THE REGULATORY ROLES OF PyrR AND Crc IN PYRIMIDINE METABOLISM IN *PSEUDOMONAS AERUGINOSA*

Monal V. Patel, B.S.

Dissertation Prepared for the Degree of

DOCTOR OF PHILOSOPHY

UNIVERSITY OF NORTH TEXAS

August 2001

APPROVED:

Gerard A. O'Donovan, Major Professor
Robert C. Benjamin, Committee Member
Mark A. Farinha, Committee Member
Mark S. Shanley, Committee Member
Olivia M. White, Committee Member
Earl G. Zimmerman, Chair of the Department of Biological Sciences
Warren Burggren, Dean of the College of Arts and Sciences
C. Neal Tate, Dean of the Robert B. Toulouse School of Graduate Studies

Patel, Monal V., The regulatory roles of PyrR and Crc in pyrimidine metabolism in *Pseudomonas aeruginosa*. Doctor of Philosophy (Molecular Biology), August 2001, 184 pp., 14 tables, 92 illustrations, references, 124 titles.

The regulatory gene for pyrimidine biosynthesis has been identified and designated *pyrR*. The *pyrR* gene product was purified to homogeneity and found to have a monomeric molecular mass of 19 kDa. The *pyrR* gene is located directly upstream of the *pyrBC'* genes in the *pyrRBC'* operon. Insertional mutagenesis of *pyrR* led to a 50-70% decrease in the expression of *pyrBC'*, *pyrD*, *pyrE* and *pyrF* while *pyrC* was unchanged. This suggests that PyrR is a positive activator. The upstream regions of the *pyrD*, *pyrE* and *pyrF* genes contain a common conserved 9 bp sequence to which the purified PyrR protein is proposed to bind. This consensus sequence is absent in *pyrC* but is present, as an imperfect inverted repeat separated by 11 bp, within the promoter region of *pyrR*. Gel retardation assays using upstream DNA fragments proved PyrR binds to the DNA of *pyrD*, *pyrE*, *pyrF* as well as *pyrR*. This suggests that expression of *pyrR* is autoregulated; moreover, a stable stem-loop structure was determined in the *pyrR* promoter region such that the SD sequence and the translation start codon for *pyrR* is sequestered. β-galactosidase activity from transcriptional *pyrR*::*lacZ* fusion assays, showed a two-fold in increase when expressed in a $pyrR^-$ strain compared to the isogenic $pyrR^+$ strain. Thus, *pyrR* is negatively regulated while the other *pyr* genes (except *pyrC*) are positively activated by PyrR. That no regulation was seen for *pyrC* is in keeping with the recent discovery of a second functional *pyrC* that is not regulated in *P. aeruginosa*.

Gel filtration chromatography shows the PyrR protein exists in a dynamic equilibrium, and it is proposed that PyrR functions as a monomer in activating *pyrD*, *pyrE* and *pyrF* and as a dimeric repressor for *pyrR* by binding to the inverted repeat. A related study discovered that the catabolite repression control (Crc) protein was indirectly involved in *pyr* gene regulation, and shown to negatively regulate expression of PyrR at the posttranscriptional level.

ACKNOWLEDGMENTS

I would like to gratefully acknowledge the opportunity provided to me by Dr. Gerard A. O'Donovan, and his continuing encouragement and generous support. I wish to also thank Dr. Alan P. Kumar for his guidance through the enchanted woods of pyrimidine research. And lastly, but by no means least I thank my parents Dr. Vinod D. Patel and Mrs. Sudha V. Patel for their unconditional love and support, without which I know could not have achieved this and traveled so far.

TABLE OF CONTENTS

LIST OF TABLES

LIST OF ILLUSTRATIONS

INTRODUCTION

Pseudomonads.

The pseudomonads are a group of obligate aerobes that use oxygen as the final electron acceptor. Some members can also use nitrate in lieu of oxygen in anaerobic respiration and thus can grow anaerobically. The genus is non-fermentative and near ubiquitous in soil and water. A striking feature of the genus is extreme nutritional versatility of its member species, in particular Pseudomonas aeruginosa, the subject of this dissertation. The biochemical studies of Stanier *et al.*, (1966) provided the early evidence for the physiological diversity of the aerobic pseudomonads and revealed the capacity of *Pseudomonas* species to metabolize a wide range of low-molecular weight organic compounds. Some species metabolize over 100 different compounds, and *Pseudomonas aeruginosa* in particular, has the ability to utilize numerous classes of compounds as carbon and energy sources such as sugars, fatty acids, dicarboxylic acids, tricarboxylic acids, some alcohols, polyalcohols and glycols, aromatic compounds, amino acids, amines and other organic molecules. In addition to being able to grow at temperatures as high as 43°C, *P. aeruginosa* and some other *Pseudomonas* species can grow in temperatures as low as 4°C. This physiological and genetic adaptability makes many pseudomonads important as pathogens of both plants and animals (Spiers *et al*., 2000; Yamamoto *et al*., 2000). The type species, *P. aeruginosa* is a recently designated global pathogen (Goldberg, 2000) and in humans it acts opportunistically by initiating infections

in individuals whose resistance is low. The production of the exopolysaccharide alginate is known to play several roles in the pathogenicity of *P. aeruginosa*, and its conversion to mucoidy is the major cause of infections in cystic fibrosis (CF) patients (Pederson, 1992; Koch & Høiby, 1993). Moreover, *P. aeruginosa* produces a green pigment known as pyoverdin that is also a major factor in virulence.

In the absence of the conventional Embden-Meyerhof-Parnas (EMP) mode of glycolysis, pseudomonads employ a number of alternative catabolic pathways to utilize carbohydrates, especially glucose and gluconate as carbon and energy sources. In *P. aeruginosa*, the Entner-Doudoroff pathway (ED) is the central metabolic route for the dissimilation of glucose to pyruvate and glyceraldehyde-3-phosphate (Entner & Doudoroff, 1952; Conway, 1992). The first step of glucose metabolism in *P. aeruginosa* is the conversion of glucose to glucose-6-phosphate by the *glk*-encoded glucokinase, followed by the formation of 6-phosphogluconate catalyzed by the *zwf*-encoded glucose-6-phosphate dehydrogenase. The next step involves the first of the two ED specific enzymes 6-phosphogluconate dehydratase, encoded by *edd* which converts of 6-phosphogluconate to 2-keto-3-deoxy-6-phosphogluconate (KDPG). The second specific enzyme aldolase, encoded by *eda* catalyzes the formation of pyruvate and glyceraldehyde-3-phosphate. These compounds, are then further metabolized by the conventional pathways, the EMP glycolytic pathway and the tricarboxylic acid (TCA) cycle.

Pyrimidine metabolism.

Pyrimidine and purine nucleotides are the essential substrates for the informational macromolecules ribonucleic acid (RNA) and deoxyribonucleic acid (DNA) which are required for cellular growth, and for the transmission of genetic information to succeeding generations. Two main pathways are involved in the formation of pyrimidine ribonucleotides, namely the biosynthetic pathway (Fig. 1) and the salvage pathway (Fig. 2). The biosynthetic pathway produces uridine 5'-triphosphate (UTP), cytidine-5'-triphosphate and deoxythymidine-5'-triphosphate (dTTP) and deoxycytidine-5'-triphosphate (dCTP), while the salvage pathway is responsible for the recycling of pyrimidine compounds released primarily from the degradation of messenger RNA. The biosynthetic pathway has been studied extensively in bacteria (Yates & Pardee, 1956a, 1956b, 1957; Beckwith *et al*., 1962; Hayward & Belser, 1965; Yan & Demerec, 1965; Hutson & Downing, 1968; Foltermann *et al*., 1981; Grogan & Gunsalus, 1993), fungi (Lacroute, 1968; Caroline, 1969), plants (Kafer & Thornburg, 1999) and mammals (Hager & Jones, 1967; Nakinishi *et al*., 1968; Jones, 1980). This pathway is ubiquitous except for a few obligate parasites (Jones, 1980) and follows the same sequence in all organisms studied thus far (Grogan & Gunsalus, 1993; O'Donovan & Neuhard, 1970). However, although the sequences are almost the same, variation exists in the regulation and organization of the enzymes within different organisms.

The salvage pathway has been studied in detail by Beck (1995) in more than 40 different bacteria and their mutants. Unlike the biosynthetic pathway, salvage circuits

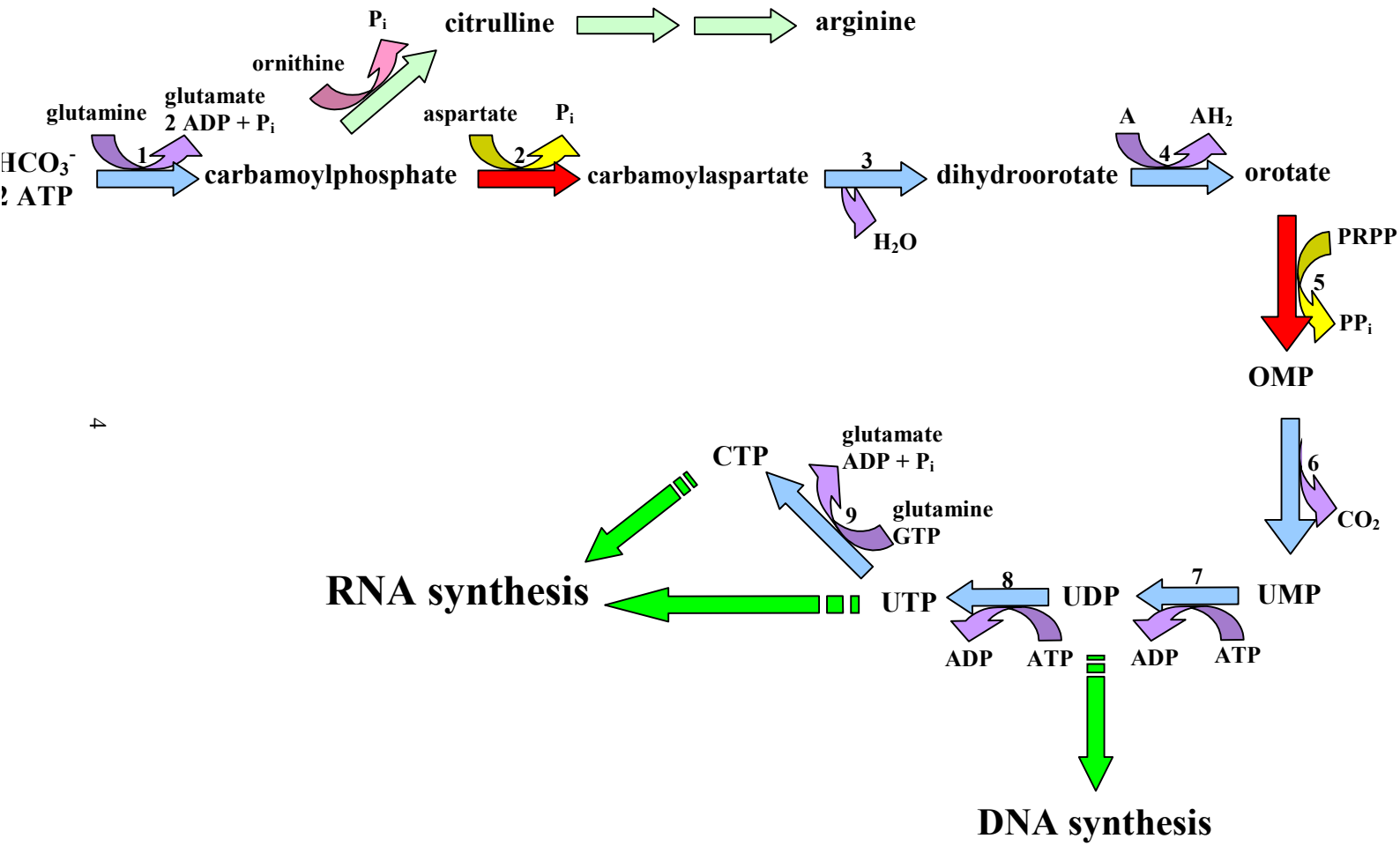
Pi
citrulline
arginine
ornithine
glutamine
glutamate
2 ADP + Pi
aspartate
Pi
A
AH2
HCO3-
? ATP
1
carbamoylphosphate
2
carbamoylaspartate
3
dihydroorotate
4
orotate
H2O
PRPP
5
PPi
OMP
6
CO2
CTP
glutamate
ADP + Pi
9
glutamine
GTP
RNA synthesis
UTP
8
UDP
7
UMP
ADP
ATP
ADP
ATP
DNA synthesis

Fig. 1. The pyrimidine biosynthetic pathway in *Pseudomonas aeruginosa*. The gene symbols and enzymes they encode: 1, *pyrA* (*carAB*) – carbamoylphosphate synthetase (CPSase); 2, *pyrBC'* – aspartate transcarbamoylase (ATCase); 3, *pyrC* – dihydroorotase (DHOase); 4, *pyrD* – dihydroorotate dehydrogenase (DHOdehase); 5, *pyrE* – orotate phosphoribosyltransferase (OPRTase); 6, *pyrF* – OMP decarboxylase (OMPdecase); 7, *pyrH* – UMP kinase; 8, *ndk* – nucleoside diphosphate kinase; 9, *pyrG* – CTP synthase.

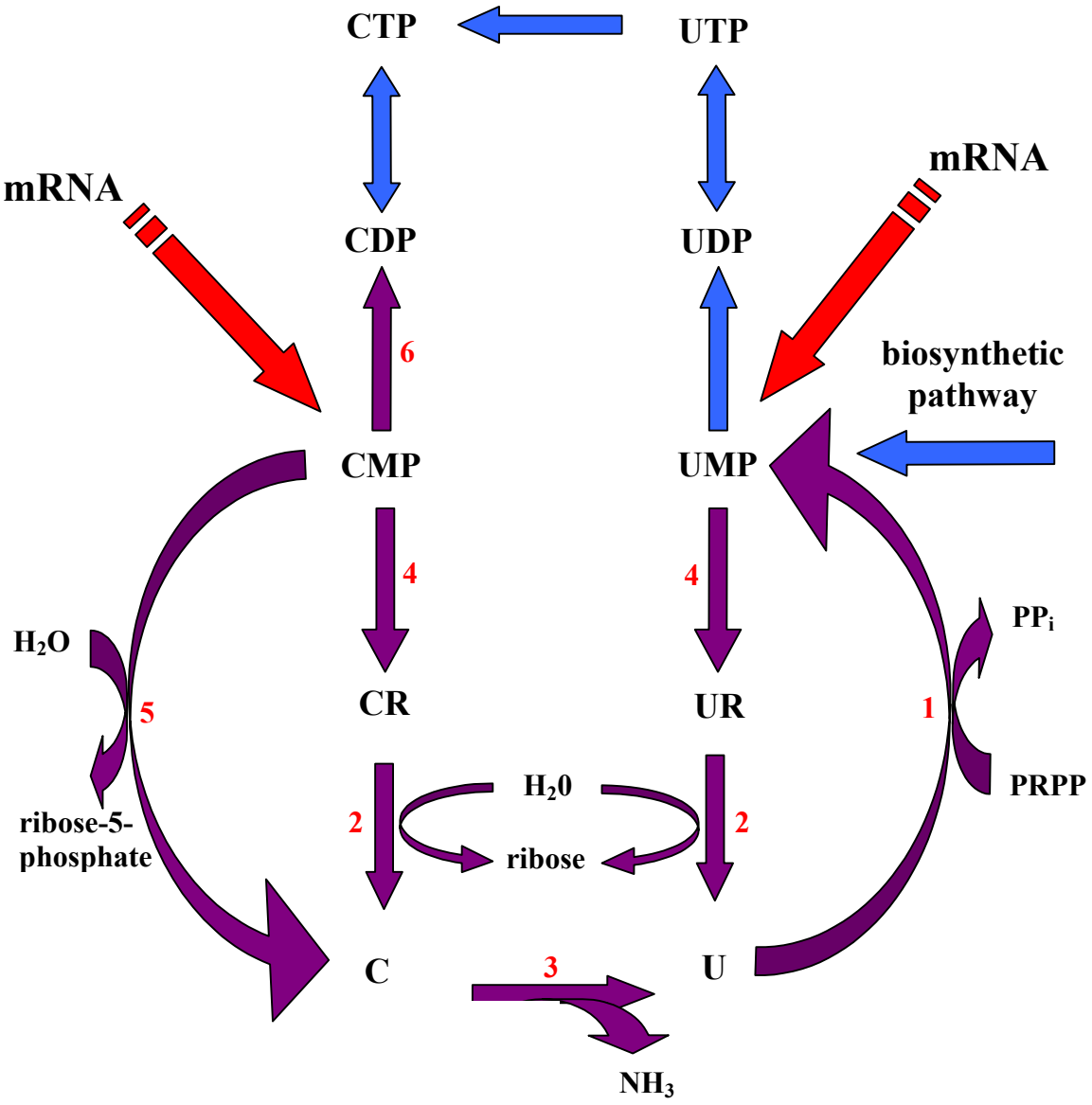

Fig. 2. The pyrimidine salvage pathway in *P. aeruginosa*. Gene symbols and the enzymes they encode: 1, *upp* – uracil phosphoribosyltransferase (UPRTase); 2, *nuh* – nucleoside hydrolase; 3, *codA* – cytosine deaminase; 4, 5'-nucleotidase; 5, *cmg* – CMP glycosylase; 6, *cmk* – CMP kinase.

differ from organism to organism. While the pyrimidine biosynthetic pathway is missing in some obligate parasites, no organism is completely devoid of a salvage pathway.

Pyrimidine biosynthetic pathway

The first step of pyrimidine biosynthesis involves carbamoylphosphate synthetase (CPSase) which catalyzes the reaction between bicarbonate and ammonium ions or more favorably glutamine, and two molecules of adenosine-5'-triphosphate (ATP) to form one molecule of carbamoylphosphate and adenosine-5'-diphosphate (ADP) (Anderson & Meister, 1965; Kalman *et al*., 1966). Both the arginine and pyrimidine biosynthetic pathways require carbamoylphosphate (Abdelal *et al*., 1969). The next step in the pyrimidine pathway involves the carbamoylation of the amino group of aspartate to give carbamoylaspartate and an inorganic phosphate molecule. This reaction is catalyzed by aspartate transcarbamoylase (ATCase) and is the first step unique to pyrimidine biosynthesis. The third reaction involves the cyclization of carbamoylaspartate with the elimination of a molecule of water to produce dihydroorotate, a reaction catalyzed by the enzyme dihydroorotase (DHOase). The fourth step of the process is the oxidation of dihydroorotate to orotate by the enzyme dihydroorotate dehydrogenase (DHOdehase). Next, the transfer of ribose-5'-phosphate from 5'-phosphoribosyl-1'-pyrophosphate (PRPP) to orotate forms orotidine-5'-monophosphate (OMP), a reaction catalyzed by orotate phosphoribosyltransferase (OPRTase). The decarboxylation of OMP by the enzyme OMP decarboxylase (OMPdecase) in the next step produces uridine-5'-monophosphate (UMP), which serves as a precursor for all pyrimidine nucleotides

including the pyrimidine nucleoside triphosphates, uridine-5'-triphosphate (UTP) and subsequently cytidine-5'-triphosphate (CTP). In sequential steps, UMP is phosphorylated to uridine-5'-diphosphate (UDP) by the highly specific UMP kinase, then further phosphorylation by the non-specific nucleoside diphosphate kinase yields UTP. The transfer of an amino group from glutamine by the enzyme CTP synthetase, completes the pathway converting UTP to CTP.

Pseudomonas pyrimidine salvage pathway

The salvage pathway, which varies from organism to organism, is responsible for the recycling of pyrimidine bases, nucleosides and nucleotides. The melting pot for recycling is replenished primarily with mononucleotides from mRNA degradation. The salvage circuits are integral processes in all cells; in prototrophs salvage provides a balance between RNA synthesis and the biosynthetic pathway, while supplying all the necessary pyrimidine requirements in auxotrophs (O'Donovan & Shanley, 1995). In *P. aeruginosa*, the feeding of Pyr^- mutants with exogenous uracil, uridine, cytosine or cytidine satisfies the pyrimidine requirement. Exogenous uracil is transported into the cell by the *uraA* encoded enzyme, uracil permease, and is then converted to uridine 5' monophosphate (UMP). This reaction is catalyzed by the enzyme uracil phosphoribosyltransferase (UPRTase), encoded by the *upp* gene. As in the biosynthetic pathway described above, UMP is phosphorylated to UDP and thence to UTP, before being converted to CTP by CTP synthetase (Fig. 2). Cytosine is transported into the cell by cytosine permease (*codB*), while the transport of exogenous uridine and cytidine into

the cell occurs via uridine permease encoded by *nup*. Once in the cell, all three of these compounds are ultimately converted to uracil. Cytosine is oxidatively deaminated to uracil by cytosine deaminase encoded by *codA*, uridine is irreversibly hydrolyzed to uracil and ribose by a non-specific nucleoside hydrolase encoded by *nuh*, and cytidine is hydrolyzed to cytosine, which is then converted to uracil by cytosine deaminase.

Regulation of pyrimidine biosynthesis in *Escherichia coli.*

Prokaryotic organisms regulate their *pyr* genes by a variety of transcriptional and translational attenuation mechanisms. The pyrimidine biosynthetic pathway in *E. coli* is regulated at the level of enzyme synthesis by attenuation (Roof *et al*., 1982; Turnbough *et al*., 1983) and at the level of enzyme activity by allosteric inhibition (Gerhart & Pardee, 1962, 1964). The *pyrBI* genes encoding ATCase and the *pyrE* gene specifying OPRTase have upstream leader sequences that allow attenuation control. In the case of the extensively studied *pyrBI*, there are two promoters, P_2 at -350 nucleotides and P_1 at -160 nucleotides upstream from the translational start of *pyrB*. Regardless of which promoter is used, termination of the transcript occurs 40 bases upstream from the start of *pyrB*. This *rho*-independent terminator region is high in G+C residues enabling the formation of a stem-loop secondary structure. This stem-loop is followed by a typical stretch of uridine residues. The mechanism of attenuation (Fig. 3) is such that when intracellular UTP levels are high, the RNA polymerase transcribes the message through the stretch of uridine residues thereby allowing the formation of the terminator loop. The structural genes are therefore not transcribed. At low UTP levels, the RNA polymerase pauses at

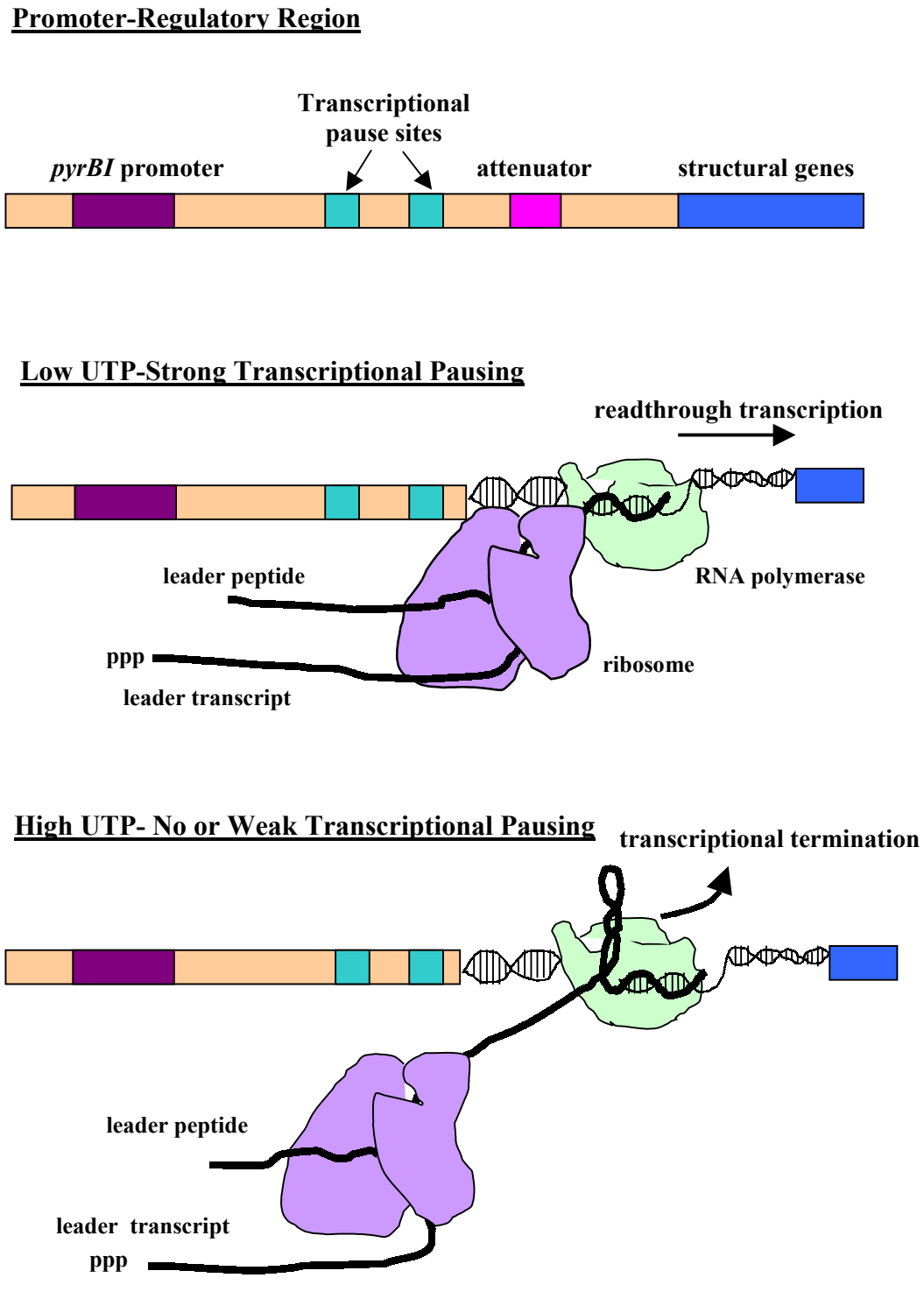

Fig. 3. Mechanism of attenuation control of the *pyrBI* operon in *Escherichia coli*.

the stretch of uridine residues, this pause is long enough to allow the ribosome to catch up to the RNA polymerase. Transcription and translation then become closely coupled which prevents the terminator loop from forming and allows transcription of the *pyrBI* operon (Navre & Schachman, 1983).

Control of enzyme activity occurs at three steps in the pyrimidine pathway. In *E. coli*, the first step is catalyzed by CPSase encoded by *carAB*, and is inhibited by UMP and activated by ornithine and inosine-5'-monophosphate (IMP). The second step is catalyzed by ATCase, encoded by *pyrBI*, is inhibited by CTP and activated by ATP (Foltermann *et al*., 1981). The step catalyzed by *pyrG* encoded, CTP synthetase, is inhibited by CTP and activated by UTP (Long & Pardee, 1967; Long & Koshland, 1978). In *Pseudomonas*, the same three steps are strongly influenced by pyrimidine and purine nucleotide effectors (Chu & West, 1990). CPSase enzyme activity is inhibited by UMP and activated by ornithine and N-acetylornithine (Abdelal *et al*., 1983), while activity of the *pyrBC'* encoded ATCase is inhibited by ATP, CTP and UTP with ATP exerting the greatest inhibition (Isaac & Holloway, 1968; Condon *et al*., 1976; Schurr *et al*., 1993; Vickrey, 1993).

Regulation of the *pyr* operon in *Bacillus subtilis.*

In enteric bacteria, separate unlinked genes or operons encode the six-enzymatic steps of pyrimidine biosynthesis, whereas in *Bacillus* these genes are arranged in an operon and transcribed as a single message. A novel mechanism for regulation of the *pyr* operon in *B. subtilis*, proposed by Lu *et al*., (1995) describes transcriptional attenuation, controlled

at three sites within the 5' end of the *pyr* transcript, by a UMP-dependent RNA binding protein encoded by the first gene of the operon, *pyrR* (Fig. 4). At high pyrimidine nucleotide levels, UMP binds to the PyrR protein forming a PyrR-UMP complex which in turn binds to a specific sequence on the *pyr* mRNA. This binding alters the secondary structure of the *pyr* message and promotes the formation of a *rho*-independent terminator, resulting in reduced expression of the pyrimidine genes that lie downstream from the binding site (Lu *et al*., 1995, Lu & Switzer, 1996; Turner *et al*., 1998; Switzer *et al*., 1999). In addition, this regulatory protein, PyrR, has the catalytic salvage activity of uracil phosphoribosyltransferase (UPRTase).

Regulation of pyrimidine biosynthesis in *Pseudomonas aeruginosa.*

Pyrimidine metabolism has not been extensively investigated in pseudomonads and although previous studies have explored the regulation of pyrimidine biosynthesis (Isaac & Holloway, 1968; Condon *et al*., 1976), significant control at the level of gene expression could not be substantiated. Unlike the *pyr* gene arrangement found in *B. subtilis*, the pyrimidine genes in *P. aeruginosa* are scattered throughout the auxotrophic portion of the chromosome (Fig. 5).

In this research study, the presence of the regulatory protein, PyrR, in *P. aeruginosa* was identified and shown to regulate expression of the downstream pyrimidine biosynthetic genes, *pyrD*, *pyrE* and *pyrF* as well as expression of the *pyrR* gene.

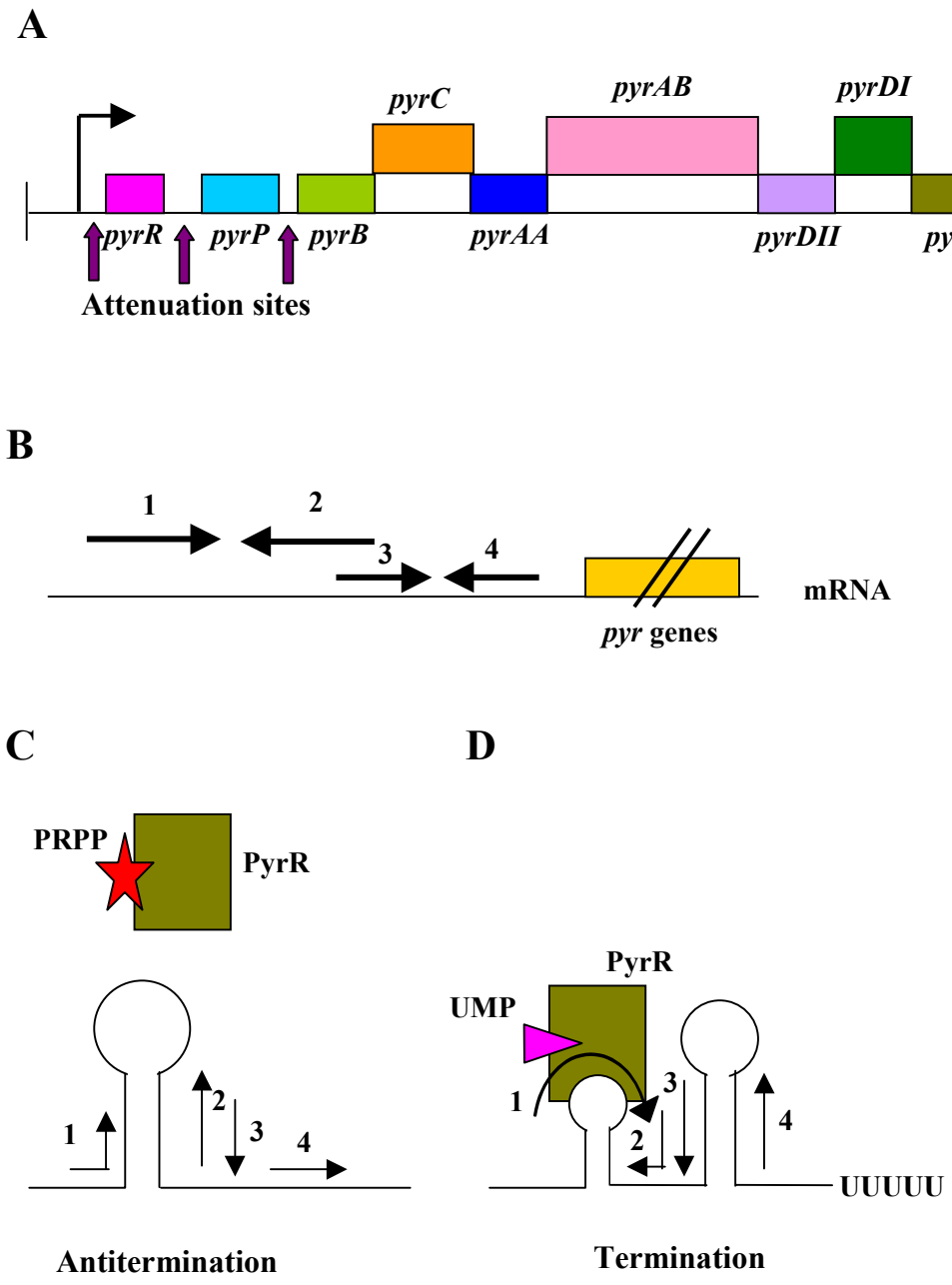

Fig.4. Mechanism of attenuation control of the *pyr* operon in *Bacillus subtilis*. Adapted from Lu & Switzer (1996).

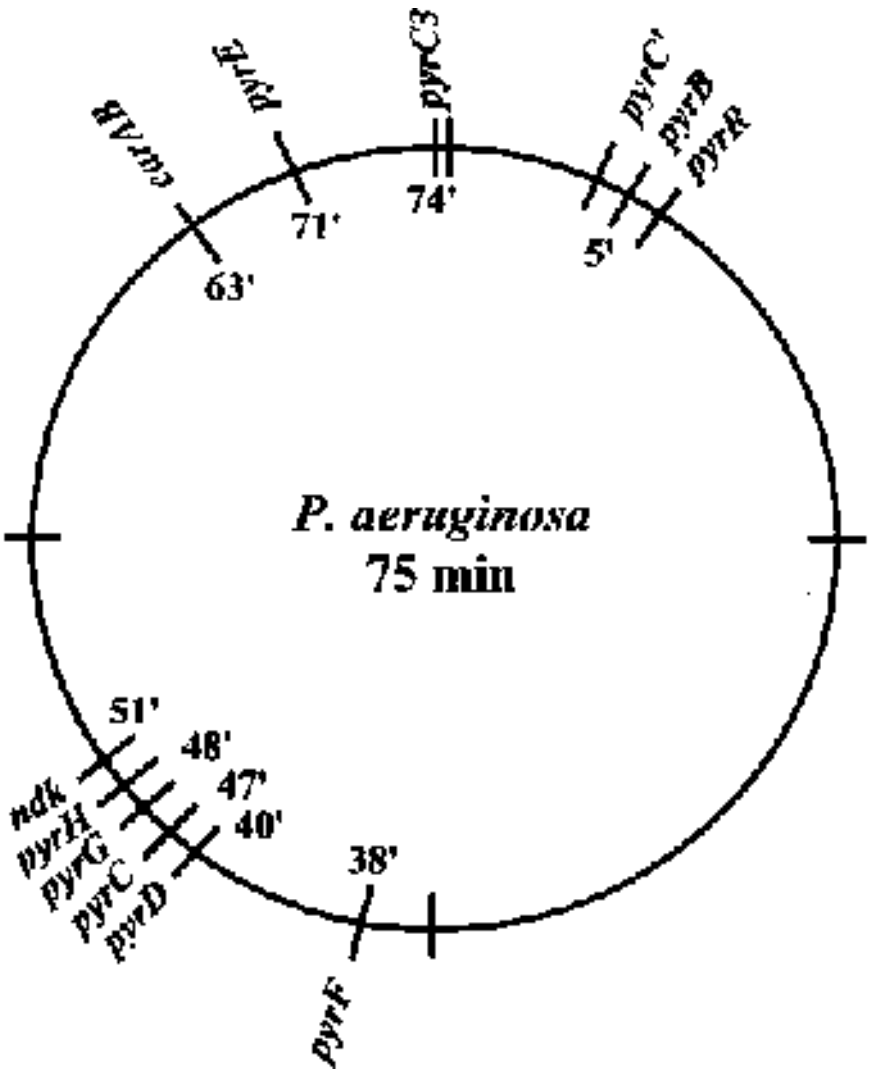

Fig. 5. Arrangement of the pyrimidine genes on the *P. aeruginosa* chromosome.

Catabolite repression control.

When an organism is supplied with two different carbon sources in its growth medium, it generally utilizes them sequentially rather than simultaneously. This preference by an organism to utilize one carbon source over another in the presence of both is known as catabolite repression control (CRC). In *E. coli* and other Gram negative enteric bacteria, glucose is the preferred carbon source and its catabolite repression control involves the catabolite activator protein (CAP), also referred to as the cAMP receptor protein (CRP) encoded by the *crp* gene. In these enterics, transport of glucose is driven by the phosphoenolpyruvate (PEP)-dependent transport system (PTS) and the binding of the signal molecule, cyclic AMP (cAMP) to CAP. This cascade system induces adenylate cyclase activity, which in turn increases the intracellular cAMP concentration. In the presence of glucose, cAMP levels are low and the constitutively expressed CAP is not bound by cAMP therefore does not activate transcription of the repressed structural genes, e.g. *lacZYA* for lactose utilization. However as the glucose source is depleted, the intracellular levels of cAMP increase and the CAP-cAMP complex forms which can bind to the promoter region of the repressed genes and enhance transcriptional initiation. Though the molecular mechanism of catabolite repression control has been extensively characterized in *E. coli* and *S. typhimurium*, it is yet to be fully characterized in *P. aeruginosa*. Unlike the glucose effect on catabolite repression found in *E. coli*, catabolite repression control of inducible catabolic pathways in *Pseudomonas* does not appear to involve a cAMP-mediated mechanism (Siegel *et al*., 1977; Philips & Mulfinger, 1981). Acetate and tricarboxylic acid cycle intermediates,

such as succinate have been shown to be the strongest repressing substrates in *Pseudomonas* (Hylemon & Phibbs, Jr., 1972; Smyth & Clarke, 1975; Collier *et al*., 1996). So far, the only protein shown definitively to be involved in catabolite repression control in *P. aeruginosa*, is the Crc protein (MacGregor *et al*., 1992). Though its function is yet to be identified, studies have recently shown that the Crc protein is involved in the regulation of several pathways. These include the expression of branched-chain keto acid dehydrogenase (BCKAD) encoded by the *bkd* operon (Hester *et al*., 2000a; 2000b), glucose-6-phosphate dehydrogenase (Wolff *et al*., 1991; Siegel *et al*., 1977) and amidase (Smyth & Clarke, 1975; Farin & Clarke, 1978) in *Pseudomonas*. The recent studies by Hester *et al*. (2000a; 2000b) showed that the Crc protein affected expression of BkdR, a positive transcriptional regulator of the *bkd* operon. The mechanism of action by Crc on BkdR is not known, however Phibbs and coworkers have shown that the Crc protein has all the necessary structural features to cleave a phosphodiester bond yet lacks the ability to bind DNA. Therefore, it is thought that perhaps the Crc protein, when activated, cleaves the mRNA at a specific site within the secondary structure thereby affecting expression at the posttranscriptional level. In *P. aeruginosa*, the *crc* gene that encodes the Crc protein is located –80 bp upstream of the *pyrE* gene, which encodes orotate phosphoribosyltransferase, and the two genes are divergently transcribed (Fig. 6). Divergent transcription is a relatively common type of gene organization, approximately 40% of all transcription units in *E. coli* are transcribed from divergent promoters (Opel *et al*., 2001). Of these, approximately 60% contain one or more operon or gene-specific regulatory genes.

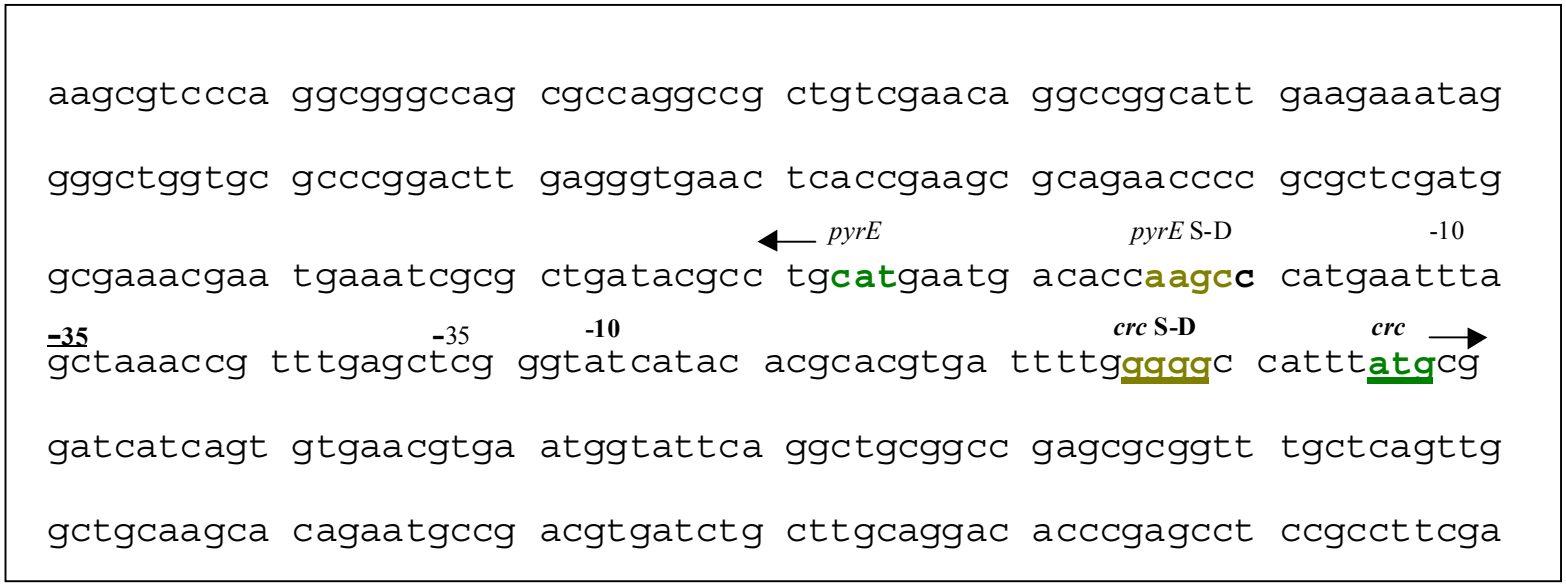

Fig. 6. Partial nucleotide sequence of the *P. aeruginosa pyrE* and *crc* genes showing the 80 bp intergenic region (MacGregor *et al*. (1996).

The purpose of this aspect of the research study is to explore any possible involvement of Crc in pyrimidine metabolism in *P. aeruginosa*.

Dicarboxylate transport in *Pseudomonas*.

In *Pseudomonas*, the pyrimidine biosynthetic pathway is a six-step process leading to UMP. Of the pyrimidine biosynthetic pathway intermediates, it has been shown in *E. coli* and *S. typhimurium* that orotate can satisfy the pyrimidine requirement of *pyr* mutants, only when glycerol is used as the carbon and energy source (Baker *et al*., 1996); glucose and orotate cannot satisfy this requirement. It has also been reported that a C4-dicarboxylate transport protein, DctA, encoded by the *dctA* gene is required in *E. coli* and *S. typhimurium* since *dctA* mutants in these organisms are unable to utilize succinate, malate or fumarate as sole carbon and energy sources. In addition, succinate was found to compete with orotate for entry into the enteric cell (Baker *et al.*, 1996). Therefore, the *dctA* gene product, in addition to transporting C4-dicarboxylates, mediates the transport of orotate, a cyclic monocarboxylate.

The effect of succinate on the transport of orotate into the *Pseudomonas* cell was investigated in the present study with the aim to identify in *Pseudomonas* the same dicarboxylate transport system as seen in *E. coli* (Baker *et al*., 1996).

MATERIALS AND METHODS

Bacterial strains, plasmids, media and growth conditions.

The bacterial strains and plasmids used in this study are listed in Tables 1a and 1b. Bacteria were grown in Luria-Bertani (LB) enriched medium (Bertani, 1951), *Pseudomonas* minimal medium supplemented with Hutner's Metals 44 (Ornston & Stanier, 1966) or in *Escherichia coli* minimal medium (Miller, 1972). For biparental mating experiments, transconjugants were selected for on *Pseudomonas* isolation agar (PIA, Difco). Antibiotics were added at the following concentrations: ampicillin, 100 μg ml^{-1}; gentamicin, 20 μg ml^{-1}; kanamycin 50 μg ml^{-1} for *E. coli*, and carbenicillin, 600 μg ml^{-1}, gentamicin, 100 μg ml^{-1}, tetracyclin, 100 μg ml^{-1} for *P. aeruginosa*. The carbon sources used were glucose at 0.2% or succinate at 10 mM. *P. aeruginosa* AK903 and PAO1 wild type strains were employed throughout this study. All *E. coli* and *P. aeruginosa* strains were grown at 37°C with shaking at 250 rpm.

Preparation of competent cells.

All *E. coli* competent cells for transformation were prepared using the calcium chloride method of Dagert & Ehrich (1979) with slight modifications. The cultures were grown in 50 ml LB medium to an optical density (OD) of 0.2 – 0.4 at 600 nm and chilled on ice for 10 min. The cells were harvested by centrifugation at 1875 ***g*** at 4°C for 15 min, the cell pellet was resuspended in 20 ml of ice-cold 0.1 M $CaCl_2$ and incubated

Table 1a. Bacterial strains used in this study**.**

Strains	Description or relevant phenotype	Source or reference
E. coli		
DH5α	*ΔrecA1 argF lacIZYA*	Bethesda Research Laboratory
SM10	*thi*-1 *thr leu tonA lacY supE recA*::RP4-2-Tc::Mu (Km^R)	De Lorenzo & Timmis (1994)
BL21	F^- *ompT gal dcm lon hsdS*$_B$ ($r_B^- m_B^-$)	Amersham Pharmacia Biotech.
JM109	*recA1 endA1 gyrA96 hsdR17 supE44 relA1* Δ (*lac-proAB*) (*F' traD36 proAB lacI*^{q} ZΔM15)	New England Biolabs, Inc.
P. aeruginosa		
AK903	restriction minus derivative of PAO1; addition of casamino acids	Potter & Loutit (1982)
PAO1	wild type	*Pseudomonas* Stock Center
PAO8023	*crc::*Cb^R	*Pseudomonas* Stock Center
PAO8020	*crc*::Tc^R	*Pseudomonas* Stock Center
PAO8017	*crc*$^-$ *pyrE*$^-$	*Pseudomonas* Stock Center
PAO0114	*pyrD*	*Pseudomonas* Stock Center
MVP7401	*pyrR::*Gm^R derivative of AK903	This study
MVP7402	*out* derivative of PAO1	This study
MVP7403	*out* derivative of PAO0114	This study
MVP7404	recruited strain derivative of PAO8017	This study

Table 1b. Plasmids used in this study.

Plasmid	Description or relevant phenotype	Source or reference
pUC18	Amp^R *lacΔZM15*	New England Biolabs
pUC41	11.8 kb insert containing the *pyrRBC'* fragment in pUC18	Vickery (1993)
pCR™II	Amp^R Kan^R PCR cloning vector	Invitrogen
pGmΩ1	*bla aacC1*; gentamicin cassette with omega loops on both ends	Schweizer (1993)
pGEX-2T	Amp^R GST gene fusion vector	Amersham Pharmacia Biotech.
pRTP1	Amp^R *rpsL oriT cos*	Stibitz *et al*. (1986)
pQF50	Amp^R promoterless - *lacZ* transcriptional fusion vector	Farinha & Kropinski (1990a)
pQF52	Amp^R promoterless - *lacZ* translational fusion vector	Park *et al*. (1997)
pPZ352	PAO1 crc^-	MacGregor *et al*. (1991)
pMVP1	*P. aeruginosa pyrR* ; ~800 bp insert in pCR™II (correct orientation)	This study
pMVP2	*P. aeruginosa pyrR* ; ~800 bp insert in pCR™II (wrong orientation)	This study
pMVP3	*pyrR*::Gm^R in pMVP1, interrupted by a Gm cassette at a *Aat*II site	This study
pMVP4	~2.3 kb *pyrR*::Gm^R fragment from pMVP3 in pRTP1	This study
pMVP5	*P. aeruginosa upp*; ~900 bp insert in pCR™II (correct orientation)	This study
pMVP6	*P. aeruginosa upp*; ~900 bp insert in pCR™II (wrong orientation)	This study
pMVP10	*P. aeruginosa pyrR*; ~510 bp insert in pGEX-2T	This study
pMVP11	*P. aeruginosa upp*; ~600 bp insert in pGEX-2T	This study
pMVP50	*P. aeruginosa pyrR* promoter region; ~320 bp insert in pQF50	This study
pMVP52	*P. aeruginosa pyrR* promoter region; ~310 bp insert in pQF52	This study

on ice for 20-25 min. The cells were centrifuged at 833 ***g*** at 4°C for 15 min, the pellet was resuspended in 0.7 ml of ice-cold 0.1 M $CaCl_2$ and incubated on ice overnight. The next day, glycerol was added to the cells at a concentration of 15%, the competent cells were separated into 150 µl aliquots and stored at -80°C for up to 3 months.

Transformation of *E. coli*.

Transformations of *E. coli* were carried according to the method of Huff *et al*., (1990). Approximately 40 ng of plasmid DNA was mixed with 150 µl of calcium chloride prepared competent cells and the mixture were incubated on ice for 20 min. The cells were then heat shocked at 42°C for exactly 2 min, 1 ml of LB was added to the cells and incubated at 37°C for 1 h with shaking. After 1 h, the cells were plated on LB medium, and the transformed cells were selected for with the appropriate antibiotic.

Preparation of cell extracts for *pyr* assays.

P. aeruginosa PAO1 and its derivatives were grown in *Pseudomonas* minimal medium in the presence of appropriate supplements. The cultures (50 ml) were grown to an OD of 0.6 at 600 nm, harvested and resuspended in 1 ml of 40 mM potassium phosphate buffer (pH 7.0). The cell suspension was ruptured by sonication. The extract was centrifuged at 12,000 ***g*** at 4°C for 5 min, and 300 µl of the supernatant was withdrawn for assay of dihydroorotate dehydrogenase. The remaining extract was centrifuged at 12,000 ***g*** at 4°C for a further 25 min. The supernatant (clarified extract) was transferred to a sterile microcentrifuge tube for assay of the other pyrimidine

enzymes. Protein concentration was determined by the method of Bradford (1976) with bovine serum albumin as the standard (Fig. 7).

Aspartate transcarbamoylase (ATCase) assay.

ATCase enzyme assays were performed using the method described by Gerhart & Pardee (1962) with modification. The specific activity (μmol min^{-1} mg^{-1}) was determined by monitoring the enzymatic production of carbamoylaspartate (CAA) in 10 min at 37°C using the colorimetric method of Prescott & Jones (1969). A 1 ml reaction volume contained the following components: 40 μl of Tri-buffer, pH 9.5 (Ellis & Morrison, 1982), (51 mM diethanolamine, 51 mM *N*-ethylmorpholine and 100 mM MES), 50 μl of 100 mM potassium aspartate (pH 9.5), 100 μl of 50 mM carbamoylphosphate (dilithium salt), 10 μl of clarified extract, 800 μl ddH_2O. In addition to the reaction tubes, a control was also prepared by substituting the clarified extract for ddH_2O. The ATCase assay tubes were prepared in advance, without the addition of carbamoylphosphate, and preincubated at 37°C for 2 min. The reaction was initiated by the addition of carbamoylphosphate and the tubes were incubated at 37° for 10 min. After 10 min, the reaction was terminated by the addition of 1 ml of color mix (2 parts of 5 mg ml^{-1} of antipyrine in 50% sulfuric acid (v/v) with 1 part of 8 mg ml^{-1} of 2, 3-butanedione monoxime in 5% acetic acid (v/v)). The reaction tubes were mixed by vortexing, and incubated at 65°C for 2 h in the light to allow development of the color. The tubes were capped with marbles to minimize evaporation. After 2 h, the absorbance at 466 nm was

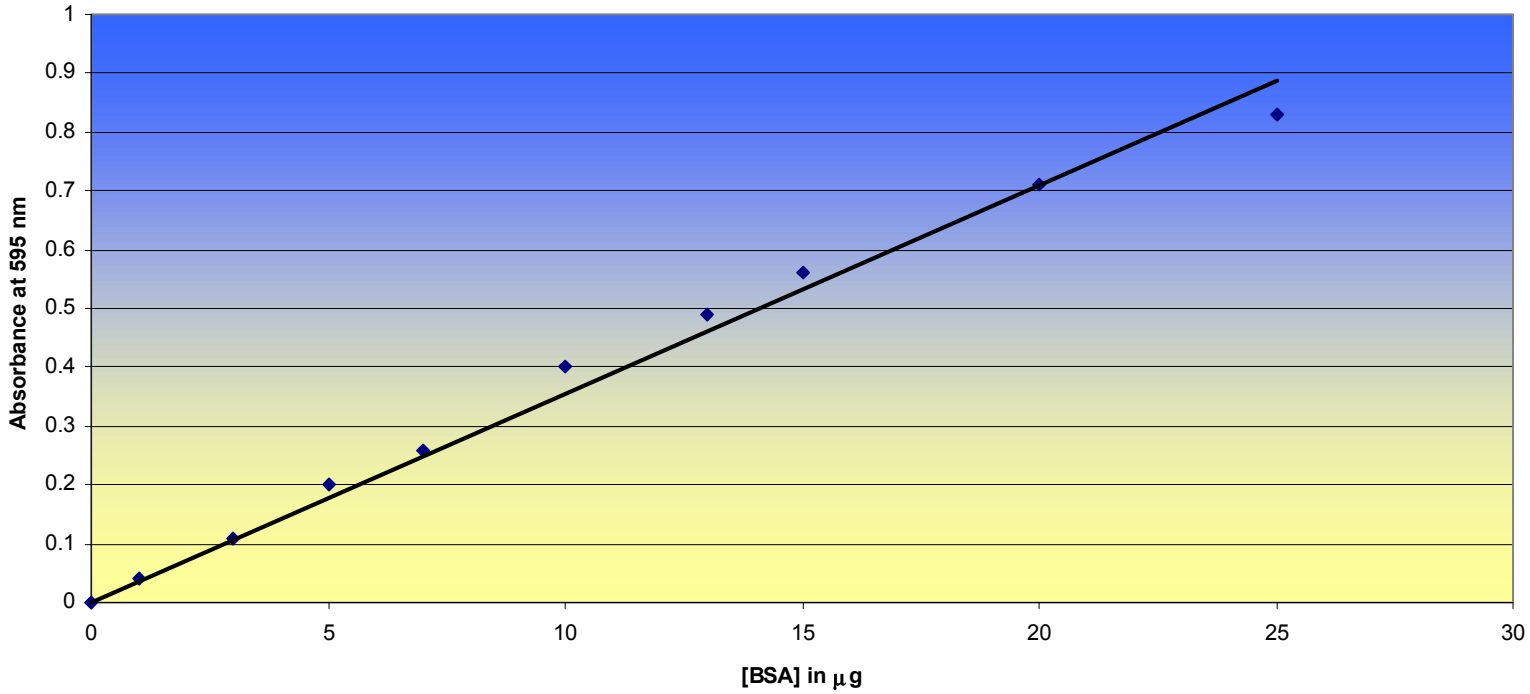

Fig. 7. Bradford protein standard curve

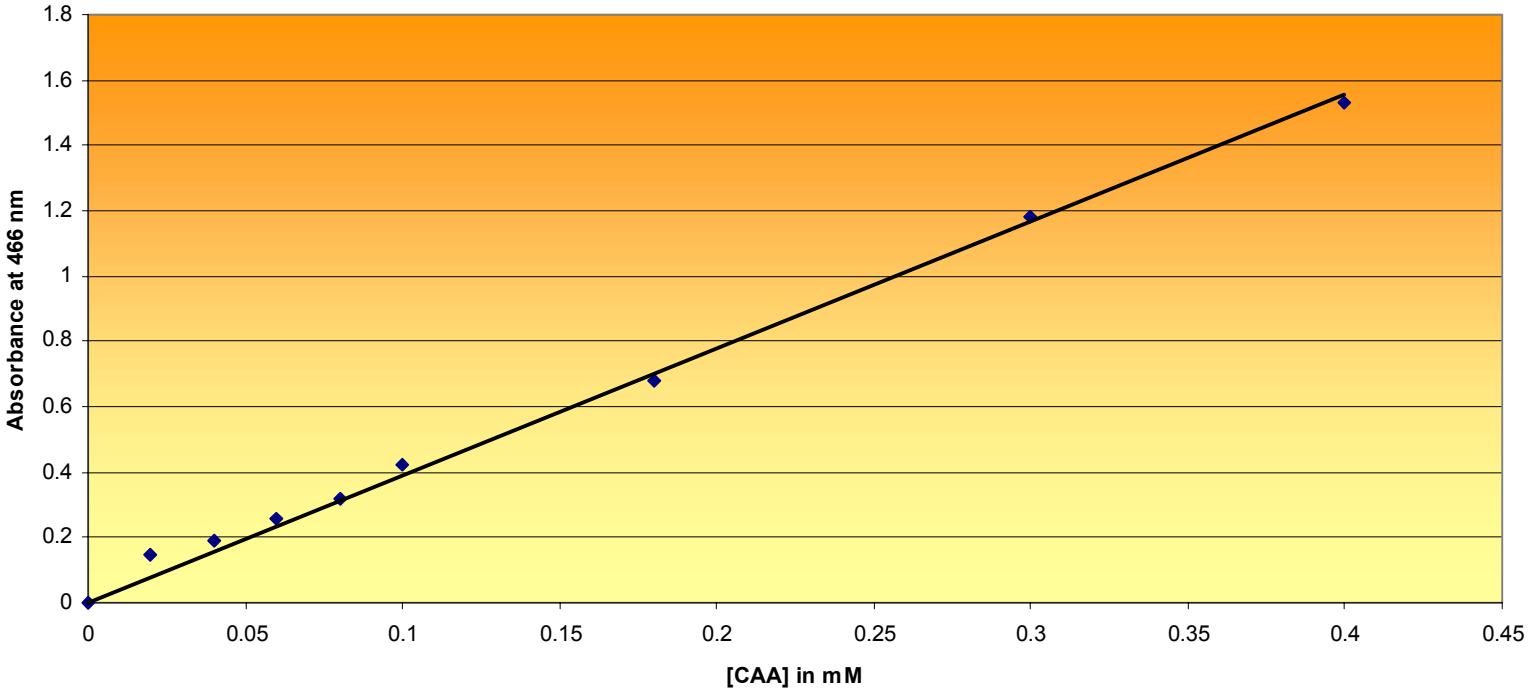

Fig. 8. Carbamoylaspartate standard curve

measured, using the control tube to blank the spectrophotometer. The mmoles of CAA produced were determined using a CAA standard curve, prepared with known concentration of CAA ranging from 0 to 450 nM in the standard assay reaction mix and under the same color development conditions (Fig. 8).

Dihydroorotase (DHOase) assay.

The DHOase assay tubes contained the following components in a 1 ml reaction volume: 100 µl of 1 M Tris (pH 8.6), 100 µl of 10 mM EDTA, 100 µl of 20 mM dihydroorotate (in 0.1 M phosphate buffer, pH 7.5), 10 µl clarified extract and 690 µl of ddH_2O (Beckwith *et al*., 1962; Schwartz & Neuhard, 1975). The DHOase assay tubes were prepared in advance, without the dihydroorotate, and pre-incubated at 37°C for 2 min. The reaction was initiated by the addition of dihydroorotate and the tubes were incubated at 37°C for 10 min. After 10 min, the reaction was terminated by the addition of 1 ml of color mix as described for the ATCase assay. The tubes were vortexed and incubated at 65°C for 2 h in the light. The absorbance was measured at 466 nm. A control tube containing all reaction components except dihydroorotate was used to blank the spectrophotometer.

Dihydroorotate dehydrogenase assay.

Dihydroorotate dehydrogenase activity was measured spectrophotometrically by monitoring the conversion of dihydroorotate to orotate at 290 nm. The dihydroorotate dehydrogenase reaction mix was prepared in a quartz cuvette containing the following

components in a 1 ml reaction volume: 0.1 M Tris (pH 8.6), 6 mM $MgCl_2$, 1 mM dihydroorotate (in 0.1 M phosphate buffer, pH 7.5), 50 µl cell extract (from 5 min centrifugation at 12 000 ***g***) and ddH_2O to a 1 ml total volume. The reaction cuvette was prepared in advance, without the dihydroorotate, and incubated at 37°C for 2 min. The reaction was initiated with the addition of dihydroorotate, and the A_{290} units were noted immediately, this was the blank reading. The cuvette was then incubated at 37°C for 10 min, after which the A_{290} units were measured. The blank reading was subtracted from the 10 min reading. An increase in absorbance of 1.93 is equivalent to a change in substrate concentration of 1 mM (relative to the blank value, [Beckwith *et al*., 1962; Schwartz & Neuhard, 1975]).

Orotate phosphoribosyltransferase (OPRTase) assay.

OPRTase activity was measured spectrophotometrically by the method of Smith *et al*., (1980). The conversion of orotate to OMP was monitored at 295 nm. The OPRTase reaction mix was prepared in a quartz cuvette containing the following components in a 1 ml reaction volume: 0.1 M Tris (pH 8.6), 6 mM $MgCl_2$, 0.25 mM orotate, 0.6 mM 5-phosphoribosyl-1-pyrophosphate (PRPP), 50 µl clarified extract and ddH_2O to a 1 ml total volume. The reaction cuvette was prepared in advance, without the orotate, and incubated at 37°C for 2 min. The reaction was initiated with the addition of orotate, and the A_{295} units were recorded immediately, this was the blank reading. The cuvette was then incubated at 37°C for 10 min, after which the A_{295} units were measured. The 10 min reading was subtracted from the blank reading. A decrease in absorbance of

3.67 is equivalent to an increase in orotidine 5'-monophosphate (OMP) concentration of 1 mM (relative to the blank value, [Beckwith *et al*., 1962; Schwartz & Neuhard, 1975]).

OMP decarboxylase assay.

OMP decarboxylase activity was measured spectrophotometrically by monitoring the conversion of OMP to uridine 5'-monophosphate (UMP) at 285 nm. The OMP decarboxylase reaction mix was prepared in a quartz cuvette containing the following components in a 1 ml reaction volume: 0.1 M Tris (pH 8.6), 6 mM $MgCl_2$, 0.2 mM OMP, 50 µl clarified extract and ddH_2O to a 1 ml total volume. The reaction cuvette was prepared in advance, without the OMP, and incubated at 37°C for 2 min. The reaction was initiated with the addition of OMP, and the A_{285} units were noted immediately, this was the blank reading. The cuvette was then incubated at 37°C for 10 min, after which the A_{285} units were measured. The 10 min reading was subtracted from the blank reading. A decrease in absorbance of 1.38 is equivalent to a decrease in OMP concentration of 1 mM (relative to the blank value, [Beckwith *et al*., 1962; Schwartz & Neuhard, 1975]).

Cloning of the *pyrR* gene.

An 800 bp DNA fragment containing the *pyrR* gene was amplified from pUC41 plasmid (Fig. 9., Vickrey, 1993) by the Polymerase Chain Reaction (PCR, Saiki *et al*., 1988) with two synthetic oligonucleotides: oligo-1 (5'-TCCCATCGATGTCAGCGAGG-3') and oligo-2 (5'-GAGCAGCTCGCGGGGCAATC-3'). The gene product was amplified using *Taq* polymerase, which creates 3'-T overhangs, enabling direct ligation of the PCR

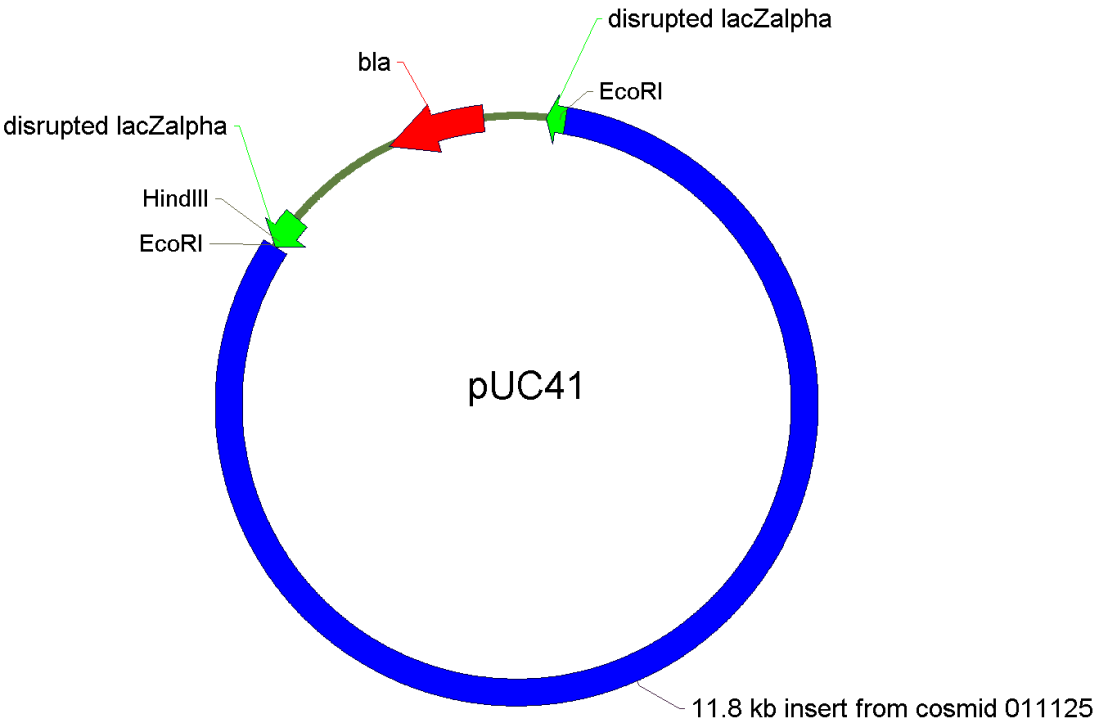

Fig. 9. Schematic diagram of pUC41 (Vickrey, 1993), derived from an *Eco*RI digest of pUC18. The 11.8 kb insert contains the *P. aeruginosa pyrRBC*' open reading frames (ORF's) taken from cosmid 011125 (obtained from B. W. Holloway).

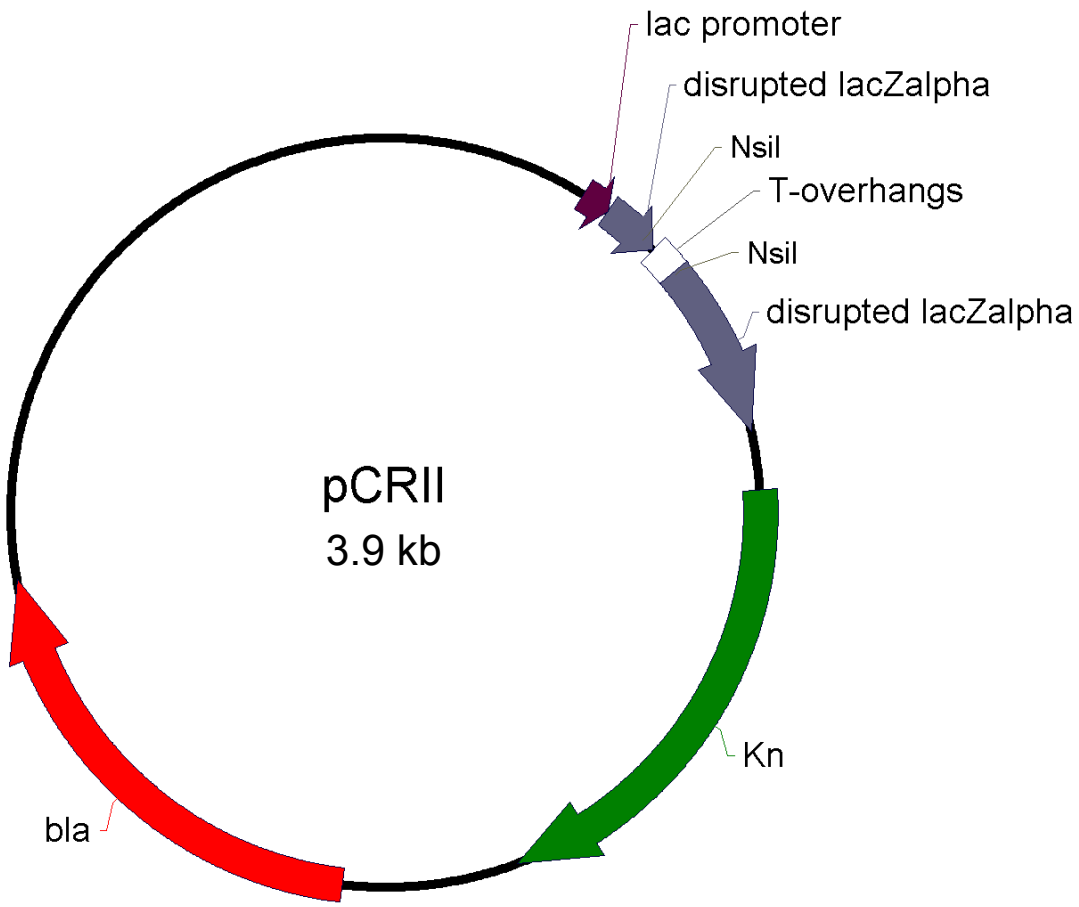

Fig. 10. Schematic diagram of pCRII cloning vector (Invitrogen). The multiple cloning site is located within the disrupted *lacZ*α gene to allow for blue/white selection, Kn corresponds to kanamycin resistance gene and *bla* corresponds to the *β*-lactamase gene which confers ampicillin resistance.

product into the pCRII vector from The Original TA Cloning Kit (Fig. 10., Invitrogen). After transformation of *E. coli* DH5α, clones containing the *pyrR* insert were selected on LB+kanamycin, with isopropyl-β-D-thiogalactopyranoside (IPTG) at 0.03% and 5-bromo-4-chloro-3-indolyl-*β*-D-galactoside (X-gal) at 0.003%. Restriction enzyme digests determined the orientation of the *pyrR* inserts. The resulting clone, pMVP1 (Fig. 11) had the *pyrR* gene inserted in the correct orientation and pMVP2 (Fig. 12) had the *pyrR* gene inserted in the opposite orientation to the *lac* promoter on the vector.

DNA sequencing.

Sequencing of double-stranded DNA was performed with the Sequenase® kit (U.S. Biochemicals Corp.) based on the dideoxy method of Sanger *et al*., (1977). All reactions were carried out according to manufacturer's specifications. The oligonucleotides used for the sequencing of the *pyrR* gene are listed in Table 2.

Table 2. Synthetic oligonucleotides used for sequencing.

Primer	Sequence (5'-3')	Usage	Supplier
pPA PE	TTGGCGTCTGTCGGCAT	Sequencing of *pyrR* gene	Vickrey (1993)
PAR-1F	CCATTATGCTTTCGCCACCG	Sequencing of *pyrR* gene	IDT[a]
PAR-1R	TGCGCGGCAGGAGTTCGGCG	Sequencing of *pyrR* gene	IDT[a]
PAR-2R	AGGGTCACGCTGGCCGGACG	Sequencing of *pyrR* gene	IDT[a]
PAR-3R	CCTGGTCGTTGAGCTGCAGC	Sequencing of *pyrR* gene	IDT[a]

[a] IDT, Intergrated DNA Technologies, Coralville, IA.

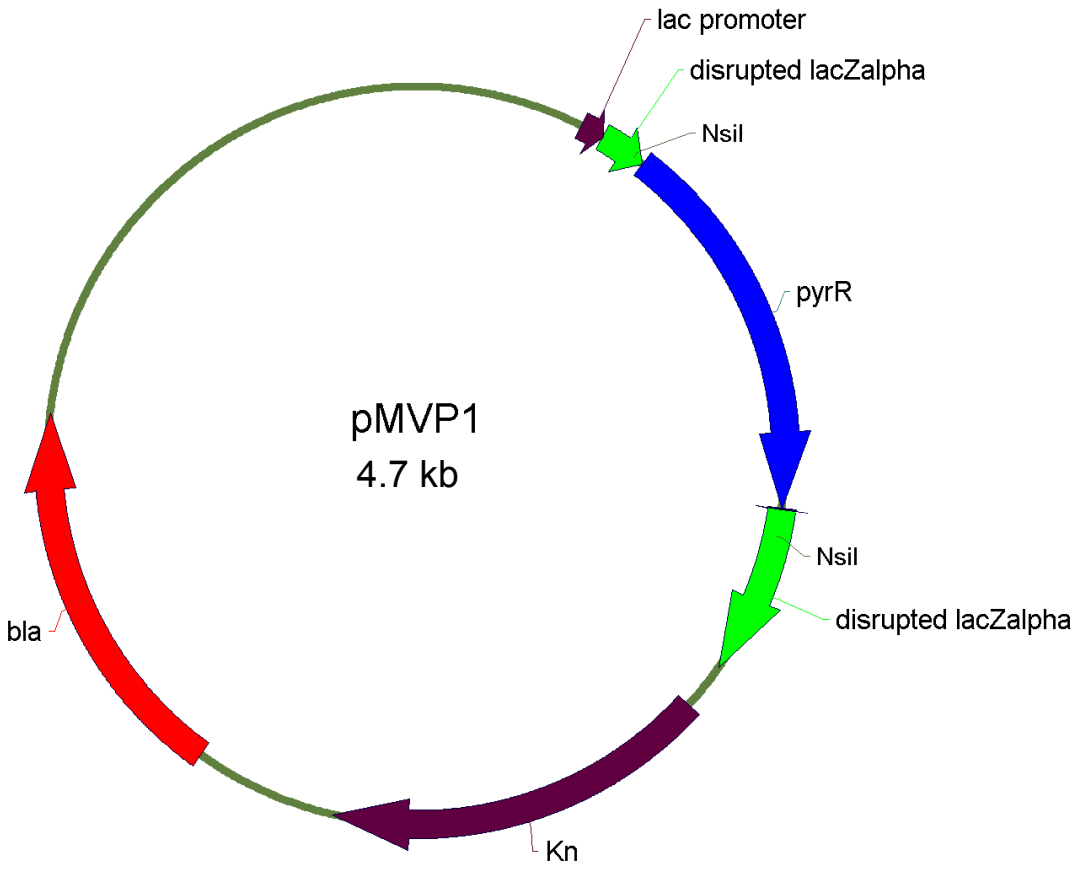

Fig. 11. Construction of pMVP1 derived from pCRII vector (Invitrogen). The resulting 4.7 kb plasmid includes an 800 bp fragment containing the *P. aeruginosa pyrR* gene, cloned in the same orientation as the *lac* promoter.

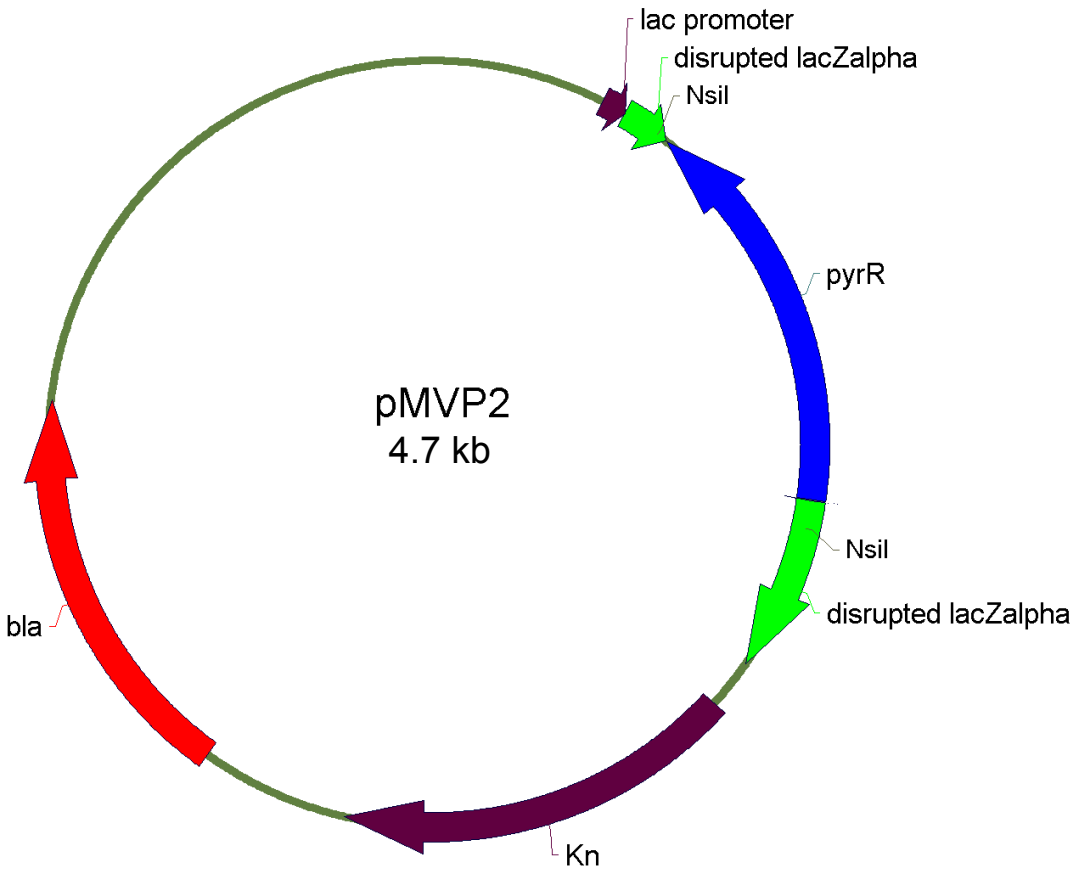

Fig. 12. Construction of pMVP2 derived from pCRII vector (Invitrogen). The resulting 4.7 kb plasmid includes an 800 bp fragment, containing the *P. aeruginosa pyrR* gene cloned in the opposite orientation to the *lac* promoter.

Cassette mutagenesis.

A 1.6-kb *Sma*I fragment containing the gentamicin resistance (Gm) cassette was isolated from plasmid pGMΩ1 (Fig. 13., Schweizer, 1993) by digestion with *Sma*I and agarose purification (Amersham Pharmacia Biotech.). The Gm cassette was cloned into the *Aat*II located 178 bp into the *pyrR* gene on plasmid pMVP1. The resulting plasmid, pMVP3 (Fig. 14) was digested with *Nsi*I to give a 2.4-kb fragment containing the *pyrR*::Gm region. The fragment was agarose purified and the 5'-overhangs generated from the *Nsi*I digestion were "filled in" with T4 DNA polymerase. This *pyrR*::Gm fragment was cloned into the conjugation vector, pRTP1 ([digested with *Bam*HI and made blunt], Fig. 15., Stibitz *et al*., 1986) and the resulting gene replacement plasmid, pMVP4 (Fig. 16), was transformed into *E. coli* SM10 (Simon *et al*., 1983) and used for biparental mating with AK903.

Biparental mating experiment: *pyrR* cassette knockout into *P. aeruginosa* AK903.

The gene replacement plasmid, pMVP4, was mobilized into *P. aeruginosa* AK903, by biparental mating as described by Gambello & Iglewski (1991). Cells taken from overnight cultures were used for the mating (Fig. 17), 1 ml of *P. aeruginosa* AK903 (recipient strain) cells grown at 37°C in LB were transferred to a sterile microcentrifuge tube, centrifuged at 12,000 ***g*** for 1 min. The supernatant was removed and 1 ml of *E. coli* SM10 cell harboring the *pyrR* knockout plasmid (donor strain) grown in *E. coli* minimal medium supplemented with 0.2% glycerol, 0.2% casamino acids, 1 mM $MgSO_4$, and

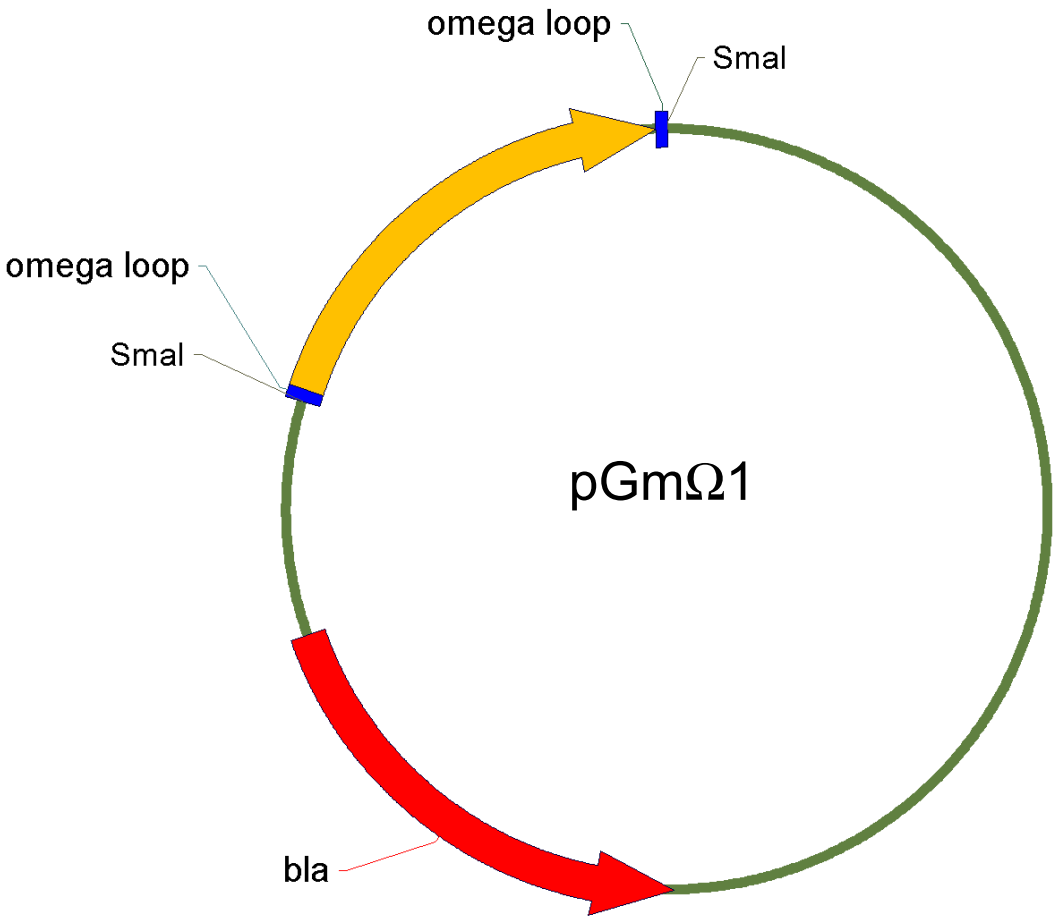

Fig. 13. Schematic diagram of plasmid pGmΩ1 (Schweizer, 1993), containing the 1.6 kb gentamicin resistant gene cassette for site-specific insertion and deletion mutagenesis. The omega loops denote flanking regions containing the transcription and translation stop signals of the Ω interposon, in inverted orientation.

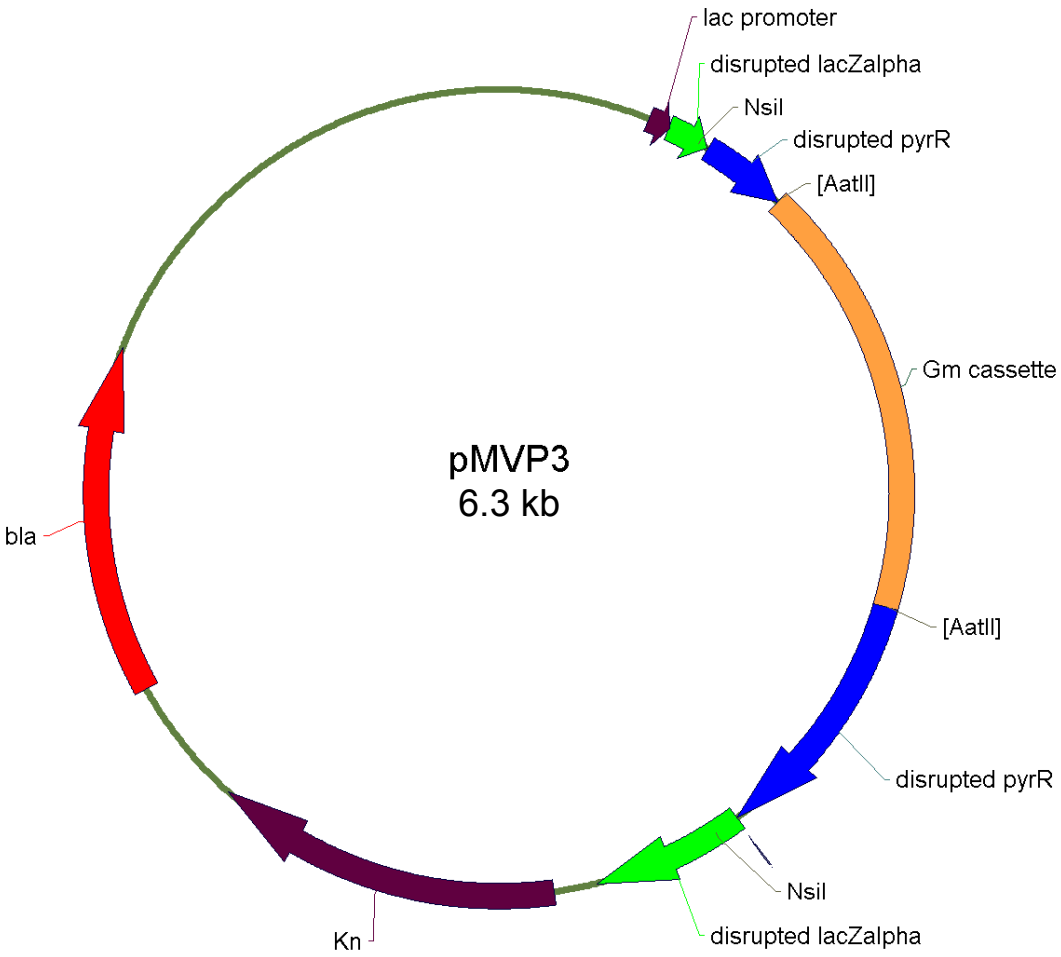

Fig. 14. Construction of pMVP3, derived from pMVP1. The resulting 6.3 kb plasmid contains a 1.6 kb gentamicin (Gm) cassette fragment, digested from pGmΩ1 (Schweizer, 1993), cloned into the *Aat*II restriction site of the *pyrR* gene. Expression of the *pyrR* gene is inactivated by the insertion of the Gm cassette.

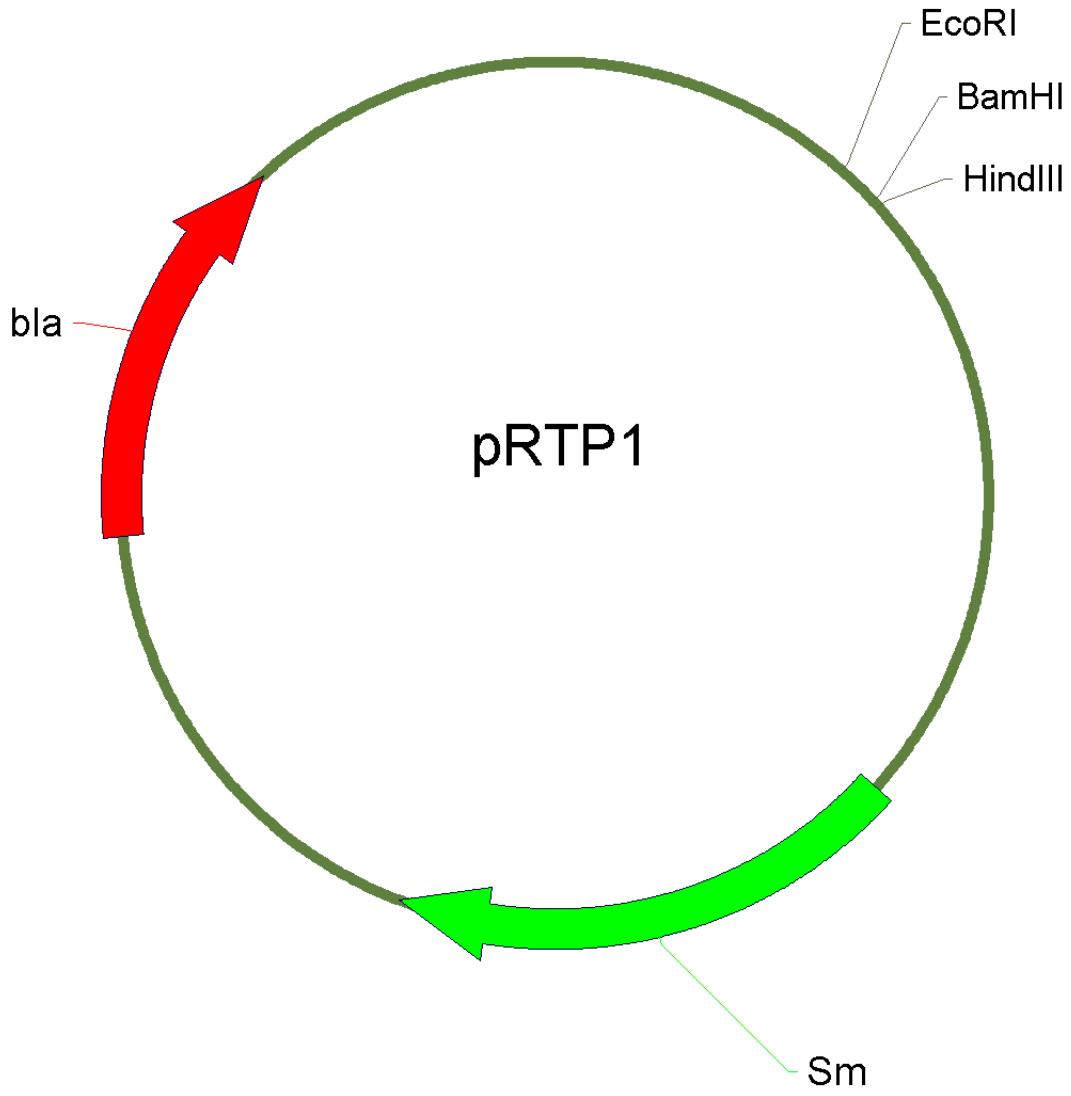

Fig. 15. Schematic diagram of the conjugation vector, pRTP1 (Stibitz *et al*., 1986). Sm corresponds to streptomycin sensitivity and *bla* corresponds to *β*-lactamase conferring ampicillin resistance.

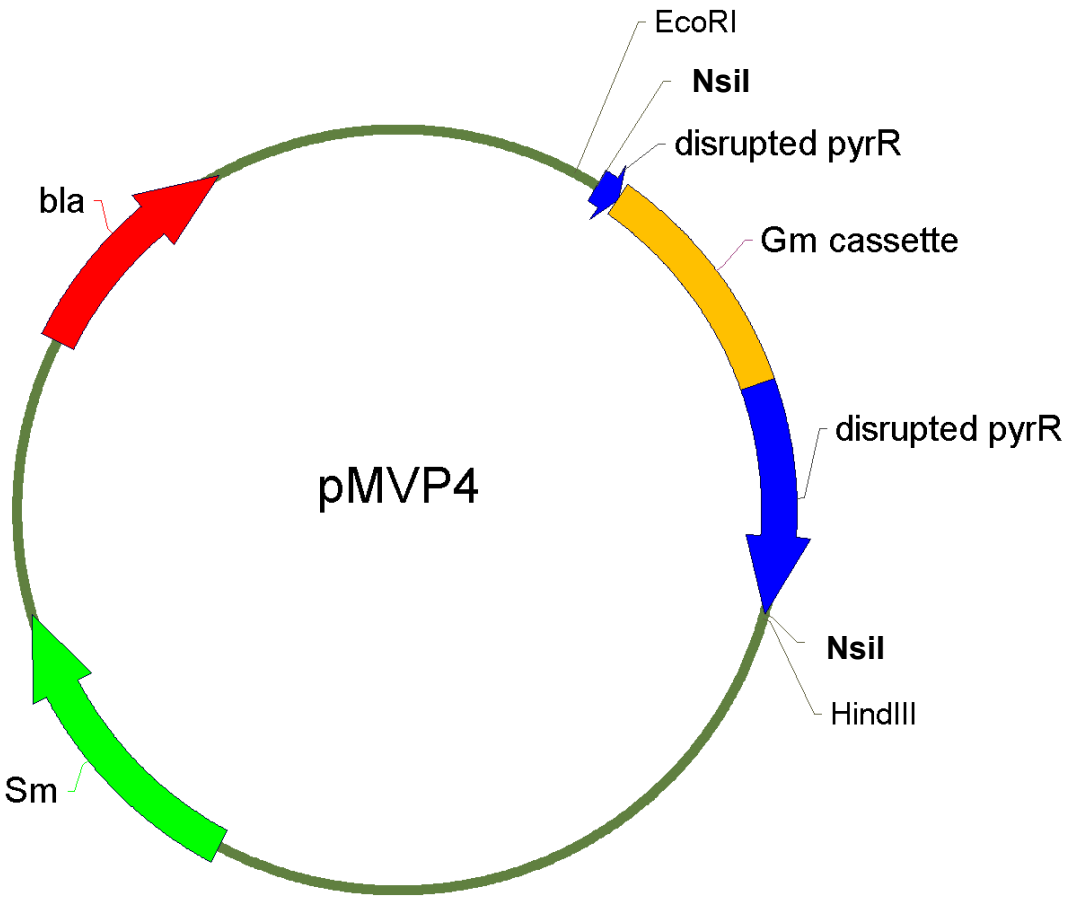

Fig. 16. Construction of pMVP4, derived from pMVP3. The ~2.4 kb *Nsi*I *pyrR*::Gm fragment from pMVP3 was treated with T4 DNA polymerase and blunt end ligated into the conjugation vector, pRTP1 digested with *Bam*HI and blunt-ended (Stibitz *et al*., 1986). Sm corresponds to streptomycin sensitivity and *bla* corresponds to *β*-lactamase conferring ampicillin resistance.

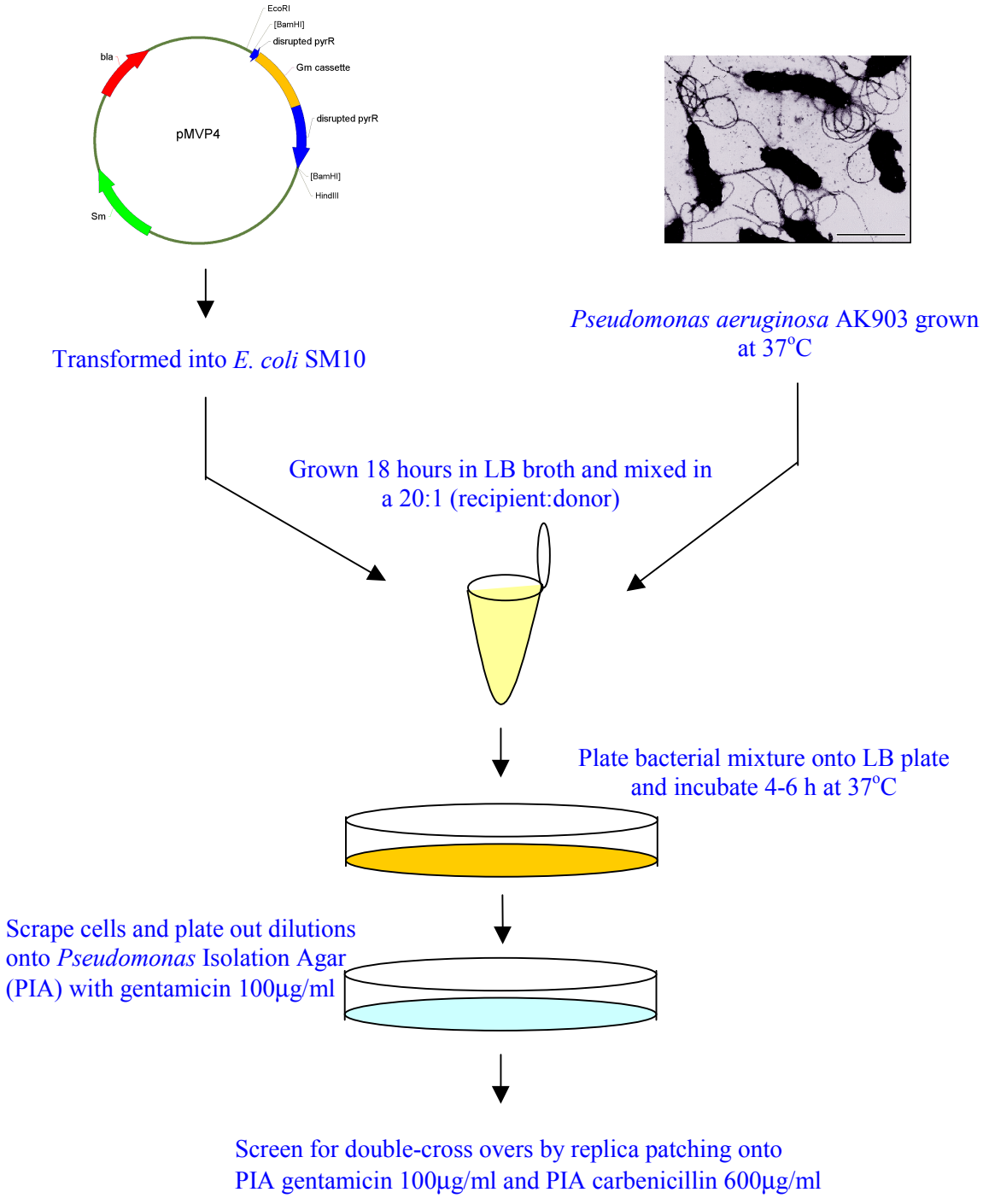

Fig. 17. Diagrammatic representation of the biparental mating procedure.

0.002% B1 (thiamine), was transferred to the same microcentrifuge tube and centrifuged at 12,000 ***g*** for 1 min to pellet the cells. The supernatant was removed and the cells were vortexed, to thoroughly mix the recipient cells with the donor cells. The mixed cells were then plated onto LB medium that had been pre-warmed at 37°C, and then incubated at 37°C for a further 4-6 h. After incubation, 2 ml of sterile 1X PBS (pH 7.3) were added to the plate, the cells were scraped using a sterile glass hockey stick and transferred into a sterile 15 ml conical tube. Serial dilutions of the cells were plated onto PIA+gentamicin and incubated at 37°C overnight to select for single-crossover events. The gentamicin resistant colonies that appeared after overnight incubation were replica plated onto PIA+gentamicin and PIA+carbenicillin to select for double-crossover events. The transconjugants that were gentamicin resistant (Gm^R) and carbenicillin sensitive (Cb^S) had lost the vector sequence conferring the Cb^R allele, and had therefore undergone a double crossover event.

Cloning of the *upp* gene.

A 940 bp DNA fragment containing the *upp* gene was amplified from *P. aeruginosa* chromosomal DNA by PCR (Saiki *et al*., 1988) with two synthetic oligonucleotides: oligo-1 (5'-TCGTTGTTGAACAGGCAGTC-3') and oligo-2 (5'-AAGGCGACGAACAGCATCT-3'). The *upp* gene product was amplified using *Taq* polymerase, which created 3'-T overhangs, enabling direct ligation of the PCR product into the pCR®II vector from The Original TA Cloning® Kit (Fig. 10., Invitrogen). After transformation into *E. coli* DH5α, clones containing the *upp* insert were selected on

LB+kanamycin, with IPTG at 0.03% and X-gal at 0.003%. Restriction enzyme digests determined the orientation of the *upp* inserts. The resulting clone, pMVP5 (Fig. 18) had the *upp* gene inserted in the correct orientation and pMVP6 (Fig. 19) had the *upp* gene inserted in the opposite orientation to the *lac* promoter on the vector.

RNA isolation.

The procedure for RNA preparation was essentially the same as that described by Park *et al*. (1997). *P. aeruginosa* PAO1 was grown in minimal medium to an OD_{600} of 0.4 - 0.5. A 30 ml portion of the culture was transferred to a pre-chilled centrifuge tube, and the chilled cultured was centrifuged at 30,000 ***g*** at 4°C for 15 min. The cell pellet was resuspended in 3 ml of a solution containing 0.02 M sodium acetate (pH 5.2), 1 mM EDTA, and 0.2% diethylpyrocarbonate (DEPC), and then sodium dodecyl sulfate (SDS) was added to a final concentration of 0.5% (w/v). An equal volume of phenol was added to the cell extract, vortexed for 30 s and then incubated at 65°C for 5 min with gentle shaking. The mixture was then centrifuged at 30,000 ***g*** at room temperature for 15 min and the aqueous phase (top layer) was transferred to a fresh conical tube. An equal volume of phenol:chloroform (1:1) was added, the mixture was vortexed briefly and centrifuged at 30,000 ***g*** at room temperature for 15 min. The aqueous phase was transferred to a sterile, siliconized 25 ml Corex® centrifuge tube, three volumes of ice-cold 100% ethanol was added and the mixture was incubated at -80°C overnight (or 30

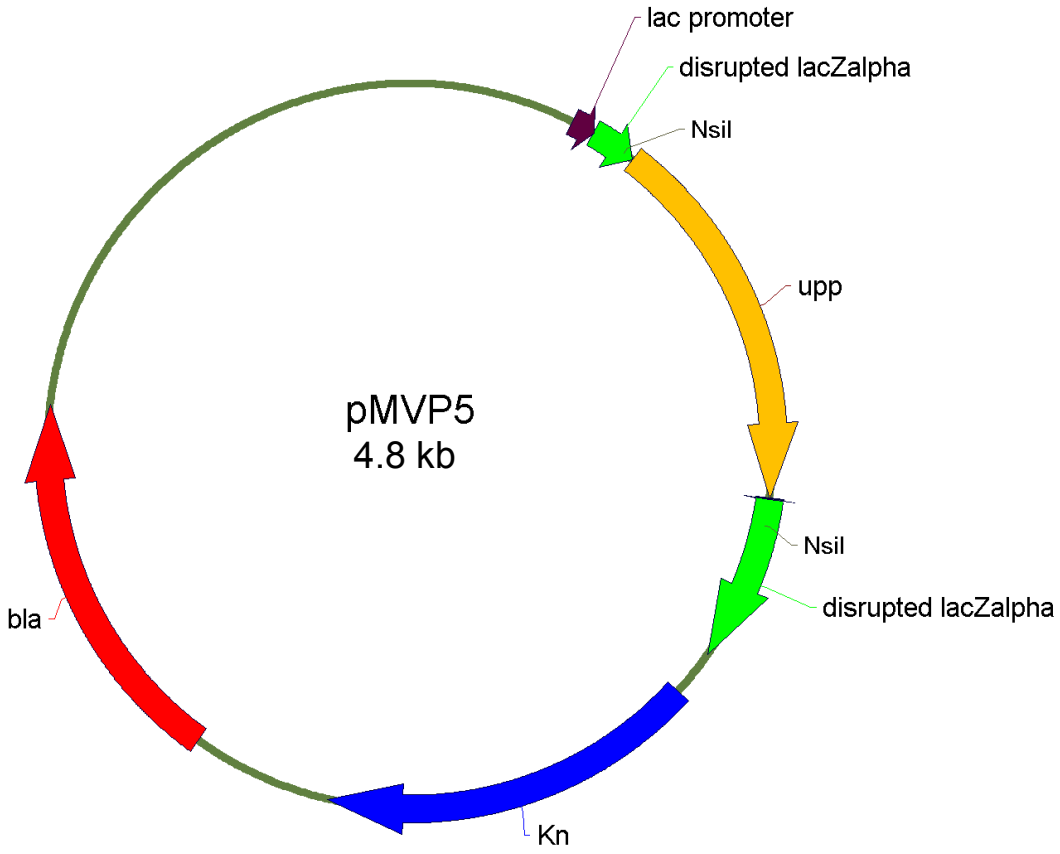

Fig. 18. Construction of pMVP5 derived from pCRII vector (Invitrogen). The resulting 4.8 kb plasmid includes a 900 bp fragment containing the *P. aeruginosa upp* gene, cloned in the same orientation as the *lac* promoter.

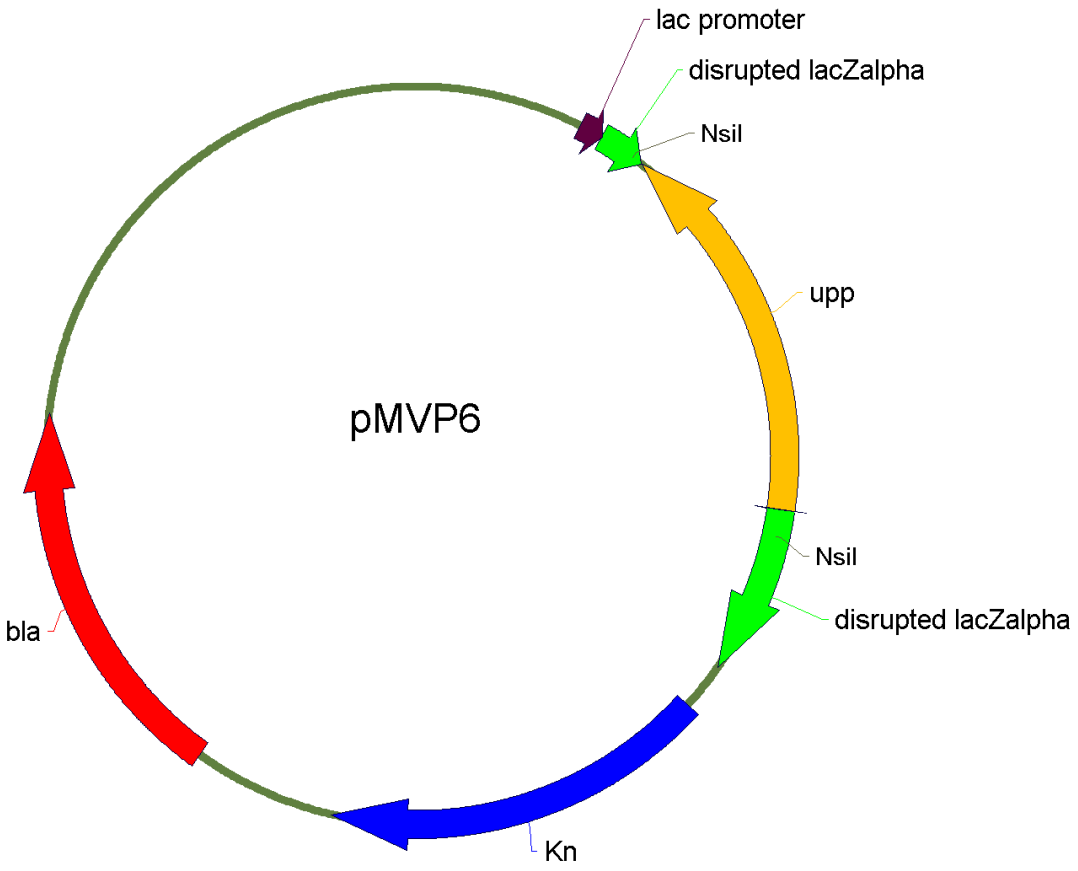

Fig. 19. Construction of pMVP6 derived from pCRII vector (Invitrogen). The resulting 4.8 kb plasmid includes a 900 bp fragment containing the *P. aeruginosa upp* gene, cloned in the opposite orientation to the *lac* promoter.

min if time was restricted). The RNA precipitate was collected by centrifugation at 14,000 ***g*** at 4°C for 30 min, the RNA pellet was resuspended in 300 µl of DEPC-treated TE buffer composed of 10 mM Tris and 1 mM EDTA (pH 8.0). The RNA was extracted three times with an equal volume of phenol, phenol:chloroform and then chloroform, centrifuging at 12,000 ***g*** at 4°C for 15 min between each extraction. The RNA was precipitated with the addition of one tenth volume of 3M sodium acetate (pH 5.2), two volumes of 100% ethanol and centrifuging at 12,000 ***g*** at 4°C for 15 min. The pellet was washed with 1 ml of 70% ethanol followed by 90% ethanol and allowed to air dry. The dried RNA pellet was resuspended in 100 µl of DEPC-treated water. The RNA was visualized by formaldehyde agarose gel electrophoresis (Fig. 20) and was quantified by absorbance spectroscopy at 260 nm.

End labeling of nucleic acid probe.

End-lableled oligonucleotides were used for primer extension analysis and end-labeled PCR products were used for gel mobility shift assays. The end-labeling reaction was prepared in a microcentrifuge tube and contained 120-150 ng of DNA, 50 µCi of γ-^{32}P-ATP, 1X polynucleotide kinase reaction buffer, 10 units of T4 polynucleotide kinase in ddH_2O (or DEPC treated ddH_2O for probes to be used in primer extension analysis). The reaction was incubated at 37°C for 1 h. A 1 µl aloiquot of the reaction was transferred to a sterile microcentrifuge tube for scintillation counts before purifying the probe. The unincorporated nucleoside triphosphates were removed from the remainder of

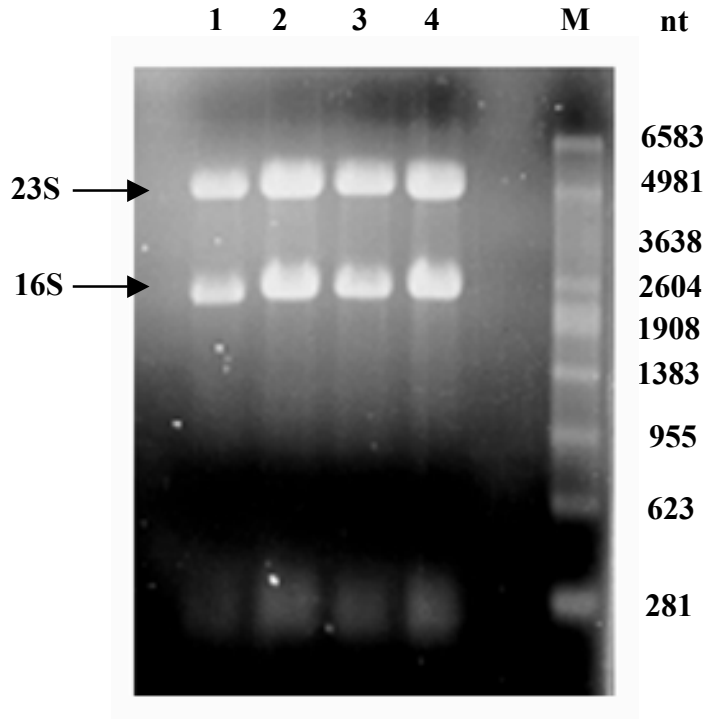

Fig. 20. Analysis of *P. aeruginosa* total RNA preparation by formaldehyde agarose gel electrophoresis. Lanes: 1, 8 µg RNA isolated from cells grown in *Pseudomonas* minimal medium (Psmm); 2, 8 µg RNA isolated from cells grown in Psmm and 2 mM uracil; 3, 10 µg RNA isolated from cells grown in Psmm and 1 mM orotate; 4, 10 µg RNA isolated from cells grown in Psmm, 2 mM uracil and 1 mM orotate; M, RNA marker (Promega).

the reaction using a *TE Micro* SELECT-D, G-25 spin column (5 Prime → 3 Prime, Inc.). The spin column was placed in a collection tube and centrifuged at 12,000 ***g*** for 20 seconds to remove the TE storage buffer. The column was transferred to a fresh collection tube, the labeling reaction was applied directly to the center of the gel bed and allowed to sit undisturbed for 1 min and then centrifuged at 12,000 ***g*** for 20 seconds. The labeled nucleic acid was recovered in the collection tube in approximately 20 µl of TE buffer. A 1 µl aliquot of the purified probe was transferred to a sterile microcentrifuge tube and the counts per min (cpm) per microliter before and after column purification were determined using a scintillation counter. The percent of radioisotope incorporated was calculated by dividing the cpm-after by the cpm-before and multiplying by 100. According to manufacturer's specifications, greater than 60% incorporation is acceptable.

Primer hybridization and extension.

Primer extension analysis was used to identify the transcriptional start sites of *pyrR* and *pyrBC'*. The technique involves hybridizing a radiolabeled oligonucleotide probe derived entirely from within the gene of interest, to complementary RNA, and extending it using reverse transcriptase. The hybridization reaction was prepared in a PCR tube. Twenty micrograms of total RNA were mixed with 3 µl of freshly mixed 10X hybridization buffer (0.2 M Tris, pH 8.0, 1 M NaCl, 1 mM EDTA) and 5 x 10^5 cpm of radiolabeled primer. DEPC-treated water was added to a final volume of 30 µl. The annealing reaction was performed between 95°C and 60°C with 3.5°C steps over 2 h in a

thermal cycler. The salts were removed from the reaction mixture by ethanol precipitation. The purified pellet was resuspended in 25 µl of reverse transcriptase reaction mixture containing 3.5 µl of 4 mM dNTPs, 5 µl of 5X reverse transcriptase reaction buffer, 1 µl of actinomycin D (1 mg ml^{-1}), 50 units of RNasin, 10 units of AMV reverse transcriptase in 13.25 µl of DEPC-treated ddH_2O. Actinomycin D was included to prevent self-copying of the primer by reverse transcriptase. The hybridization and extension reaction was performed at 42°C for 1 h and 30 min. The extension reaction was terminated by addition of EDTA at 20 mM and RNase at 0.4 mg ml^{-1} and further incubated at 37°C for 30 min. The DNA strand was recovered by two extractions with phenol:chloroform, a chloroform extraction and ethanol precipitation. The nucleic acid pellet was resuspended in 4 µl of ddH_2O and 4 µl of sequencing loading dye (U.S. Biochemicals Corp.), the sample was electrophoresed on a denaturing 4% acrylamide 7 M urea sequencing gel alongside a sequencing ladder from the same primer, and visualized by autoradiography.

***In vitro* expression of PyrR.**

The *P. aeruginosa* PyrR protein was expressed using an *E. coli* S30 Extract System for Circular DNA (Promega) which simplifies the transcription/translation of DNA sequences cloned into plasmid vectors. This technique allows for the identification and characterization of polypeptides based on the method described by Zubay (1973). One microgram of pMVP1 plasmid DNA purified with the spin-midi kit (Bio 101) was used as the DNA template and mixed with 5 µl of Amino Acid Mixture Minus

Methionine, 20 µl of S30 Premix Without Amino Acids, 15 µCi of [^{35}S] methionine (NEN Dupont) and 15 µl of S30 Circular Extract. Nuclease-free water was added to a final volume of 50 µl, the components were mixed by gentle vortexing and then centrifuged at 12,000 ***g*** for 5 s to bring the reaction mixture to the bottom of the tube. The reaction was incubated at 37°C for 2 h and then terminated by placing the tube on ice for 5 min. A 5 µl aliquot of the reaction mixture was transferred to a fresh tube and concentrated by acetone precipitation to remove the polyethyleneglycol (PEG) from the extract. To accomplish this, 20 µl of acetone was added to the 5 µl reaction mixture, placed on ice for 15 min and centrifuged at 12,000 ***g*** at 4°C for 5 min. The supernatant was aspirated and the pellet was dried for 15 min under vacuum and resuspended in 10 µl ddH_2O. The expressed protein was analyzed by sodium dodecyl sulfate polyacrylamide gel electrophoresis (SDS-PAGE) and visualized by autoradiography.

Sodium dodecyl sulfate polyacrylamide gel electrophoresis (SDS-PAGE).

SDS-PAGE is a rapid method routinely used to quantify, compare and characterize proteins. This method denatures proteins into their individual subunits and separates them based primarily on their molecular weights (Laemmli, 1970). The SDS binds along the polypeptide chain, masking the overall charge making the reduced SDS-protein complex proportional to its molecular weight. Samples were electrophoresed on a 15% SDS polyacrylamide separating gel with a 5% stacking gel using a Mini-Protean II electrophoresis apparatus (Bio-Rad). The 15% separating gel was prepared by mixing 5 ml of acrylamide stock solution A (30% w/v acrylamide and 0.8% w/v *N'N'*-bis-

methylene-acrylamide in ddH_2O), 2.5 ml of denaturing solution B (1.5 M Tris-HCl, pH 8.8, 0.4% w/v SDS in ddH_2O) and 2.5 ml of ddH_2O. Twenty milligrams of ammonium persulfate was added and dissolved in the gel solution by gentle vortexing. Just prior to casting, 5 µl of *N,N,N',N'*-tetramethylene-ethylenediamine (TEMED) was added, and mixed into the solution by gentle inversion. The gel was cast immediately, leaving a 2 cm gap at the top for the stacking gel. *N*-butanol was layered above the gel to prevent drying and to ensure a flat surface for the separating gel/stacking gel interface. The gel was allowed to polymerize at room temperature for 1 h. After polymerization, the *N*-butanol layer was washed off with ddH_2O and the stacking gel was cast. The 5% stacking gel was prepared by mixing 0.67 ml of solution A, 1 ml of denaturing solution C (0.5 M Tris-HCl, pH 6.8. 0.4% w/v SDS), 2.3 ml of ddH_2O, 10 mg of ammonium sulfate and finally 5 µl of TEMED. Immediately after casting, the gel comb was inserted to form the loading wells and the gel was allowed to polymerize at room temperature for 1 h. The gel was placed in a Mini Protean II electrophoresis tank and filled with denaturing electrophoresis running buffer (25 mM Tris, 192 mM glycine and 0.1% w/v SDS, pH 8.3). The samples were prepared by mixing four parts of protein sample with 1 part of 5X SDS sample buffer (60 mM Tris-HCl, pH 6.8, 25% glycerol v/v, 2% SDS w/v, 14.4 mM β-mercaptoethanol, and 0.1% w/v bromophenol blue) in a sterile microcentrifuge tube. Pre-stained broad range markers were used as standards (Bio-Rad). The samples and the standards were boiled for 2 min, cooled, loaded onto the gel and electrophoresed for 1 h 15 min at 150 V. The proteins were stained with Coomassie Blue staining solution (45% methanol (v/v), 10% glacial acetic acid (v/v), 0.1% Coomassie Brilliant Blue R-250 (w/v)

in ddH_2O) for 20 min with gentle rocking. The gel was then rinsed with ddH_2O and destained with 10% methanol (v/v), 10% glacial acetic acid (v/v) in ddH_2O overnight in a sealed container. The molecular masses of the proteins markers were: myosin, 209 kDa; β-galactosidase, 124 kDa; BSA, 80 kDa; ovalbumin, 49.1 kDa, carbonic anhydrase, 34.8 kDa, soybean trypsin inhibitor, 28.9 kDa, lysozyme, 20.6 kDa and aprotinin, 7.1 kDa.

Construction of the *pyrR*::*lacZ* transcriptional fusion.

A 320 bp DNA fragment incorporating the *pyrR* promoter region was amplified from pUC41 (Vickrey, 1993) by PCR (Saiki *et al*., 1988) with two synthetic oligonucleotides containing engineered enzyme restriction sites at the 5' end: oligo-1 (5'-CGCGGATCCAACGGCCGTTTCAACC-3') has a *Bam*HI site and oligo-2 (5'-CCCAAGCTTGAGTTCGGCGGGATTG-3') has a *Hin*dIII site. The PCR product was purified from an agarose gel, digested with *Bam*HI and *Hin*dIII, and ligated into the *Bam*HI/*Hin*dIII sites of the broad-host-range *lacZ* transcriptional fusion vector, pQF50 (Farinha & Kropinski, 1990a) which contains a promoter-less *lacZ* gene (Fig. 21). After transformation into *E. coli* DH5α, *lacZ*-positive clones were selected on LB+ampicillin, IPTG at 0.03% and X-gal at 0.003%. The resultant plasmid, pMVP50 (Fig. 22), was confirmed by restriction enzyme digests.

Construction of *pyrR*::*lacZ* translational fusion.

A 310 bp DNA fragment containing the *pyrR* translational start (MSLP) and

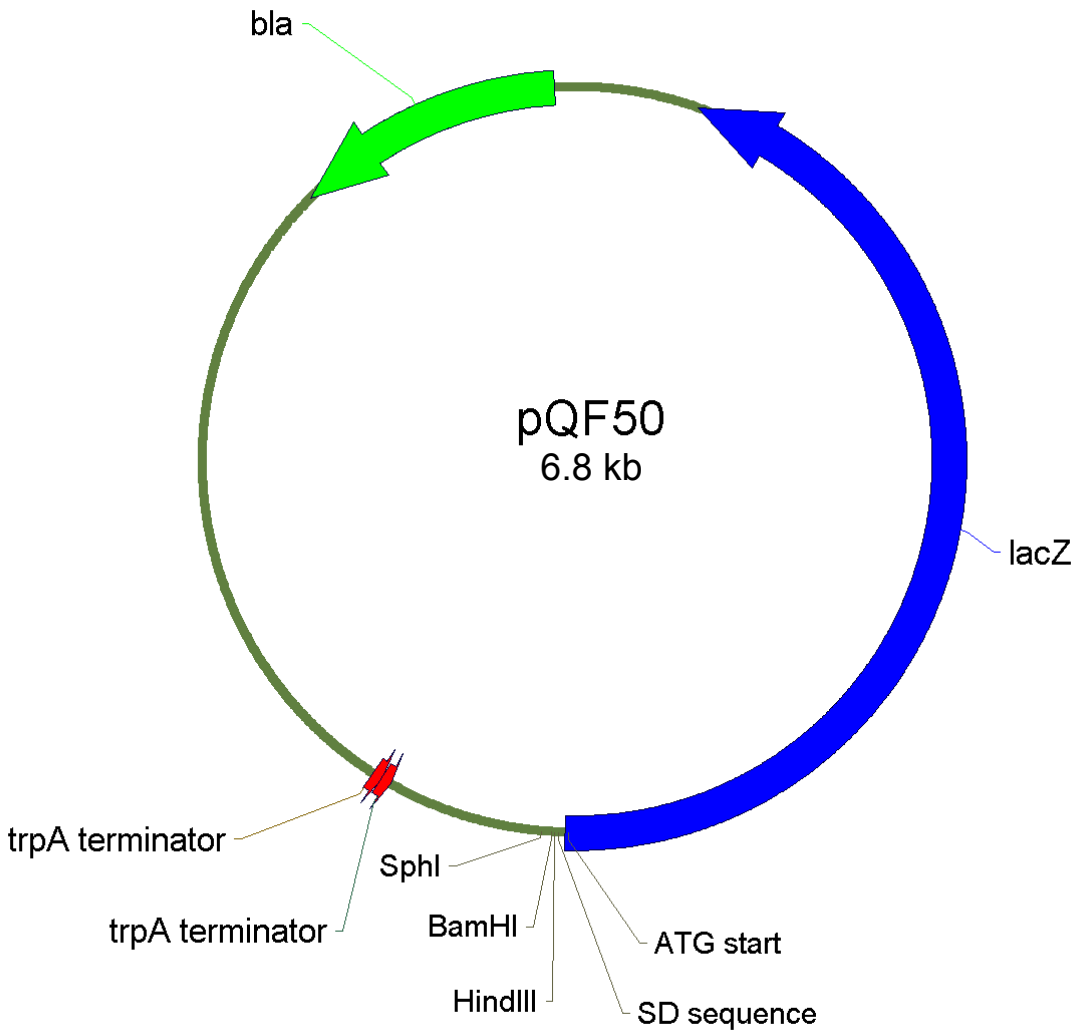

Fig. 21. Schematic diagram of the broad-host-range plasmid pQF50 (Farinha & Kropinski, 1990a), which utilizes the promoterless *lacZ* gene derived from pCB267 (Schneider & Beck, 1986). Two artificial *trpA* terminators are inserted in tandem upstream of the multiple cloning site, to prevent read through transcription from the *bla* promoter.

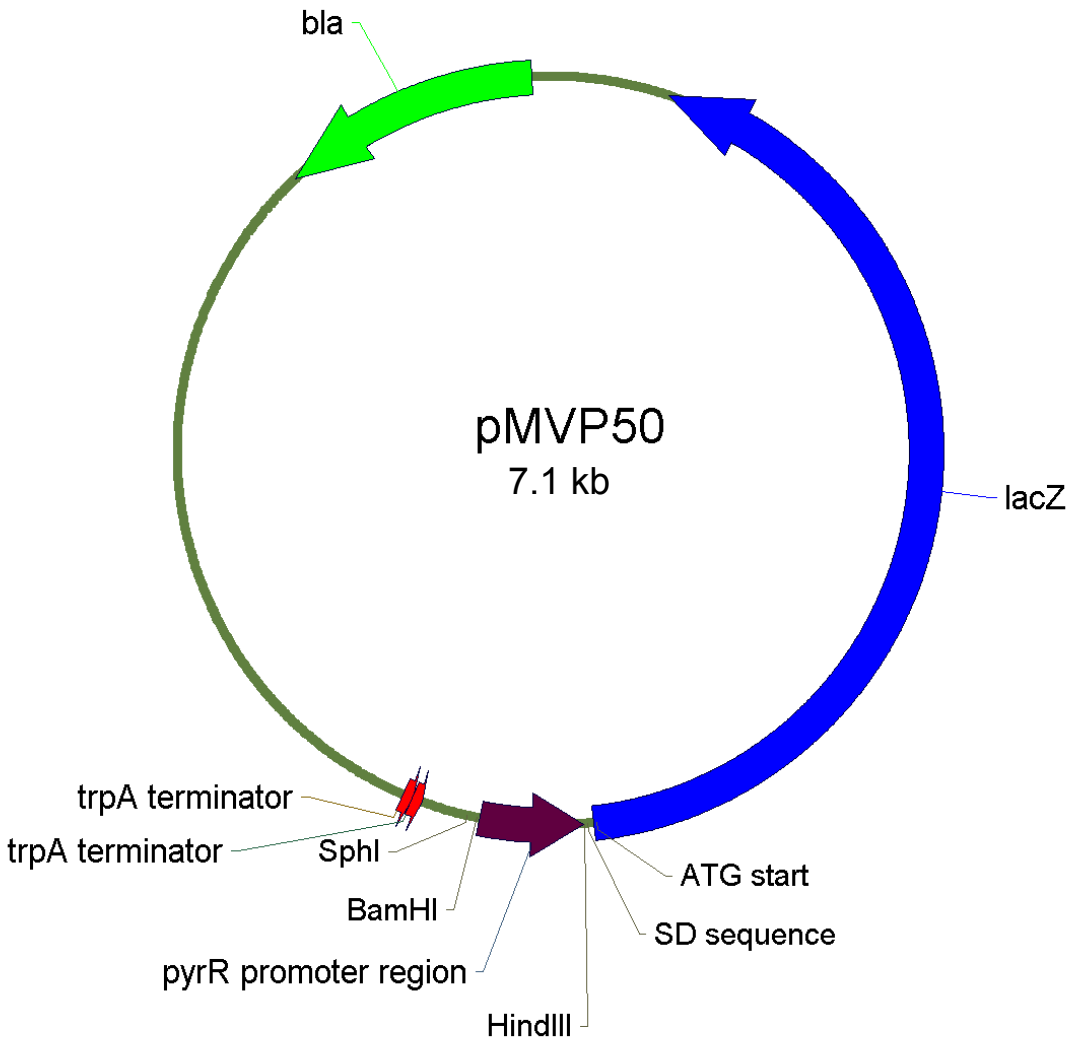

Fig. 22. Construction of pMVP50, *pyrR*::*lacZ* transcriptional fusion, derived from pQF50 (Farinha & Kropinski, 1990a). A 300 bp fragment containing the *P. aeruginosa* *pyrR* promoter region was inserted into the *Bam*HI-*Hin*dIII sites of pQF50.

upstream promoter region was amplified from pUC41 (Vickrey, 1993) by PCR (Saiki *et al*., 1988) with two synthetic oligonucleotides designed to generate *Hin*dIII and *Sma*I restriction sites at the 5' ends of oligo-1 and 2 respectively: oligo-1 (5'-CCCCCCCAAGCTTAAC GGCCGTTTCAACCT-3') and oligo-2 (5'-TCCTCCTCCCCCGGGATTGGGTAGGCT CAT-3'). The amplified PCR product was agarose purified, digested with *Hin*dIII and *Sma*I and, ligated into *Hin*dIII-*Sma*I-cleaved pQF52 (Fig. 23., Park *et al*., 1997). After transformation into *E. coli* DH5α, the resultant plasmid, pMVP52 (Fig. 24), was selected on LB+ampicillin, 0.3% IPTG and 0.003% X-gal.

Electroporation.

The *lacZ* fusion plasmids were electroporated into *P. aeruginosa* by the method of Farinha & Kropinski (1990b). Logarithmically growing cells of OD_{600} ~0.5 were used to make electrocompetent cells. One milliliter of culture was centrifuged 12,000 *g* for 3-5 min, the supernatant was discarded and the cells were washed with 1 ml of MOPS buffer (1 mM of MOPS, 15% glycerol,v/v) for a total of 10 washes. After the final wash, the cells were resuspended in 50 µl of MOPS buffer. The 50 µl of electrocompetent cells were mixed with ~500 ng of plasmid (1-5 µl) and pipetted into an electroporation cuvette (0.1 cm gap). The plasmid DNA was electroporated into the host cells using the Gene Pulser II System (Bio-Rad), set at the following parameters: resistance at 400 Ω; capacitance at 25 µF, and voltage at 2.5 kV. After applying the electrical pulse, 1 ml of

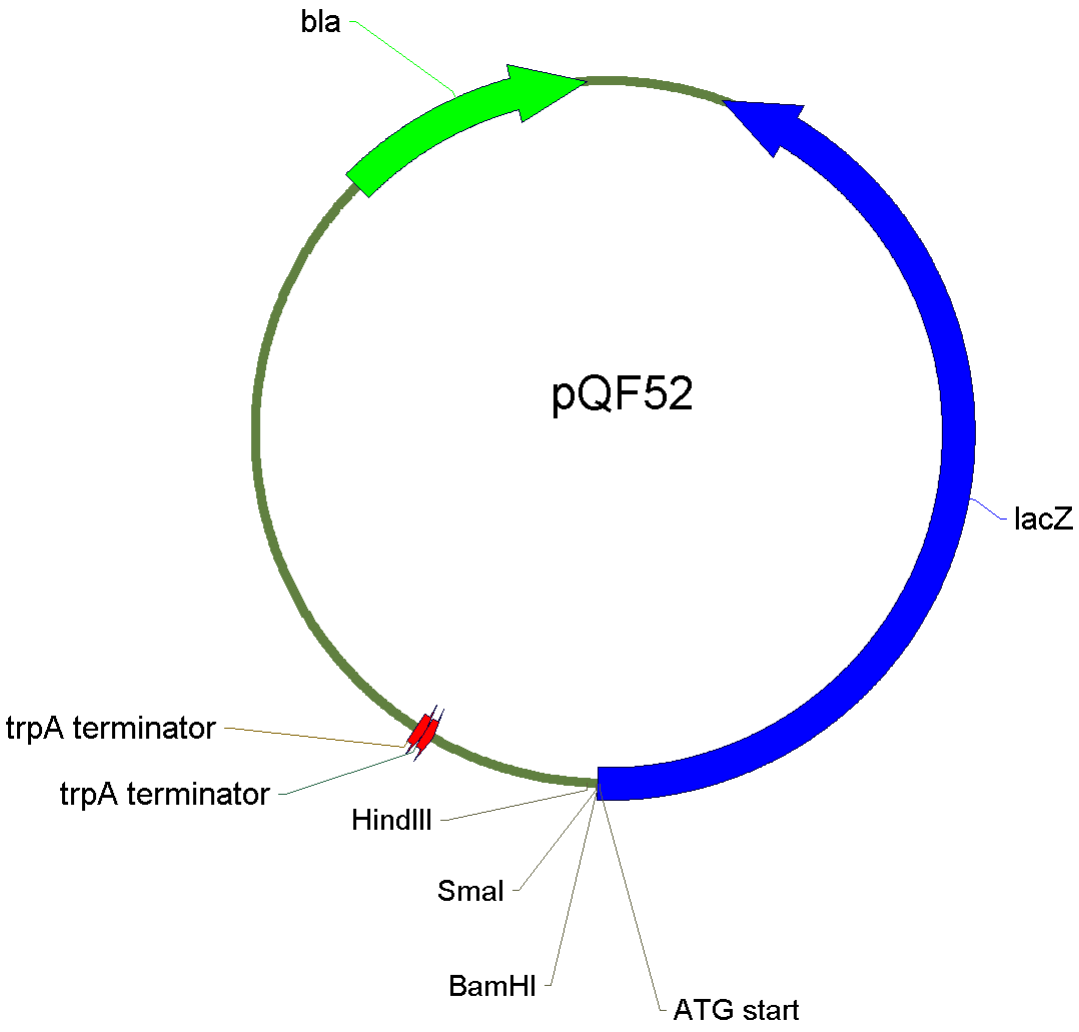

Fig. 23. Schematic diagram of the *lacZ* translational fusion vector, pQF52 (Park *et al*., 1997), derived from pQF50 (Farinha & Kropinski, 1990a). The *lacZ* gene is cloned in the opposite orientation to that of the *bla* gene to eliminate basal level expression of *β*-galactosidase.

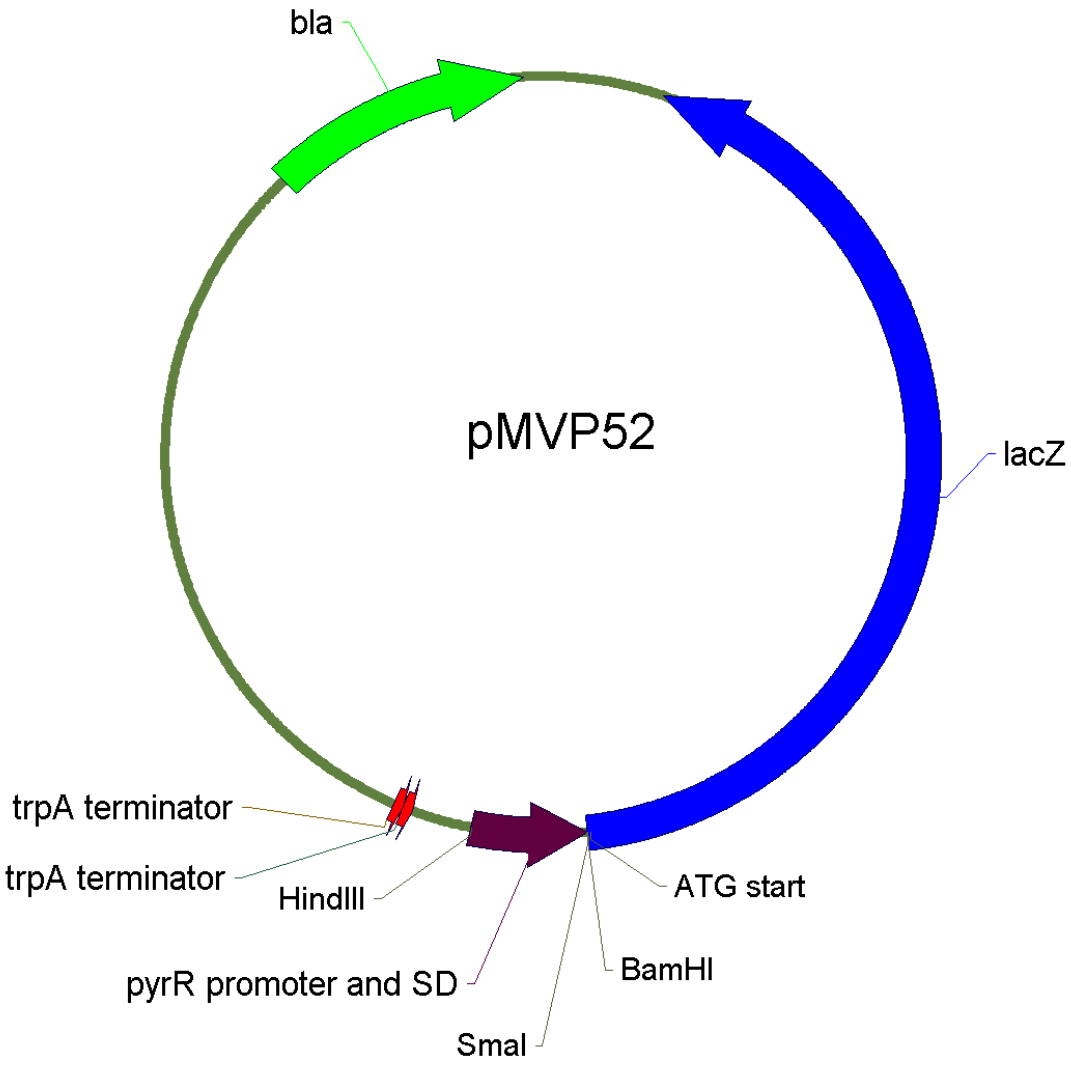

Fig. 24. Construction of pMVP52, *pyrR*::*lacZ* translational fusion, derived from pQF52 (Park *et al*., 1997). A ~310 bp fragment containing the *P. aeruginosa pyrR* promoter region, Shine-Dalgarno sequence and the sequence of the first 4 amino acids of the *pyrR* gene was inserted into the *Hin*dIII-*Sma*I sites of pQF52.

LB broth was added to the cuvette and the cells were incubated at 37°C for 1 h with shaking. The cells harboring the fusion plasmid were selected on LB+carbenicillin.

β-Galactosidase assay.

β-galactosidase specific activity was determined by the method of Miller (1972). Logarithmically (OD_{600} ~0.6) growing cultures were cooled by placing on ice for 20 min to prevent further growth, and the OD_{600} was measured and recorded. High level β-galactosidase activity was assayed by adding 0.1 ml of the culture to 0.9 ml of Z buffer, pH 7.0 (60 mM $Na_2HPO_4 \cdot 7H_2O$, 40 mM $NaH_2PO_4 \cdot H_2O$, 10 mM KCl, 1 mM $MgSO_4 \cdot 7H_2O$, 50 mM β-mercaptoethanol). The cells were lysed by the addition of 2 drops of chloroform, 1 drop of a 0.1% SDS solution, and vortexing for 10 seconds. The lysed cells were incubated at 28°C for 5 min. The reaction was initiated by the addition of 200 µl of *o*-nitrophenol-β-galactoside (ONPG)(4 mg ml^{-1} ONPG in Z buffer, pH 7.0), and vortexed briefly. The reaction tubes were assayed for 15 min at 28°C, and the color reaction was stopped by the addition of 0.5 ml of 1 M Na_2CO_3. The A_{420} units were measured using a control tube, containing all reaction components except cells, to blank the spectrophotometer. The A_{550} units were also measured to correct for light scattering due to cell debris. The specific activity of β-galactosidase was calculated as follows:

$$\frac{1000 \times (A_{420} - 1.75 \times A_{550})}{t \times v \times OD_{600}} = \text{units of } \beta\text{-galactosidase}$$

where t = the time of the reaction (min), and v = the volume of culture per reaction (ml). One unit of β-galactosidase hydrolyzes 1 nmol ONPG min^{-1} (mg protein)$^{-1}$.

Expression of *pyrR*.

A 510 bp DNA fragment of the intact *pyrR* gene was amplified from pMVP1 by PCR with two synthetic oligonucleotides designed to generate *Bam*HI and *Eco*RI restriction sites at the 5' ends: oligo-1 (5'-CGCGGATTCCTACCCAATCCCGCC-3') and oligo-2 (5'-CCGGAATTCAGGAAGCGGAGGAAAG-3'). The PCR product was agarose purified, digested with *Bam*HI and *Eco*RI, and ligated into the *Bam*HI/*Eco*RI sites of the pGEX-2T gene fusion vector (Fig. 25., Amersham Pharmacia Biotech). The resulting plasmid, pMVP10 (Fig. 26), was sequenced to confirm that the GST::PyrR fusion was translated in-frame. The pGEX-2T vector features a *tac* promoter for inducible, high-level expression of fusion proteins with glutathione S-transferase (GST) (Smith & Johnson, 1988). The GST gene isolated from *Schistosoma japonicum* contains an ATG start and ribosome-binding site. The resulting fusion protein is be purified by affinity chromatography using the GST purification system from Amersham Pharmacia Biotech.

Purification of the PyrR protein.

A culture of *E.coli* BL21 harboring pMVP10 was grown in LB+ampicillin (4 liters) to an OD_{600} ~ 0.8. Fusion protein expression was induced with the addition of IPTG at 0.1 mM. The culture was incubated for an additonal 4 h at 37°C with shaking. The cells were harvested by centrifugation at 10,000 ***g*** at 4°C for 45 min, and the cell pellet was resuspended in 200 ml of cold phosphate buffered saline (1X PBS), containing 137 mM NaCl, 2.7 mM KCl, 4.3 mM $Na_2HPO_4.7H_2O$ and 1.4 mM KH_2PO_4, pH 7.3. The cells were broken by passage through a French pressure cell (Aminco) at 20,000 lb psi.

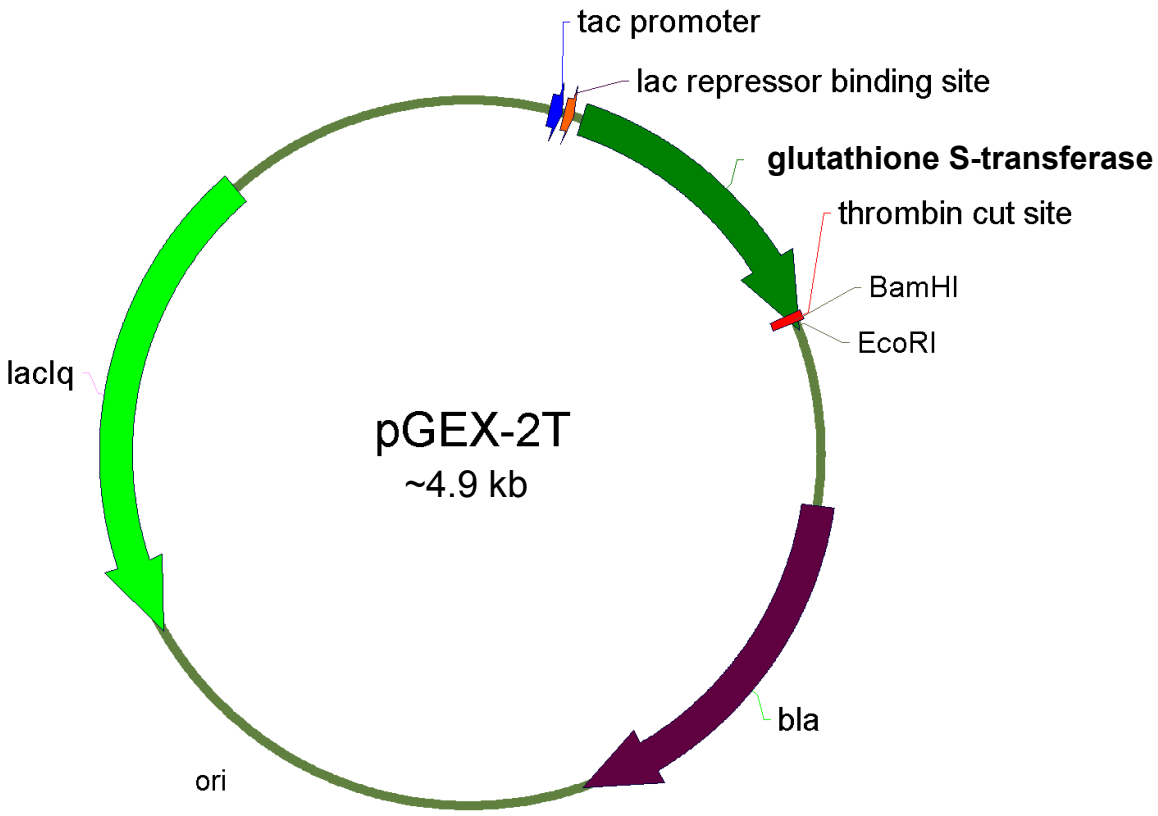

Fig. 25. Schematic diagram of pGEX-2T, glutathione S-transferase fusion vector (Smith & Johnson, 1988, Amersham Pharmacia Biotech.), an expression vector for inducible, high-level intracellular expression of genes as fusions with GST, which are then purified by affinity chromatography.

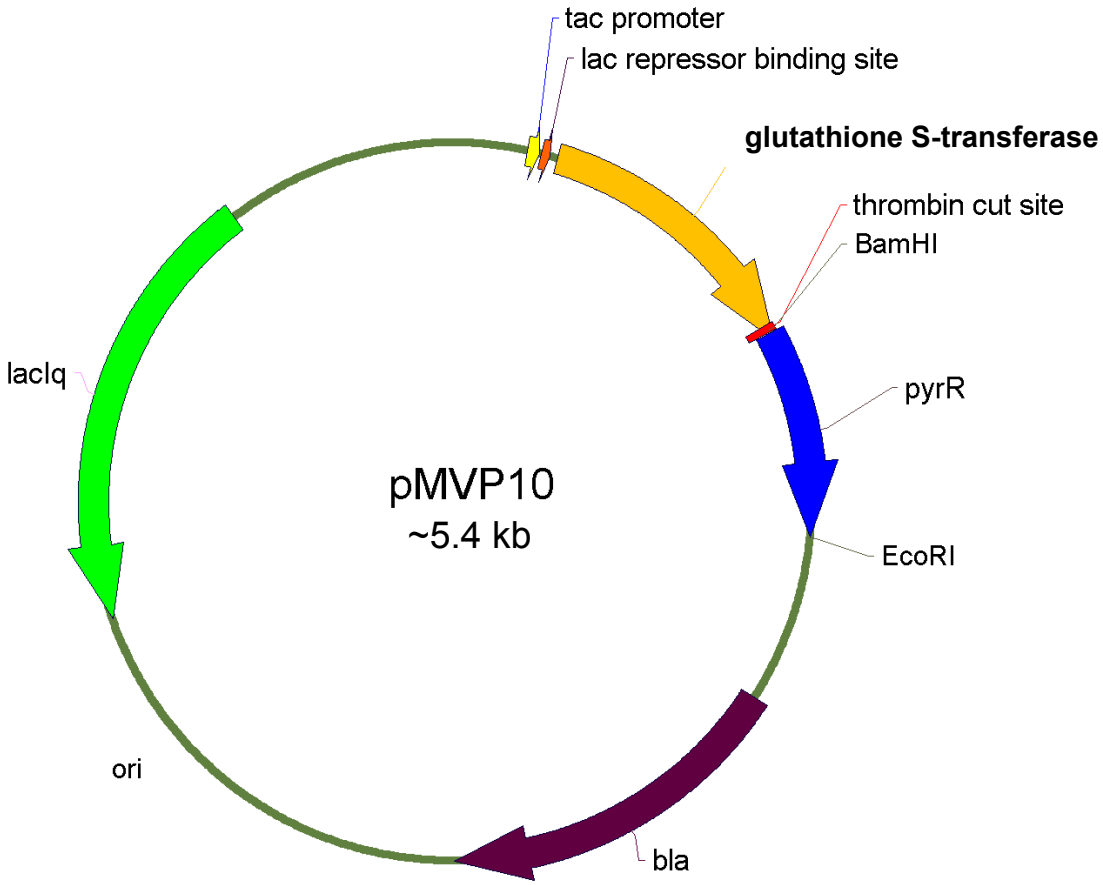

Fig. 26. Construction of pMVP10 derived from pGEX-2T (Smith & Johnson, 1988; Amersham Pharmacia Biotech.). Plasmid pMVP10 has a ~510 bp fragment containing an intact *pyrR* gene inserted into the *Bam*HI-*Eco*RI sites of the expression vector, pGEX-2T. The glutathione S-transferase::*pyrR* gene fusion is expressed from the *tac* promoter.

The crude extract was treated with DNase at 37 μg ml^{-1}, Triton X-100 at 0.1%, dithiothreitol (DTT) at 5 mM and incubated at 4°C overnight with gentle stirring. The crude extract was then centrifuged at 32,000 ***g*** for 30 min and the supernatant was subjected to ammonium sulfate fractionation. The fraction precipitating between 30 and 40% saturation was resuspended in 5 ml ice-cold 1X PBS, pH 7.3 and the lysate was dialyzed against the same buffer at 4°C overnight. The dialyzed solution was subjected to affinity chromatography using the Pharmacia glutathione sepharose 4B matrix. Batch purification was carried out as specified by the manufacturer. The GST:PyrR fusion protein was eluted from the matrix two times with 2 ml of 10 mM reduced glutathione. The eluted fractions that contained the GST:PyrR fusion were combined and dialyzed against 1X PBS (pH 7.3) overnight at 4°C. The dialyzed fusion sample was incubated with 100 units of thrombin protease overnight at 4°C, to cleave the PyrR protein from the GST tag. The cleaved sample was subjected to anion-exchange chromatography. A column was gravity packed with diethylaminoethyl (DEAE) Sepharose matrix (~ 1-2 ml bed volume), and washed with at least 3 column volumes of 1X PBS (pH7.3). The sample was loaded onto the column and the flow through was collected. The column was washed with 70 ml of 1X PBS (0 M NaCl fraction), and the GST tag eluted in this fraction. The column was again washed with 6 ml of 0.1 M NaCl to elute residual GST tag and other contaminating proteins. The PyrR protein was eluted with 3 ml of 0.2 M NaCl. All fractions were analyzed by SDS-15% PAGE. The fraction containing purified PyrR protein was dialyzed against PyrR buffer (100 mM Tris-acetate, pH 7.5, 10 mM

potassium acetate, 20% glycerol) at 4°C overnight. The purified protein (1 μg μl^{-1}) was separated into 100 μl aliquots, snap frozen in liquid nitrogen and stored at -80°C.

Expression of *upp*.

A 600 bp DNA fragment containing the intact *upp* gene was amplified from pMVP5 by PCR with two synthetic oligonucleotides designed to generate *Bam*HI and *Eco*RI restriction sites at the 5' ends: oligo-1 (5'-GCGGATCCCCCGTACATGAGATC-3') and oligo-2 (5'-CCGGAATTCAGGCTTCCTTCTGCTT-3'). The PCR product was agarose purified, digested with *Bam*HI and *Eco*RI, and ligated into the *Bam*HI/*Eco*RI sites of the pGEX-2T gene fusion vector (Fig. 25., Amersham Pharmacia Biotech). The resulting plasmid, pMVP11 (Fig. 27), was sequenced to confirm that the GST-Upp fusion was translated in-frame.

Purification of the Upp protein.

A culture of *E.coli* BL21 harboring pMVP11 was grown in LB+ampicillin (4 liters) to an OD_{600} ~ 0.8, fusion protein expression was induced with IPTG at 0.1 mM and the cells were incubated at 37°C with shaking for 4 h. The cell lysate was prepared as described previously for purification of the PyrR protein. The crude extract was subjected to ammonium sulfate fractionation. The fraction precipitating between 30 and 40% saturation was resuspended in 5 ml ice-cold 1X PBS, pH 7.3 and the lysate was dialyzed against the same buffer at 4°C overnight. The GST-Upp fusion protein was purified by affinity chromatography using the Pharmacia glutathione Sepharose 4B matrix. Batch

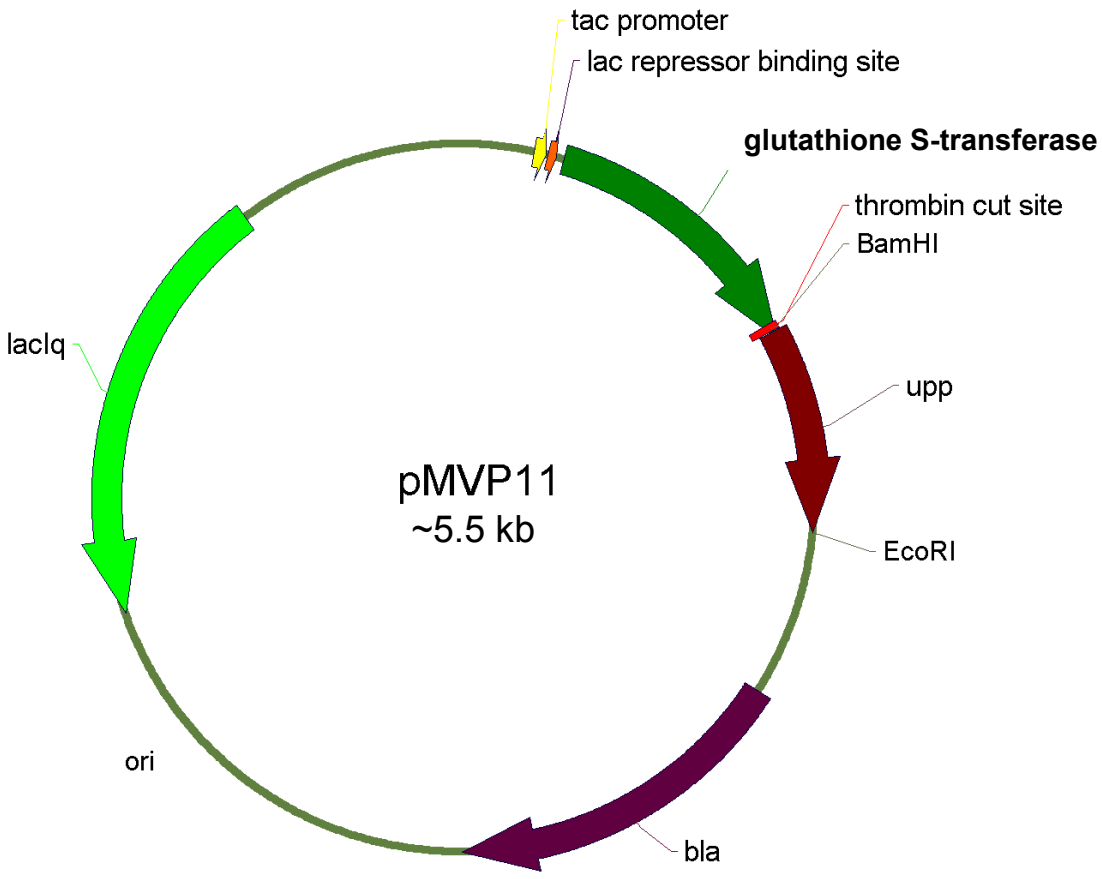

Fig. 27. Construction of pMVP11 derived from pGEX-2T (Smith & Johnson, 1988; Amersham Pharmacia Biotech.). Plasmid pMVP11 has a 600 bp fragment containing an intact *upp* gene inserted into the *Bam*HI-*Eco*RI sites of the expression vector, pGEX-2T. The glutathione S-transferase::*pyrR* gene fusion is expressed from the *tac* promoter.

purification was carried out according to manufacturer's specifications. The GST-Upp fusion protein was eluted from the matrix two times with 2 ml of 10 mM reduced glutathione. The eluted fractions containing the GST-Upp fusion were combined and dialyzed against 1X PBS (pH 7.3) overnight at 4°C. The dialyzed fusion sample was incubated with 100 units of thrombin protease overnight at 4°C, to cleave the PyrR protein from the GST tag. The fraction containing purified Upp protein was dialyzed against PyrR buffer (100 mM Tris-acetate, pH 7.5, 10 mM potassium acetate, 20% glycerol) at 4°C overnight. The purified protein was separated into 100 µl aliquots, snap frozen in liquid nitrogen and stored at -80°C.

Isolation of DNA fragments for electrophoretic mobility shift assays (EMSA).

DNA fragments containing the promoter regions of the *pyrR* (327 bp), *pyrD* (254 bp), *pyrE* (255 bp) and *pyrF* (175 bp) genes were amplified from *P. aeruginosa* chromosomal DNA by PCR (Fig. 28). The oligonucleotides used are listed in Table 3. The PCR products were agarose purified and end-labeled with γ-^{32}P using polynucleotide kinase as described earlier. These radiolabeled PCR fragments were used as DNA probes for EMSA.

Electrophoretic mobility shift assays (EMSA).

EMSA is a sensitive method for the detection of specific *in vitro* interactions of DNA and/or RNA with proteins (Ausubel *et al*., 1993), and is also commonly referred to as gel retardation or gel shift assays. Interactions between proteins and target DNA or

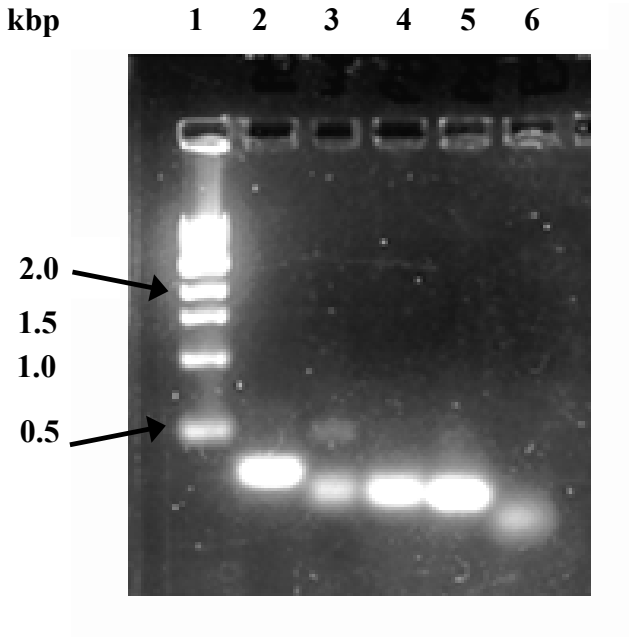

Fig. 28. Agarose gel electrophoresis analysis of PCR fragments used for EMSA assays. Lanes: 1, 1 kb DNA marker (New England Biolabs); 2, fragment of the *pyrR* upstream region (327 bp); 3, fragment of the *upp* upstream region (280 bp); 4, fragment of the *pyrD* upstream region (254 bp); 5, fragment of the *pyrE* upstream region (255 bp); 6, fragment of the *pyrF* upstream region (175 bp).

Table 3. Synthetic oligonucleotides used to generate DNA probes for EMSA

Primer	Sequence (5'→ 3')	Usage	Supplier[a]
PQF50-RF	CGCGGATCCAACGGCCGTTTCAACC	PCR of *pyrR* probe	IDT
PQF50-RR	CCCAAGCTTGAGTTCGGCGGGATTG	PCR of *pyrR* probe	IDT
PyrD-Forward	CGGCAGGGCCAATCGGGTCCTGCT	PCR of *pyrD* probe	Bio-synthesis
PyrD-Reverse	CAGTTTGAACAGCAGCTGGCGGGC	PCR of *pyrD* probe	Bio-synthesis
PADPYRE-F	GCCGTCCAGTTGGAAGGACGGGTCA	PCR of *pyrE* probe	IDT
PADPYRE-R	CGCGCTGATACGCCTGCATGAATGA	PCR of *pyrE* probe	IDT
PyrF-Forward	GTCGACTGGCTGGAGCAACTGCTC	PCR of *pyrF* probe	Bio-synthesis
PyrF-Reverse	AATCCAGGGCGACGATGATGGGGG	PCR of *pyrF* probe	Bio-synthesis

[a] IDT, Intergrated DNA Technologies, Coralville, IA; Bio-Synthesis, Lewisville, TX.

RNA, results in the formation of a protein-DNA/RNA complex. This protein-DNA/RNA complex would migrate at a slower rate through a non-denaturing polyacrylamide gel, due to a measurable decrease or shift in mobility when compared to unbound DNA or RNA. Electrophoretic mobility shift assays for RNA binding were performed by Heather Savacool-Bonner of Robert L. Switzer's Research Group, University of Illinois, Urbana, IL. The assays were carried out according to the method of Turner *et al*. (1998). The gel shift assay for DNA binding was performed using the method described by Proctor (1998) with slight modifications. A 4% non-denaturing polyacrylamide stock solution composed of 50 ml of 40% (19:1) acrylamide:bis-acrylamide, 25 ml of 5X Tris-Borate-EDTA (TBE) buffer, pH 8.0 in 500 ml of ddH_2O was prepared. The 5X TBE buffer contained 0.5 M Tris-HCl (pH 8.0), 0.5 M Boric acid and 5 mM EDTA. The 4% polyacrylamide stock solution was purified through a 0.45 μm porosity filter (Millipore) and stored at 4°C for up to 3 months. The gel was prepared by the addition 0.02 g of ammonium persulfate and 10 μl of TEMED to 10 ml of 4% polyacrylamide stock solution. The gel was pre-electrophoresed in 0.25X TBE buffer, pH 8.0 at 4°C for 45 min prior to loading the binding reactions. The following solutions required for the binding reaction were prepared;

10X Gel shift binding buffer – filter sterilized through a 0.4 μm porosity filter
0.25 M Tris-HCl, pH 8.0
0.06 M MgCl2
5 mM EDTA (sodium salt), pH 8.0
0.2 M KCl
50% glycerol, v/v

2X Reaction cocktail
0.2 volume 10X gel shift binding buffer
0.1 volume 5 mM DTT
γ-^{32}P-ATP labeled DNA probe to ~50,000 cpm/10 µl of 2X cocktail.
Adjust volume to 1.0 ml with sterile ddH_2O.

1X Dilution buffer - store at -20°C
100 µl 10X gel shift binding buffer
100 µl 5 mM DTT
100 µl 1 mg ml^{-1} bovine serum albumin (BSA)
700 µl sterile ddH_2O

The binding reactions were prepared in a volume of 20 µl and contained the following components: 5-9 µl of 1X dilution buffer, 10µl of 2X probe cocktail, and 1-5 µ*g* of purified protein. When required, the following ligands were added to the binding reaction at 0.1 mM; orotate, orotidine 5'-monophosphate (OMP), uridine 5'-monophosphate (UMP) and 5-phosphoribosyl-1-pyrophosphate (PRPP). The final volume of each binding reaction was adjusted to 20 µl and incubated at room temperature for 30 min. After incubation, 10 µl of the binding reaction were loaded onto a pre-electrophoresed 4% non-denaturing polyacrylamide gel, and the bound and unbound DNA was separated at 100 V for 30-40 min. The gel was transferred to 3 mm Whatman filter paper and dried under vacuum at 75°C for 2 h. The results were visualized by autoradiography.

The apparent dissociation constants (K_d) of PyrR for the target DNA/or ligands were determined by varying the concentration of PyrR (0.1 µ*g* to 5 µ*g*) used in the binding reaction. The concentration of radiolabeled DNA/or ligands was held constant and the density of the bands was measured using a NIH Image Version 1.61 densitometry program by Wayne Rasband.

The competitive ligand binding assays were performed by varying the concentration of one ligand in the binding reaction (0.03 mM to 1 mM), and keeping the concentration of the second ligand constant at 0.1 mM.

High performance liquid chromatography (HPLC) gel filtration.

HPLC-gel filtration was used to determine the native size of the PyrR protein. The following molecular weight protein standards were loaded onto a Protein Pak Steel 300SW (7.5 mm x 30 cm) gel filtration column (Waters Corp.) at a concentration of 15 μ*g*: blue dextran , 2,000 kDa; apoferritin, 443 kDa; β-amylase, 200 kDa; alcohol dehydrogenase, 150 kDa; and carbonic anhydrase, 29 kDa (Sigma-Aldrich Co.). The mobile phase was 50 mM Tris-acetate, pH 7.5 (Turner *et al*., 1998), which had been filtered through a 0.4 μm filter (Millipore) and degassed by vacuum and sonication. The flow rate was 1 ml min^{-1} and the detection wavelength was 214 nm and 280 nm. A standard curve of retention time *versus* molecular weight was generated. Seven micrograms of purified PyrR protein was loaded onto the column. The purified PyrR protein was loaded onto the column under the following conditions: 7 μg of PyrR alone, 7 μg of PyrR, 6 mM $MgCl_2$ and 0.2 mM PRPP pre-incubated at room temperature for 10 min, 7 μg of PyrR, 6 mM $MgCl_2$ and 2 mM PRPP pre-incubated at room temperature for 10 min and, 7 μg of PyrR, 6 mM $MgCl_2$ and 2 mM OMP pre-incubated at room temperature for 10 min. The native size of PyrR under the varying conditions was determined directly from the standard curve. The reaction in the presence of 2 mM PRPP was repeated using 50 μg of PyrR and 1 ml fractions were collected. The protein in each

fraction was concentrated by trichloroacetic acid (TCA) precipitation and analyzed on 15% SDS-PAGE, to confirm the presence of the PyrR subunit (Bollag & Edelstein, 1991).

HPLC-enzyme assays.

Enzyme activities were assayed using the reverse-phase SUPELCOSIL-LC-18-T column, 4.6 mm x 15 cm, (Supelco), which features a special surface treatment along with an octadecylsilane bonding for efficient separation of nucleotides. The mobile phase was a 0.1 M phosphate buffer, pH 5.3 prepared by mixing 86.6 ml of 1 M KH_2PO_4 and 13.2 ml of 1 M K_2HPO_4, bringing the volume up to 950 ml with ddH_2O and adjusting to pH 6.0 with 1 M KOH. An ion pairing agent, tetrabutylammonium hydrogen sulfate was added to a final concentration of 10 mM, which caused a drop in to pH 5.3, the final volume was then adjusted to 1 liter with ddH_2O. The buffer solution was filtered through a 0.4 μm filter and degassed under vacuum with sonication. The flow rate was 1.5 ml min^{-1}, and the nucleotides were detected at wavelengths 254 nm and 280 nm (Beck, 1995; Turner *et al*., 1998).

HPLC-Uracil phosphoribosyltransferase (UPRTase) assay.

The UPRTase reaction mix contained 50 mM Tris, 6 mM $MgCl_2$, 0.6 mM PRPP, 0.5 mM uracil, and either 20 μl of clarified extract or 10 μg of purified PyrR protein, in a reaction volume of 250 μl at a final pH 8.0. The reaction was initiated with the addition of uracil. Reactions with clarified extract were assayed for 10 min and reactions with

purified PyrR protein were assayed for 30 min. The reactions were terminated by the addition of an equal volume of 0.5 M perchloric acid, which denatured the proteins. The pH was adjusted to pH 7.0 by the addition of 20 µl of 1 M KOH. The tubes were incubated on ice for 5 min, and centrifuged at 12,000 ***g*** for 5 min to pellet the precipitate. The supernatant was filtered through a 0.4 µm filter and 50 µl was loaded onto the column (Beckwith *et al*., 1962; Beck. 1995).

HPLC-Orotate phosphoribosyltransferase (OPRTase) assay.

The OPRTase reaction mix contained 50 mM Tris , 6 mM $MgCl_2$, 0.6 mM PRPP, 0.5 mM orotate, and either 20 µl of clarified extract or 10 µg of purified PyrR protein, in a reaction volume of 250 µl at a final pH 8.0. The reaction was initiated with the addition of orotate. Reactions with clarified extract were assayed for 10 min and reactions with purified PyrR protein were assayed for 30 min. The reactions were terminated by the addition of an equal volume of 0.5 M perchloric acid, which denatured the proteins. The pH was adjusted to 7.0 by the addition of 20 µl of 1 M KOH. The tubes were incubated on ice for 5 min, and centrifuged at 12,000 ***g*** for 5 min to pellet the precipitate. The supernatant was filtered through a 0.4 µm filter and 50 µl was loaded onto the column.

HPLC-Orotate decarboxylase assay.

The orotate decarboxylase reaction mix contained 50 mM Tris (pH 8.0), 0.5 mM orotate, and 20 µl of clarified extract in a reaction volume of 250 µl. The reaction was initiated with the addition of orotate and was assayed for 20 min. The reactions were

terminated by the addition of an equal volume of 0.5 M perchloric acid, which denatures the proteins. The pH was adjusted to 7.0 by the addition of 20 µl of 1 M KOH. The tubes were incubated on ice for 5 min, and centrifuged at 12,000 ***g*** for 5 min to pellet the precipitate. The supernatant was filtered through a 0.4 µm filter and 50 µl was loaded onto the column.

Amino-terminal amino acid sequencing.

Edman degradation of the PyrR protein was kindly performed at the Molecular Genetics Facility of Georgia State University by Dr. John Houghton. The purified PyrR protein was separated by SDS-PAGE and then electroblotted onto a polyvinylidene difluoride (PVDF) membrane. The amino-terminal amino acid sequence was determined with a Beckman LF3200 gas-phase protein sequenator.

Western blotting.

Bacillus subtilis PyrR polyclonal antibodies, kindly supplied by Dr. Robert L. Switzer, University of Illinois, were used to show crossreactivity with the *P. aeruginosa* PyrR protein. Ten micrograms of purified PyrR protein was electrophoresed on a SDS-15% polyacrylamide gel as previously described. The gel was placed onto a 0.45µm pure nitrocellulose membrane and sandwiched with a piece of 3 mm Whatman filter paper and a Fiberpad sponge on each side. The nitrocellulose membrane, filter paper, and sponges were pre-soaked in cold transfer buffer (50 mM Tris (pH 7.5), 380 mM glycine, 0.1% SDS (w/v), and 20% methanol (v/v) in ddH_2O). The gel sandwich was placed in a Mini

Trans-Blot Electrophoretic Transfer Cell (Bio-Rad) with the gel positioned on the cathode side of the system. The protein was electroblotted onto nitrocellulose membrane at 45 V overnight at 4°C. The membrane containing transferred protein was incubated in 100 ml of blocking buffer (3% BSA w/v, 0.1% Tween 20 v/v, in TBS buffer, pH 7.5) at room temperature with gentle rocking for 2 h. The TBS buffer was prepared with 10 mM Tris-HCl, pH 7.5, 150 mM NaCl in ddH_2O. The membrane was then sealed in a hybridization bag with 25 ml of a solution containing the primary antibody, anti-*B. subtilis* PyrR, diluted 1:1000 in TBS buffer, and incubated at room temperature with gentle rocking for 1 h. The membrane was then washed with 100 ml of TNT buffer (0.1% BSA w/v, 0.1% Tween 20 v/v in TBS buffer, pH 7.5) for 15 min with gentle rocking at room temperature. The wash was repeated 3 times for a total of 4 washes at 15 min intervals. The membrane was then placed in a hybridization bag and incubated with 25 ml of a solution that contained the secondary antibody, anti-rabbit IgG alkaline phosphatase conjugate (Sigma-Aldrich Co.), diluted 1:3000 in TBS buffer, pH 7.5. The membrane was incubated with secondary antibody for 1 h at room temperature with gentle rocking. The membrane was washed 4 times with 100 ml of TNT buffer, changing the buffer every 15 min. During the washes, the following light sensitive solutions were prepared in amber flasks: 5-bromo-4-chloro-indoyl-phosphate/ nitroblutetrazolium detection reagent (BCIP/NBT, one tablet dissolved in 30 ml ddH_2O) and 20 ml stop buffer (20 mM EDTA in TBS buffer). After the washes, the membrane was incubated in the detection solution with gentle rocking, until the color developed and bands were visible. The reaction was terminated by the addition of stop solution.

Effect of carbon source on orotate utilization.

A 50 ml culture of the *P. aeruginosa pyrD* auxotroph (PAO0114) was grown in *Pseudomonas* minimal medium with glucose (0.2%) as the carbon source, and uracil (50 μg ml^{-1}) as the pyrimidine source. The optical density at 600 nm was measured. A 1 ml aliquot of the overnight culture was harvested, washed twice with 5 ml of 1X PBS (pH 7.3) and resuspended in 1 ml of the same buffer. A 100 μl aliquot of the washed cells was used as inoculum for subculturing. The strain was tested for its ability to use either uracil at 50 μg ml^{-1} or orotate at 50 μg ml^{-1} to satisfy the pyrimidine requirement. The experiment was repeated using 10 mM succinate as the carbon and energy source.

Effect of varying concentrations of succinate on orotate utilization.

Two 5 ml cultures of the *P. aeruginosa pyrD* auxotroph (PAO0114) were grown overnight in *Pseudomonas* minimal medium. One tube was grown with glucose as the carbon and energy source and uracil as the pyrimidine source at 50 μg ml^{-1}. The other tube was grown with succinate as the carbon source and uracil as the pyrimidine source at 50 μg ml^{-1}. The optical density at 600 nm was measured, a 1 ml aliquot was harvested, washed twice with 5 ml of 1X PBS (pH 7.3) and resuspended in an appropriate volume of the same buffer to yield the same concentration of cells in both tubes. Two sets of *Pseudomonas* minimal broth tubes were prepared with the following succinate concentrations: 2 mM, 5 mM, 10 mM and 20 mM. One set of tubes was inoculated with 100 μl of washed cells grown in glucose and the other set was inoculated with 100 μl of

washed cells grown in succinate. Cultures were incubated at 37°C with shaking for two days, and the optical density at 600 nm measured.

5'-Fluoroorotate plate assays.

P. aeruginosa wild type (AK903) and *crc* mutant (PAO8023) strains used for this assay were grown overnight in *Pseudomonas* minimal medium with the appropriate carbon source and supplemented with casamino acids (0.2%), uracil (50 μg ml^{-1}) and carbenicillin (600 μg ml^{-1}) when required. A 100 μl aliquot of overnight culture was plated onto *Pseudomonas* minimal medium supplemented with the appropriate carbon source and the necessary supplements. Immediately after plating, a pre-determined amount of 5'-fluoroorotate (FOA) crystals were placed in the center of the plate. Whenever a quantitative assay was required, a sterile filter disk saturated in a 1 mg ml^{-1} solution of FOA was placed in the center of the plate. All plates were incubated at 37°C overnight. Growth up to the crystal or disk was indicative of resistance to FOA while a zone of killing was indicative of sensitivity to FOA.

Competitive entry assay: radiolabeled orotate versus succinate

P. aeruginosa wild type (AK903) and *crc* mutant (PAO8023) strains were grown overnight in *Pseudomonas* minimal medium with glucose as the carbon and energy source and the appropriate antibiotic. The cells were harvested at 1875 ***g*** for 15 min, washed three times in 5 ml of 1X PBS (pH 7.3) and resuspended in 4.5 ml of the same buffer. The optical density at 600 nm was measured and the volume of the remaining

culture was adjusted with 1X PBS to yield the same concentration of cells in each tube. One milliliter of each culture was added to three separate microcentrifuge tubes, each containing 1 μCi of ^{3}H radiolabeled orotate. The tubes were incubated at room temperature for 30 min. The cells were vacuum filtered through a 0.45 μm nitrocellulose membrane, washed twice with 3 ml of 1X PBS and allowed to air dry overnight. The membrane filters containing the dry cells were placed in scintillation vials with 8 ml of scintillation fluid, and counts per min (cpm) were measured using a scintillation counter. The cpm of 1 μCi of ^{3}H-orotic acid was measured as a control. The percent of radiolabeled orotic acid that entered the cells was calculated as follows:

$$\frac{\text{cpm sample}}{\text{cpm of 1 } \mu\text{Ci of } ^{3}\text{H-orotic acid}} \times 100 = \% \text{ orotic acid uptake}$$

Isolation of *out* mutants.

Mutants defective in orotate utilization (*out* mutants) were isolated on glucose minimal medium based on their resistance to the analog 5-fluoroorotate. *P. aeruginosa* PAO1 was grown overnight in glucose minimal medium. One hundred microliters of this overnight culture were plated onto glucose minimal medium and a pre-determined amount of 5-fluoroorotate crystals were placed in the center of the plates as described above. The *P. aeruginosa pyrD* auxotroph (PAO0114) was also grown in glucose minimal medium supplemented with cytosine (0.1mM) as pyrimidine source. A 100 μl aliquot of this culture was plated onto glucose minimal medium supplemented with cytosine (0.1 mM). Pre-determined amounts of 5-fluoroorotate crystals were placed in

the center of the plates. All plates were incubated at 37°C for two days. After two days of incubation, the colonies that appeared within the zone of killing were taken to be *out* mutants as these mutants have been shown in *E. coli* by Baker *et al*., (1996) to be mapped at the *out* locus.

RESULTS AND DISCUSSION

Sequencing of the *pyrR* gene.

In light of the prevalence of *pyrR* genes in several different organisms (Ghim & Neuhard, 1994; Li *et al*., 1995; Elagöz *et al*., 1996) the nucleotide sequence of the region upstream of the *Pseudomonas aeruginosa pyrBC'* operon, encoding ATCase, was determined using pUC41 plasmid DNA as the template (Fig. 29). Computer analysis of this sequence revealed an open reading frame (ORF) of 510 nucleotides that encoded a polypeptide of 170 amino acids, with a deduced molecular mass of 19 kDa and a calculated isoelectric point of 5.2. Using the BLAST algorithm (Sonnhammer & Durbin, 1994; Altschul *et al*., 1990), this 510 bp ORF was searched against protein sequences in the GenBank database. Results revealed that the *P. aeruginosa* PyrR protein showed greatest similarity (87%) and identity (77%) with that of the *P. putida* PyrR protein (Kumar, 2000). In addition, the next closest match was found to be with the *pyrR* gene of *Thermus aquaticus* (Van de Casteele, 1997) at 63% similarity and 45% identity.

Primer extension analysis

To identify the transcription-initiation site for the *pyrR* transcript, a primer extension assay was performed using an end-labeled oligonucleotide primer. Total RNA samples were isolated from wild type *P. aeruginosa* grown under four different conditions, namely in the (i) absence of uracil, (ii) presence of uracil, (iii) presence of

-35 -10

GGAAGGCTGGCTGGCCGAACACCCGGATTGACCCATGGCAGCCGGCACGCCGCCGTTTGCCATTATGCTTT

+1 RBS

CGCCACCGCGGGCGCCTCCCTACAGCGGGCTCTCCCGGCGGCCATCCCATCGATGTCAGCGAGGAGCCACC

pyrR

ATG AGC CTA CCC AAT CCC GCC GAA CTC CTG CCG CGC ATG GCC AGC GAC CTG CGC
M S L P N P A E L L P R M A S D L R

GCC CAT CTC GCC GAG CGC GGC ATC GAG CGG CCG CGC TTC GTC GGC ATC CAT ACC
A H L A E R G I E R P R F V G I H T

GGC GGC ATC TGG GTC GCC GAG GCG CTG CTG AGG GAA CTG GGC AAC CAA GAG CCG
G G I W V A E A L L R E L G N Q E P

CTG GGC ACC CTC GAC GTC TCC TTC TAC CGC GAC GAC TTC ACC CAG AAC GGC CTG
L G T L D V S F Y R D D F T Q N G L

CAT CCG CAG GTC CGC CCG TCG GCG CTG CCG TTC GAG ATC GAC GGC CAG CAC CTG
H P Q V R P S A L P F E I D G Q H L

GTG CTG GTG GAC GAC GTG CTG ATG AGC GGC CGT ACC ATC CGC GCC GCA CTC AAC
V L V D D V L M S G R T I R A A L N

GAA CTG TTC GAC TAC GGC CGT CCG GCC AGC GTG ACC CTG GTC TGC CTG CTC GAC
E L F D Y G R P A S V T L V C L L D

CTG AAC GCC CGG GAG TTG CCT ATC CGC CCC GAC GTG GTC GGC CAG ACC CTG TCC
L N A R E L P I R P D V V G Q T L S

CTG GGT CGC GAT GAA CGG GTA AAA TTG GTC GGT CCC GCA CCG CTC GCC CTC GAG
L G R D E R V K L V G P A P L A L E

pyrB

CGC AAG GTC CTT TCC TCC GCT TCC TGA TCCTCTTCACTAGGGCCTGCCCC ATG CCG ACA
R K V L S S A S * M P T

GAC GCC AAG CGC CCG CTG CAG CTC AAC GAC CAG GGC CAG CTG CGC CAC TTC ATC

TCG CTC GAC GGA TTG CCC CGC GAG CTG CTC ACC GAA ATC CTC GAT ACC GCC GAT

TCC TTC CTG GAG GTC GGC GCC

Fig. 29. Nucleotide sequence of the 517 bp DNA fragment bearing the complete *P. aeruginosa pyrR* gene and partial *pyrB* gene. The transcriptional start site (+1), -10 and -35 sequences and the ribosomal binding site (RBS) are indicated in color. The deduced amino acid sequence of the ORF is shown, the stop and start codons are indicated in red and green, respectively. The asterisk indicates the *pyrR* stop codon. The underlined bases denote the 23 bp gap between the end of the *pyrR* gene and the start of the *pyrB* gene.

orotate and (iv) uracil and orotate. Results are shown in Fig. 30. A major extension product that corresponded to a transcription-start site (+1 position) situated 67 nucleotides upstream of the translational start codon was detected. As can be seen from Figure 29, the transcription-start was located appropriately downstream of putative –10 and –35 sequences. This promoter region contained elements typical of an activatable *Pseudomonas* σ^{70} consensus (Fig. 31., Deretic *et al*., 1989; Ronald *et al*., 1992) and, when subjected to computer analysis, revealed the formation of a putative stem-loop secondary structure encompassing the Shine-Dalgarno sequence and the AUG start codon (Fig. 32). Such secondary structure formation is typical of an autogenous mechanism of regulation (McCarthy & Gualerzi, 1990; Ohta *et al*., 2001), suggesting that *pyrR* encoded a protein that regulated its own expression. To find out if the putative *pyrR* promoter region were active, a 320 bp DNA fragment that contained the –10 and –35 sequences within the upstream region was fused to a promoter-less *lacZ* gene, pMVP50, and assayed for β-galactosidase activity. Results showed that the *lacZ* gene was expressed in wild type *P. aeruginosa* (Table. 4), confirming the presence of an active promoter located upstream of the *pyrR* gene. In addition, this confirmed the direction of transcription of *pyrR* was the same as that of the *pyrBC'* operon and the intergenic gap between *pyrR* and *pyrBC'* being only 23 bp, confirmed that *pyrR* was the first gene of a tricistronic operon *pyrRBC'*.

Sequence comparison with other known PyrR proteins.

Using a CLUSTAL W version 6.0 computer program (Higgins *et al*., 1996), a

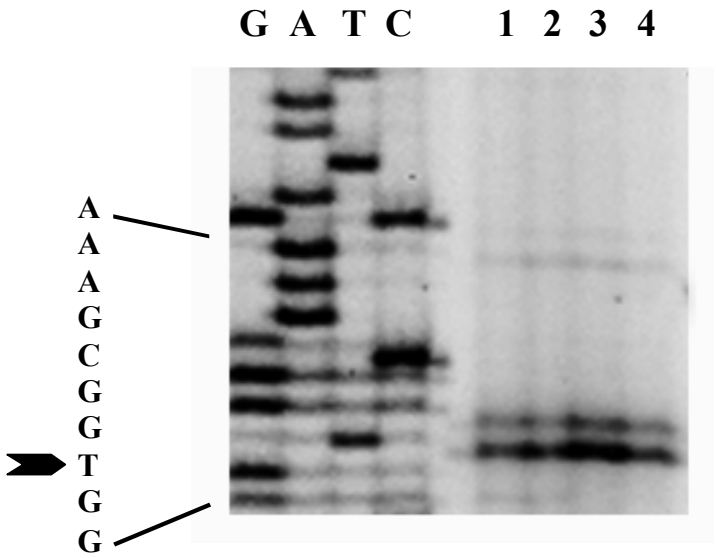

Fig. 30. Autoradiogram of primer extension analysis to determine the transcription initiation site of the *P. aeruginosa pyrR* gene. Lane 1 corresponds to total RNA isolated from wild type *P. aeruginosa* grown without the addition of supplements and lane 2, 3 and 4 correspond to total RNA isolated from wild type *P. aeruginosa* supplemented with 2 mM uracil (lane 2), 1 mM orotate (lane 3), 2 mM uracil and 1 mM orotate (lane 4). DNA sequencing termination reactions for G, A, T and C are marked. The sequence of the antisense strand is shown along the side and the arrow indicates the extended primer.

A *Pseudomonas rpoD* promoter consensus

Gene	-35	No. of nucleotides	-10	No. of nucleotides	+1
oprI	CGC**TT**GGTC	16	AAG**TAAT**GG	16	C
argF	TCC**TT**GTGT	17	TTA**TAAG**AT	-	-
catBC	ATA**TT**GGAC	17	GCG**CAAT**CC	10	A
nahR	TA**TT**GATA	17	ATA**TAAT**AA	6	A
algR2	GTC**TT**GATG	16	GCA**TAAT**CT	9	C
hutH	GCT**TT**GGAT	17	TGA**TACT**GA	-	-
Consensus	YS**TT**GR	17-18	YR**TAAT**		
pyrR	TGG**CA**GCC	18	CA**TTAT**	10	C

B *Pseudomonas* activatable *rpoD* promoter consensus

	-35	-10
nenA	A**TTGACA**AATAAAAAGCACGCTCAC--	**CATCAT**CGCGAA
nenG	T**TTATCA**ATATTGTTTGCTCCGT----	**TATCGT**TATAAC
corG	A**TTGGAC**GGCTATCAGGGTCTCGCGC-	**AATCCT**TGAACA
crcA	C**ATGACA**CGCGAATCTTAGCATT----	**CATGTT**TGAAGC
xylDEG	T**ATCTCT**AGAAAGGCCTACCCCT----	**TAGGCT**TTATGC
pyrR	C**ATGGCA**GCCGGCACGCCGCCGTTTGC	**CATTAT**GCTTTC

Fig. 31. *Pseudomonas* promoter sequences. Figure adapted from Deretic *et al*, (1989) and Ronald *et al*., (1992).

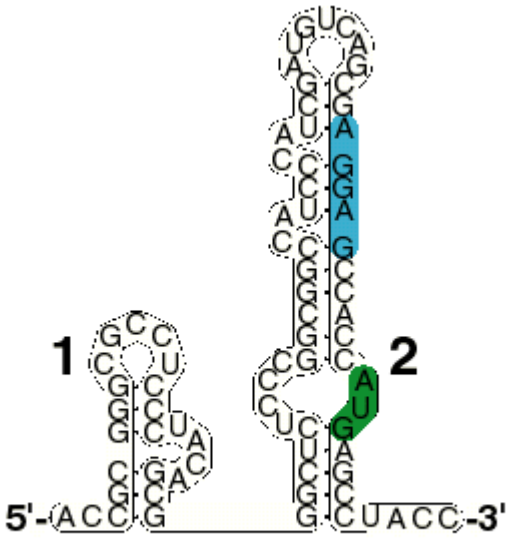

Fig. 32. RNA secondary structure of *P. aeruginosa pyrR* transcript starting with the first residue of the mRNA using the Rna Viz secondary structure computer program (De Rijk & De Wachter, 1997).

Table 4. *β*-galactosidase activity measurements of *pyrR*::*lacZ* reporter gene fusions in *P. aeruginosa* wild type, AK903 and *pyrR* mutant strain, MVP7401 under different conditions of growth.

Plasmid	**Strain**	**Genotype**	**Specific Activity (units of *β*-galactosidase[a])**			
			Glucose	Glucose + 1mM Orotate	Succinate	Succinate + 1mM Orotate
pyrR::*lacZ*	AK903	Wild type	330.5	330.2	319.8	353.3
pyrR::*lacZ*	MVP7401	*pyrR* $^{-}$	816.7	695.5	899.5	850.1

[a] One unit of *β*-galactosidase hydrolyzes 1 nmol of *o*-nitrophenol per min^{-1} mg of protein^{-1}.

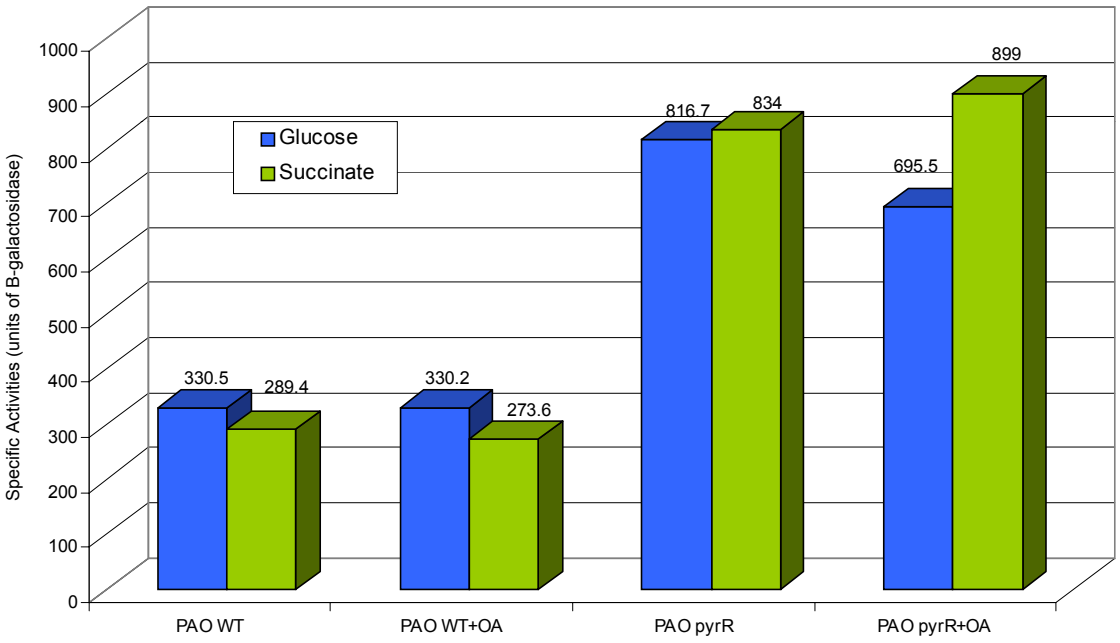

Fig. 33. Graphical representation of *β*-galactosidase activity data from Table 4.

Multiple alignment was performed to compare the *P. aeruginosa* PyrR with other known PyrR proteins (Fig. 34). *P. aeruginosa* PyrR displayed significant sequence homology to all other PyrR proteins sharing greatest homology with that of *P. putida*. In *B. subtilis*, a seven residue sequence, RGHRELP, has been shown to form a loop that is necessary for the dimerization of the PyrR protein (Tomchick *et al*., 1998). This folding conformation has been shown to be essential for the PyrR protein to bind RNA. Such a conserved stretch of amino acid residues was not present in the *P. aeruginosa* sequence, suggesting that the *Pseudomonas* PyrR protein was not likely to be a RNA binding protein. The conserved regions in the flexible loop and the central phosphoribosylpyrophosphate (PRPP) binding domain have been shown to bind to the co-regulator molecule PRPP (Fig. 34., Tomchick *et al*., 1998). In *B. subtilis*, it has been shown that bound PRPP antagonizes the binding effect of PyrR. Both of these regions are also conserved in the *Pseudomonas* PyrR proteins, suggesting that a similar mechanism of action by PRPP is in play. Also in *B. subtilis*, the residues NGK, which form the trimer loop, are necessary for the shifting between the dimeric and hexameric forms, were absent in the *P. aeruginosa* PyrR sequence. This suggested that a dimeric to hexameric shift may not occur in the *P. aeruginosa* PyrR protein. At the N-terminus of PyrR for both *P. aeruginosa* and *P. putida*, there was a stretch of 10 hydrophobic amino acids that are not present in other PyrR sequences (Fig. 35) therefore this hydrophobic region is a candidate for the dimerization domain in the *Pseudomonas* PyrR proteins. Towards the C-terminus of the *P. aeruginosa* PyrR there is a stretch of 41 amino acids that has 100% identity with that

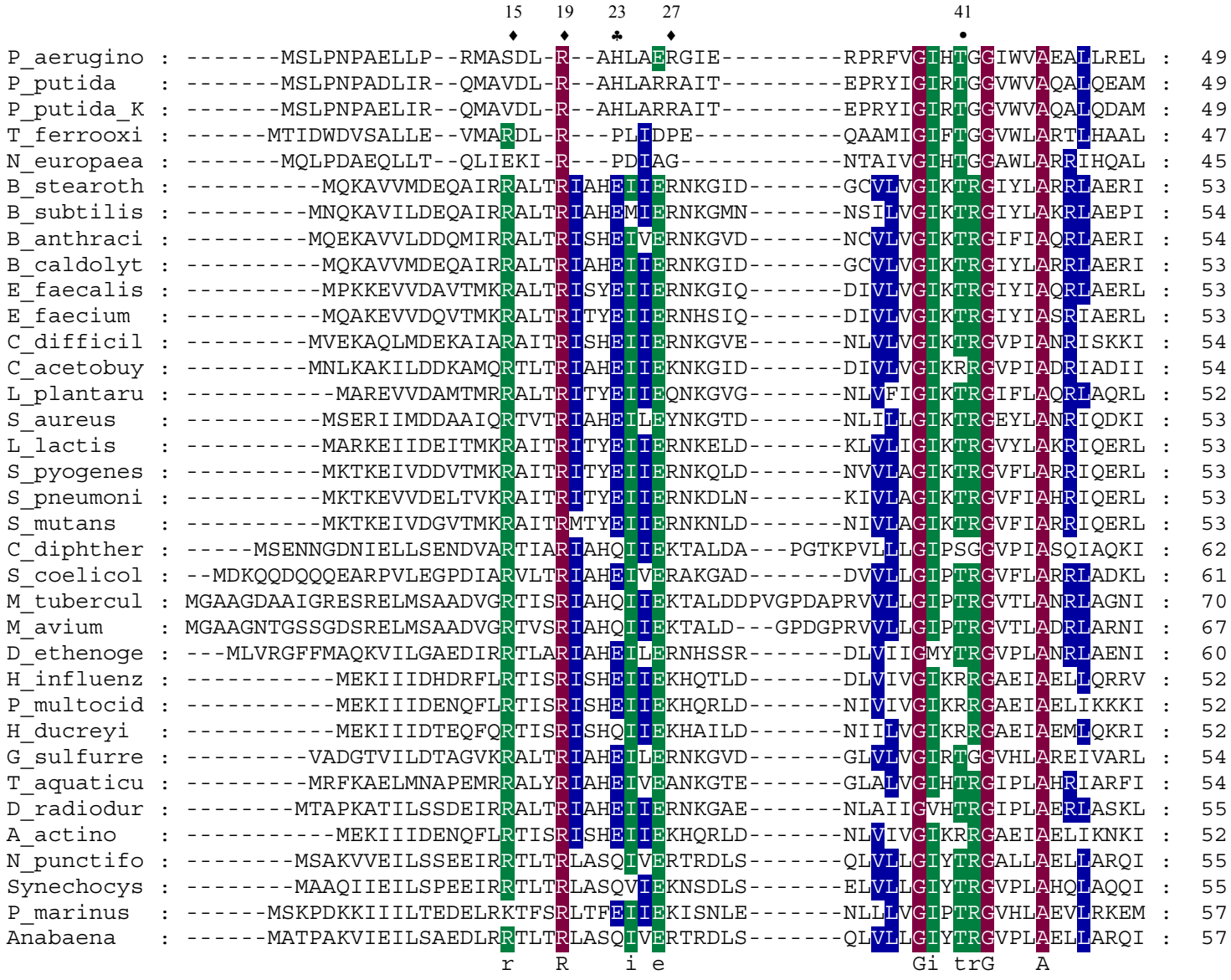
15 19 23 27 41
P_aerugino : -------MSLPNPAELLP--RMASDL-R--AHLAERGIE---------RPRFVGIHTGGIWVAEALLREL : 49
P_putida : -------MSLPNPADLIR--QMAVDL-R--AHLARRAIT---------EPRYIGIRTGGVWVAQALQEAM : 49
P_putida_K : -------MSLPNPAELIR--QMAVDL-R--AHLARRAIT---------EPRYIGIRTGGVWVAQALQDAM : 49
T_ferrooxi : ------MTIDWDVSALLE--VMARDL-R---PLIDPE----------QAAMIGIFTGGVWLARTLHAAL : 47
N_europaea : -------MQLPDAEQLLT--QLIEKI-R---PDIAG----------NTAIVGIHTGGAWLARRIHQAL : 45
B_stearoth : ----------MQKAVVMDEQAIRRALTRIAHEIIERNKGID-------GCVLVGIKTRGIYLARRLAERI : 53
B_subtilis : ---------MNQKAVILDEQAIRRALTRIAHEMIERNKGMN-------NSILVGIKTRGIYLAKRLAEPI : 54
B_anthraci : ---------MQEKAVVLDDQMIRRALTRISHEIVERNKGVD-------NCVLVGIKTRGIFIAQRLAERI : 54
B_caldolyt : ----------MQKAVVMDEQAIRRALTRIAHEIIERNKGID-------GCVLVGIKTRGIYLARRLAERI : 53
E_faecalis : ----------MPKKEVVDAVTMKRALTRISYEIIERNKGIQ-------DIVLVGIKTRGIYIAQRLAERL : 53
E_faecium : ----------MQAKEVVDQVTMKRALTRITYEIIERNHSIQ-------DIVLVGIKTRGIYIASRIAERL : 53
C_difficil : ---------MVEKAQLMDEKAIARAITRISHEIIERNKGVE-------NLVLVGIKTRGVPIANRISKKI : 54
C_acetobuy : ---------MNLKAKILDDKAMQRTLTRIAHEIIEKNKGID-------DIVLVGIKRRGVPIADRIADII : 54
L_plantaru : -----------MAREVVDAMTMRRALTRITYEIIEQNKGVG-------NLVFIGIKTRGIFLAQRLAQRL : 52
S_aureus : ----------MSERIIMDDAAIQRTVTRIAHEILEYNKGTD-------NLILLGIKTRGEYLANRIQDKI : 53
L_lactis : ----------MARKEIIDEITMKRAITRITYEIIERNKELD-------KLVLIGIKTRGVYLAKRIQERL : 53
S_pyogenes : ----------MKTKEIVDDVTMKRAITRITYEIIERNKQLD-------NVVLAGIKTRGVFLARRIQERL : 53
S_pneumoni : ----------MKTKEVVDELTVKRAITRITYEIIERNKDLN-------KIVLAGIKTRGVFIAHRIQERL : 53
S_mutans : ----------MKTKEIVDGVTMKRAITRMTYEIIERNKNLD-------NIVLAGIKTRGVFIARRIQERL : 53
C_diphther : -----MSENNGDNIELLSENDVARTIARIAHQIIEKTALDA---PGTKPVLLLGIPSGGVPIASQIAQKI : 62
S_coelicol : --MDKQQDQQQEARPVLEGPDIARVLTRIAHEIVERAKGAD-------DVVLLGIPTRGVFLARRLADKL : 61
M_tubercul : MGAAGDAAIGRESRELMSAADVGRTISRIAHQIIEKTALDDPVGPDAPRVVLLGIPTRGVTLANRLAGNI : 70
M_avium : MGAAGNTGSSGDSRELMSAADVGRTVSRIAHQIIEKTALD---GPDGPRVVLLGIPTRGVTLADRLARNI : 67
D_ethenoge : ---MLVRGFFMAQKVILGAEDIRRTLARIAHEILERNHSSR-------DLVIIGMYTRGVPLANRLAENI : 60
H_influenz : -----------MEKIIIDHDRFLRTISRISHEIIEKHQTLD-------DLVIVGIKRRGAEIAELLQRRV : 52
P_multocid : -----------MEKIIIDENQFLRTISRISHEIIEKHQRLD-------NIVIVGIKRRGAEIAELIKKKI : 52
H_ducreyi : -----------MEKIIIDTEQFQRTISRISHQIIEKHAILD-------NIILVGIKRRGAEIAEMLQKRI : 52
G_sulfurre : ---------VADGTVILDTAGVKRALTRIAHEILERNKGVD-------GLVLVGIRTGGVHLAREIVARL : 54
T_aquaticu : ---------MRFKAELMNAPEMRRALYRIAHEIVEANKGTE-------GLALVGIHTRGIPLAHRIARFI : 54
D_radiodur : --------MTAPKATILSSDEIRRALTRIAHEIIERNKGAE-------NLAIIGVHTRGIPLAERLASKL : 55
A_actino : -----------MEKIIIDENQFLRTISRISHEIIEKHQRLD-------NLVIVGIKRRGAEIAELIKNKI : 52
N_punctifo : --------MSAKVVEILSSEEIRRTLTRLASQIVERTRDLS-------QLVLLGIYTRGALLAELLARQI : 55
Synechocys : --------MAAQIIEILSPEEIRRTLTRLASQVIEKNSDLS-------ELVLLGIYTRGVPLAHQLAQQI : 55
P_marinus : ------MSKPDKKIIILTEDELRKTFSRLTFEIIEKISNLE-------NLLLVGIPTRGVHLAEVLRKEM : 57
Anabaena : ------MATPAKVIEILSAEDLRRTLTRLASQIVERTRDLS-------QLVLLGIYTRGVPLAELLARQI : 57
r R i e Gi trG A

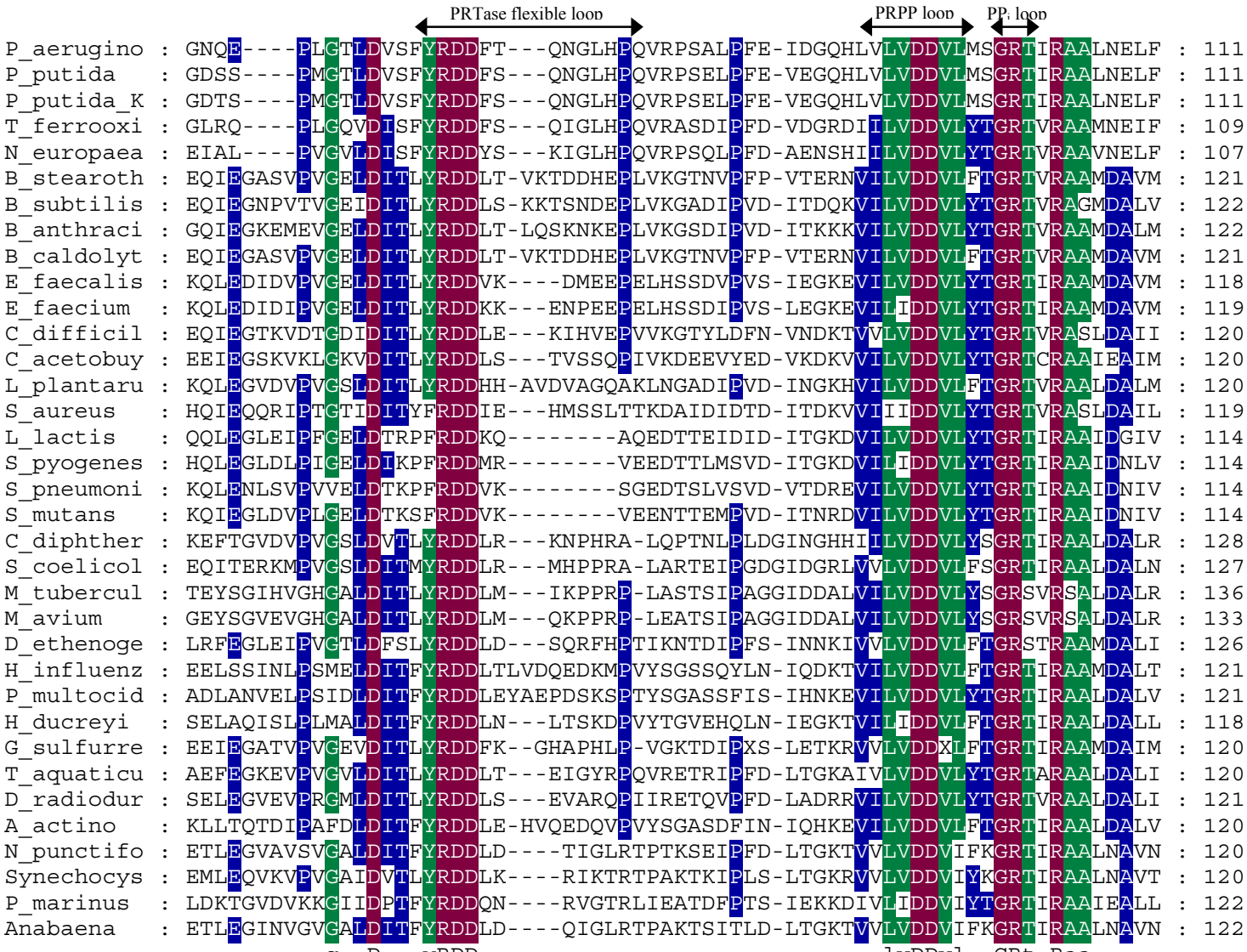
PRTase flexible loop
PRPP loop
PP, loop
P_aerugino : GNQE----PLGTLDVSFYRDDFT---QNGLHPQVRPSALPFE-IDGQHLVLVDDVLMSGRTIRAALNELF : 111
P_putida : GDSS----PMGTLDVSFYRDDFS---QNGLHPQVRPSELPFE-VEGQHLVLVDDVLMSGRTIRAALNELF : 111
P_putida_K : GDTS----PMGTLDVSFYRDDFS---QNGLHPQVRPSELPFE-VEGQHLVLVDDVLMSGRTIRAALNELF : 111
T_ferrooxi : GLRQ----PLGQVDISFYRDDFS---QIGLHPQVRASDIPFD-VDGRDIILVDDVLYTGRTVRAAMNEIF : 109
N_europaea : EIAL----PVGVLDISFYRDDYS---KIGLHPQVRPSQLPFD-AENSHIILVDDVLYTGRTVRAAVNELF : 107
B_stearoth : EQIEGASVPVGELDITLYRDDLT-VKTDDHEPLVKGTNVPFP-VTERNVILVDDVLFTGRTVRAAMDAVM : 121
B_subtilis : EQIEGNPVTVGEIDITLYRDDLS-KKTSNDEPLVKGADIPVD-ITDQKVILVDDVLYTGRTVRAGMDALV : 122
B_anthraci : GQIEGKEMEVGELDITLYRDDLT-LQSKNKEPLVKGSDIPVD-ITKKKVILVDDVLYTGRTVRAAMDALM : 122
B_caldolyt : EQIEGASVPVGELDITLYRDDLT-VKTDDHEPLVKGTNVPFP-VTERNVILVDDVLFTGRTVRAAMDAVM : 121
E_faecalis : KQLEDIDVPVGELDITLYRDDVK----DMEEPELHSSDVPVS-IEGKEVILVDDVLYTGRTIRAAMDAVM : 118
E_faecium : KQLEDIDIPVGELDITLYRDDKK---ENPEEPELHSSDIPVS-LEGKEVILIDDVLYTGRTIRAAMDAVM : 119
C_difficil : EQIEGTKVDTGDIDITLYRDDLE---KIHVEPVVKGTYLDFN-VNDKTVVLVDDVLYTGRTVRASLDAII : 120
C_acetobuy : EEIEGSKVKLGKVDITLYRDDLS---TVSSQPIVKDEEVYED-VKDKVVILVDDVLYTGRTCRAAIEAIM : 120
L_plantaru : KQLEGVDVPVGSLDITLYRDDHH-AVDVAGQAKLNGADIPVD-INGKHVILVDDVLFTGRTVRAALDALM : 120
S_aureus : HQIEQQRIPTGTIDITYFRDDIE---HMSSLTTKDAIDIDTD-ITDKVVIIIDDVLYTGRTVRASLDAIL : 119
L_lactis : QQLEGLEIPFGELDTRPFRDDKQ--------AQEDTTEIDID-ITGKDVILVDDVLYTGRTIRAAIDGIV : 114
S_pyogenes : HQLEGLDLPIGELDIKPFRDDMR--------VEEDTTLMSVD-ITGKDVILIDDVLYTGRTIRAAIDNLV : 114
S_pneumoni : KQLENLSVPVVELDTKPFRDDVK--------SGEDTSLVSVD-VTDREVILVDDVLYTGRTIRAAIDNIV : 114
S_mutans : KQIEGLDVPLGELDTKSFRDDVK--------VEENTTEMPVD-ITNRDVILVDDVLYTGRTIRAAIDNIV : 114
C_diphther : KEFTGVDVPVGSLDVTLYRDDLR---KNPHRA-LQPTNLPLDGINGHHIILVDDVLYSGRTIRAALDALR : 128
S_coelicol : EQITERKMPVGSLDITMYRDDLR---MHPPRA-LARTEIPGDGIDGRLVVLVDDVLFSGRTIRAALDALN : 127
M_tubercul : TEYSGIHVGHGALDITLYRDDLM---IKPPRP-LASTSIPAGGIDDALVILVDDVLYSGRSVRSALDALR : 136
M_avium : GEYSGVEVGHGALDITLYRDDLM---QKPPRP-LEATSIPAGGIDDALVILVDDVLYSGRSVRSALDALR : 133
D_ethenoge : LRFEGLEIPVGTLDFSLYRDDLD---SQRFHPTIKNTDIPFS-INNKIVVLVDDVLFTGRSTRAAMDALI : 126
H_influenz : EELSSINLPSMELDITFYRDDLTLVDQEDKMPVYSGSSQYLN-IQDKTVILVDDVLFTGRTIRAAMDALT : 121
P_multocid : ADLANVELPSIDLDITFYRDDLEYAEPDSKSPTYSGASSFIS-IHNKEVILVDDVLYTGRTIRAALDALV : 121
H_ducreyi : SELAQISLPLMALDITFYRDDLN---LTSKDPVYTGVEHQLN-IEGKTVILIDDVLFTGRTIRAALDALL : 118
G_sulfurre : EEIEGATVPVGEVDITLYRDDFK--GHAPHLP-VGKTDIPXS-LETKRVVLVDDXLFTGRTIRAAMDAIM : 120
T_aquaticu : AEFEGKEVPVGVLDITLYRDDLT---EIGYRPQVRETRIPFD-LTGKAIVLVDDVLYTGRTARAALDALI : 120
D_radiodur : SELEGVEVPRGMLDITLYRDDLS---EVARQPIIRETQVPFD-LADRRVILVDDVLYTGRTVRAALDALI : 121
A_actino : KLLTQTDIPAFDLDITFYRDDLE-HVQEDQVPVYSGASDFIN-IQHKEVILVDDVLFTGRTIRAALDALV : 120
N_punctifo : ETLEGVAVSVGALDITFYRDDLD----TIGLRTPTKSEIPFD-LTGKTVVLVDDVIFKGRTIRAALNAVN : 120
Synechocys : EMLEQVKVPVGAIDVTLYRDDLK----RIKTRTPAKTKIPLS-LTGKRVVLVDDVIYKGRTIRAALNAVT : 120
P_marinus : LDKTGVDVKKGIIDPTFYRDDQN----RVGTRLIEATDFPTS-IEKKDIVLIDDVIYTGRTIRAAIEALL : 122
Anabaena : ETLEGINVGVGALDITFYRDDLD----QIGLRTPAKTSITLD-LTGKTVVLVDDVIFKGRTIRAALNAVN : 122
g D yRDD
lvDDvl GRt Raa

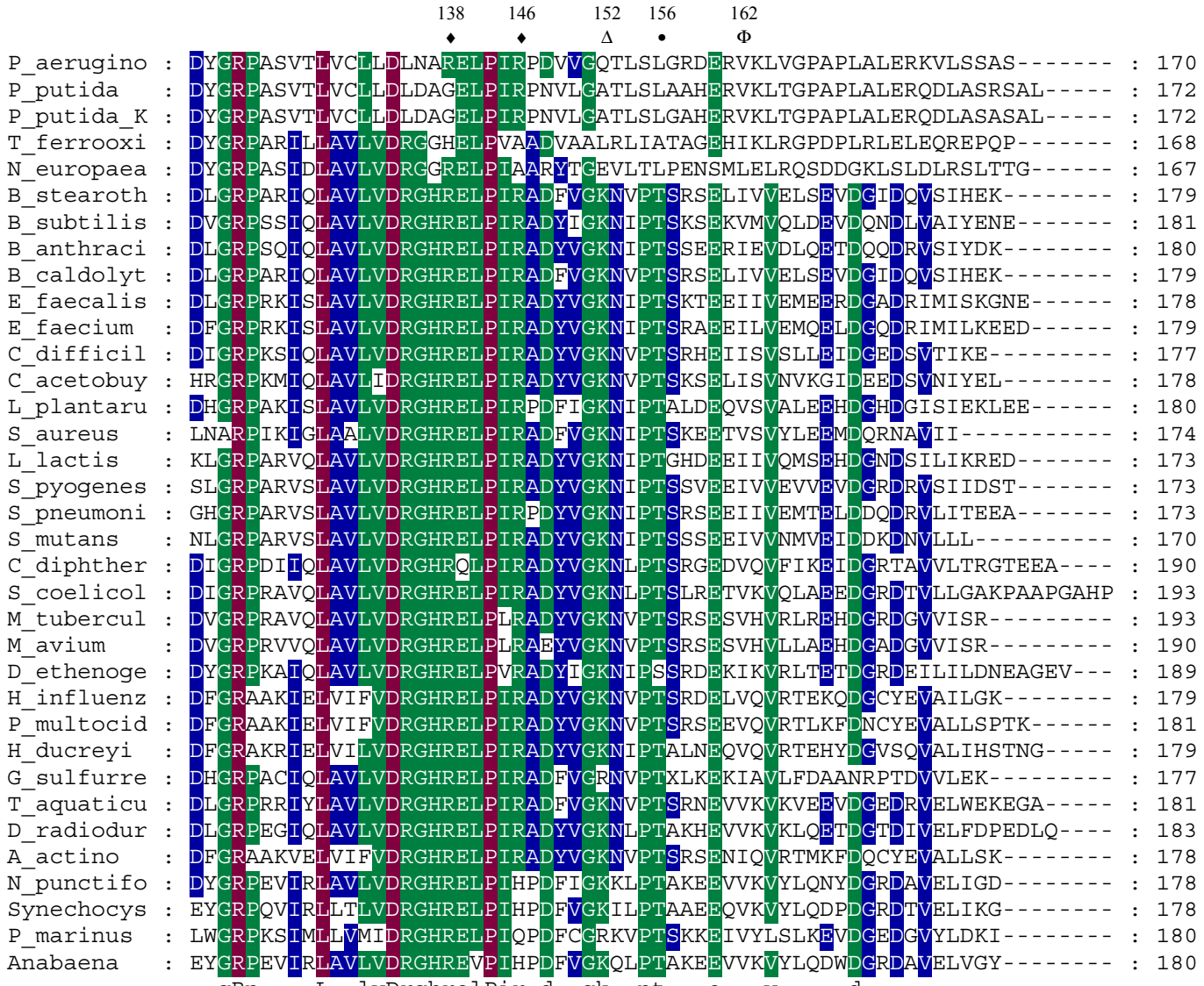
138 146 152 156 162
♦ ♦ Δ • Φ
P_aerugino : DYGRPASVTLVCLLDLNARELPIRPDVVGQTLSLGRDERVKLVGPAPLALERKVLSSAS------- : 170
P_putida : DYGRPASVTLVCLLDLDAGELPIRPNVLGATLSLAAHERVKLTGPAPLALERQDLASRSAL----- : 172
P_putida_K : DYGRPASVTLVCLLDLDAGELPIRPNVLGATLSLGAHERVKLTGPAPLALERQDLASASAL----- : 172
T_ferrooxi : DYGRPARILLAVLVDRGGHELPVAADVAALRLIATAGEHIKLRGPDPLRLELEQREPQP------- : 168
N_europaea : DYGRPASIDLAVLVDRGGRELPIAARYTGEVLTLPENSMLELRQSDDGKLSLDLRSLTTG------ : 167
B_stearoth : DLGRPARIQLAVLVDRGHRELPIRADFVGKNVPTSRSELIVVELSEVDGIDQVSIHEK-------- : 179
B_subtilis : DVGRPSSIQLAVLVDRGHRELPIRADYIGKNIPTSKSEKVMVQLDEVDQNDLVAIYENE------- : 181
B_anthraci : DLGRPSQIQLAVLVDRGHRELPIRADYVGKNIPTSSEERIEVDLQETDQQDRVSIYDK-------- : 180
B_caldolyt : DLGRPARIQLAVLVDRGHRELPIRADFVGKNVPTSRSELIVVELSEVDGIDQVSIHEK-------- : 179
E_faecalis : DLGRPRKISLAVLVDRGHRELPIRADYVGKNIPTSKTEEIIVEMEERDGADRIMISKGNE------ : 178
E_faecium : DFGRPRKISLAVLVDRGHRELPIRADYVGKNIPTSRAEEILVEMQELDGQDRIMILKEED------ : 179
C_difficil : DIGRPKSIQLAVLVDRGHRELPIRADYVGKNVPTSRHEIISVSLLEIDGEDSVTIKE--------- : 177
C_acetobuy : HRGRPKMIQLAVLIDRGHRELPIRADYVGKNVPTSKSELISVNVKGIDEEDSVNIYEL-------- : 178
L_plantaru : DHGRPAKISLAVLVDRGHRELPIRPDFIGKNIPTALDEQVSVALEEHDGHDGISIEKLEE------ : 180
S_aureus : LNARPIKIGLAALVDRGHRELPIRADFVGKNIPTSKEETVSVYLEEMDQRNAVII---------- : 174
L_lactis : KLGRPARVQLAVLVDRGHRELPIRADYVGKNIPTGHDEEIIVQMSEHDGNDSILIKRED------- : 173
S_pyogenes : SLGRPARVSLAVLVDRGHRELPIRADYVGKNIPTSSVEEIVVEVVEVDGRDRVSIIDST------- : 173
S_pneumoni : GHGRPARVSLAVLVDRGHRELPIRPDYVGKNIPTSRSEEIIVEMTELDDQDRVLITEEA------- : 173
S_mutans : NLGRPARVSLAVLVDRGHRELPIRADYVGKNIPTSSSEEIVVNMVEIDDKDNVLLL---------- : 170
C_diphther : DIGRPDILQLAVLVDRGHRQLPIRADYVGKNLPTSRGEDVQVFIKEIDGRTAVVLTRGTEEA---- : 190
S_coelicol : DIGRPRAVQLAVLVDRGHRELPIRADYVGKNLPTSLRETVKVQLAEEDGRDTVLLGAKPAAPGAHP : 193
M_tubercul : DVGRPRAVQLAVLVDRGHRELPLRADYVGKNVPTSRSESVHVRLREHDGRDGVVISR--------- : 193
M_avium : DVGRPRVVQLAVLVDRGHRELPLRAEYVGKNVPTSRSESVHVLLAEHDGADGVVISR--------- : 190
D_ethenoge : DYGRPKAIQLAVLVDRGHRELPVRADYIGKNIPSSRDEKIKVRLTETDGRDEILILDNEAGEV--- : 189
H_influenz : DFGRAAKIELVIFVDRGHRELPIRADYVGKNVPTSRDELVQVRTEKQDGCYEVAILGK-------- : 179
P_multocid : DFGRAAKIELVIFVDRGHRELPIRADYVGKNVPTSRSEEVQVRTLKFDNCYEVALLSPTK------ : 181
H_ducreyi : DFGRAKRIELVILVDRGHRELPIRADYVGKNIPTALNEQVQVRTEHYDGVSQVALIHSTNG----- : 179
G_sulfurre : DHGRPACIQLAVLVDRGHRELPIRADFVGRNVPTXLKEKIAVLFDAANRPTDVVLEK--------- : 177
T_aquaticu : DLGRPRRIYLAVLVDRGHRELPIRADFVGKNVPTSRNEVVKVKVEEVDGEDRVELWEKEGA----- : 181
D_radiodur : DLGRPEGIQLAVLVDRGHRELPIRADYVGKNLPTAKHEVVKVKLQETDGTDIVELFDPEDLQ---- : 183
A_actino : DFGRAAKVELVIFVDRGHRELPIRADYVGKNVPTSRSENIQVRTMKFDQCYEVALLSK-------- : 178
N_punctifo : DYGRPEVIRLAVLVDRGHRELPIHPDFIGKKLPTAKEEVVKVYLQNYDGRDAVELIGD-------- : 178
Synechocys : EYGRPQVIRLLTLVDRGHRELPIHPDFVGKILPTAAEEQVKVYLQDPDGRDTVELIKG-------- : 178
P_marinus : LWGRPKSIMLLVMIDRGHRELPIQPDFCGRKVPTSKKEIVYLSLKEVDGEDGVYLDKI-------- : 180
Anabaena : EYGRPEVIRLAVLVDRGHREVPIHPDFVGKQLPTAKEEVVKVYLQDWDGRDAVELVGY-------- : 180
gRp L lvDrghrelPir d gk pt e v d

Fig. 34. Aligned amino acid sequences of PyrR proteins from various organisms. Key amino acid residues are denoted by the following symbols: R (♦); E (♣); T (●); V (Φ); K (Δ). Bacterial genomes currently being sequenced: The Institute for Genomic Research (TIGR); *Bacillus anthracis* Ames, *Dehalococcoides ethenogenes*, *Enterococcus faecalis* V583, *Geobacter sulfurreducens*, *Mycobacterium tuberculosis* H37Rv, *Mycobacterium avium* 104, *Staphylococcus aureus* COL, *Streptococcus pneumoniae* type 4, and *Thiobacillus ferridoxin* ATCC 23270. The Sanger Centre (S.C.); *Clostridium difficile* 630 (epidemic type X), *Corynebacterium diphtheriae* NCTC 13129, *Streptomyces coelicolor* A3(2). Genome Therapeutics Corporation (GTC); *Clostridium acetobutylicum* ATCC 824D. Joint Genome Institute (JGI); *Enterococcus faecium* ATCC 35667, *Nitrosomonas europeae*, *Nostoc punctiforme*, *Prochlorococcus marinus* MED 4. University of Oklahoma Advanced Center for Genome Technology (OU-ACGT); *Actinobacillus actinomycetemcomitans* HK1651, *Bacillus stearothermophilus* 10, *Streptococcus pyogenes* SF370 (MI), *Streptococcus mutans* UAB159. Integrated Genomics Inc. (IGI); *E. faecium* ATCC 35667. Kazusa DNA Research Institute & Michigan State University; *Anabaena* SP PCC7120. London School of Hygiene and Tropical Medicine (LSHTM), Imperial College & Eastman Dental Institute; *Clostridium difficile* 630 (epidemic type X). Public Health Lab Service (PHLS), Degussa AG & Bielefeld University; *Corynebacterium diphtheriae* NCTC 13129. University of Minnesota; *Pasteurella multocida* Pm70. University of Washington; *Haemophilus ducreyi* 35000 HP. John Innes Centre; *Streptomyces coelicolor* A3(2). University of Massachusetts at Amherst and Exxon Corporation; *Geobacter sulferreducens*. Completed sequences*: Bacillus subtilis* (Quinn *et al*., 1991), *Bacillus caldolyticus* (Ghim & Neuhard, 1994), *Deinococcus radiodurans* (White *et al*., 1999), *Haemophilus influenzae* (Fleischmann *et al*., 1995), *Lactobacillus plantarum* (Elagöz *et al*., 1996), *Lactococcus lactis* (Bolotin *et al*., 1999), *Synechocystis* sp. PCC6803 (Kaneko *et al*., 1996), and *Thermus aquaticus* Z05 (Van de Casteele *et al*., 1997).

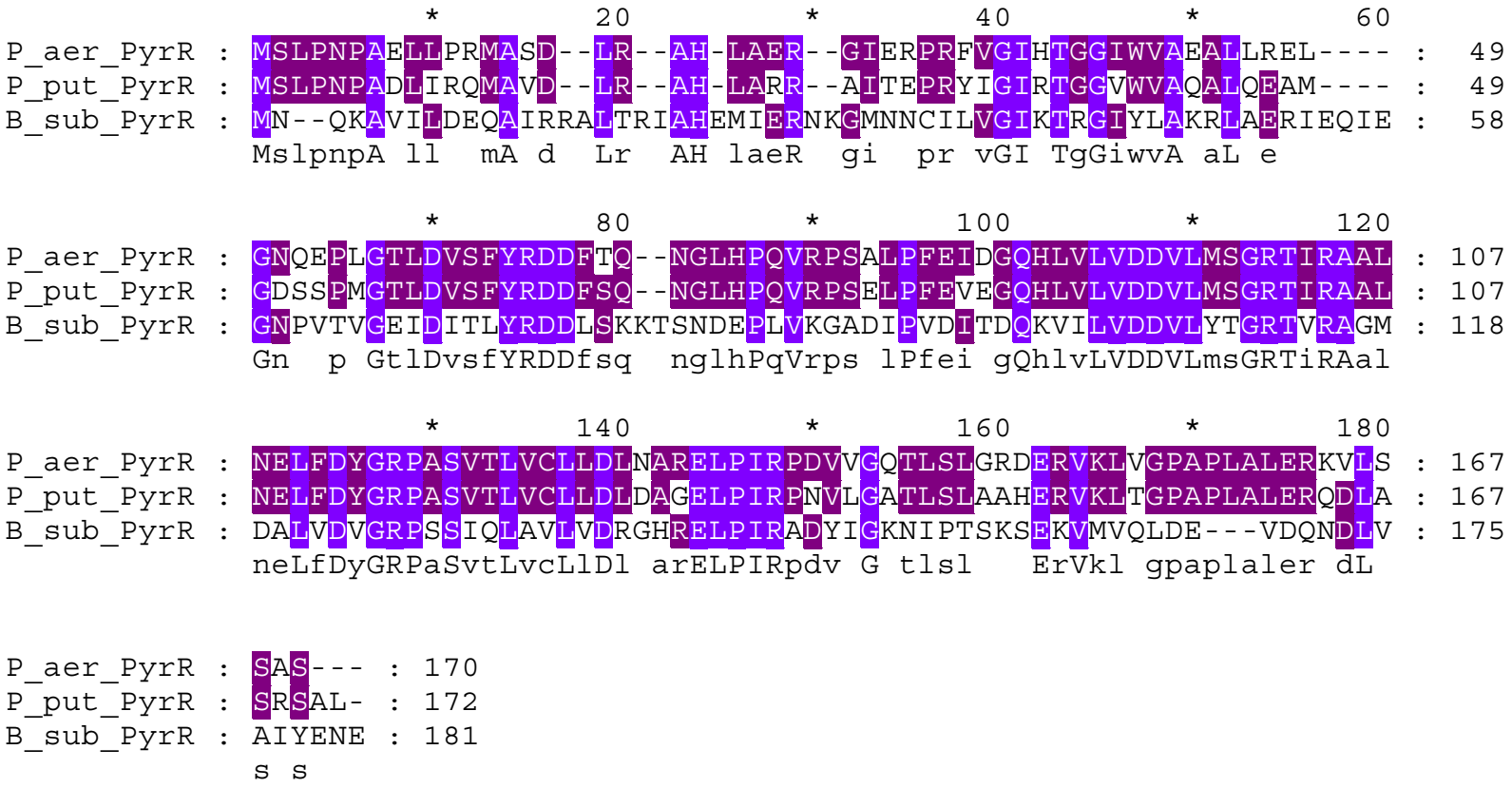

Fig. 35. Alignment of the *P. aeruginosa* and *P. putida* PyrR protein sequences with the *B. subtilis* sequence.

of *P. putida* (Fig. 35). Most of these 41 amino acids were unique to the *Pseudomonas* PyrR sequences.

***In vitro* transcription and translation analysis.**

The *P. aeruginosa pyrR* gene on a ~800 bp DNA fragment was cloned into the expression vector pCR™II (Fig. 10., Invitrogen) in the same orientation to that of the *lac* promoter, to create pMVP1 (Fig. 11). The same ~800 bp DNA fragment which contained the 510 bp *pyrR* gene was also cloned in an orientation opposite to the *lac* promoter on the pCR™II vector to create pMVP2 (Fig. 12). To determine if the *P. aeruginosa pyrR* gene encoded a protein product, an i*n vitro* transcription/translation (Zubay, 1973) was performed using plasmid pMVP1, with pMVP2 as a negative control. Based on gene sequence, the theoretical molecular mass of this PyrR protein was deduced to be 19 kDa. However on a SDS-PAGE gel, the 510 bp *pyrR* gene encoded a protein that electrophoresed at 24 kDa (Fig. 36). Such differences between actual and theoretical weights could be explained by the effect of charge on the mobility of small proteins in SDS-PAGE (Swank & Munkres, 1971; Merle & Kadenbach, 1980). The *in vitro* transcription/translation sample was also analyzed under non-denaturing conditions, the native PyrR protein migrated to a locus between the 66 kDa and 132 kDa molecular weight markers. Based on a monomer of 19 kDa, this most likely corresponded to a tetramer with an apparent molecular mass of ~80 kDa (Fig. 37).

An *in vitro* transcription/translation analysis was also performed using plasmid pMVP5 (Fig. 18) to determine the apparent molecular mass of the *P. aeruginosa* Upp

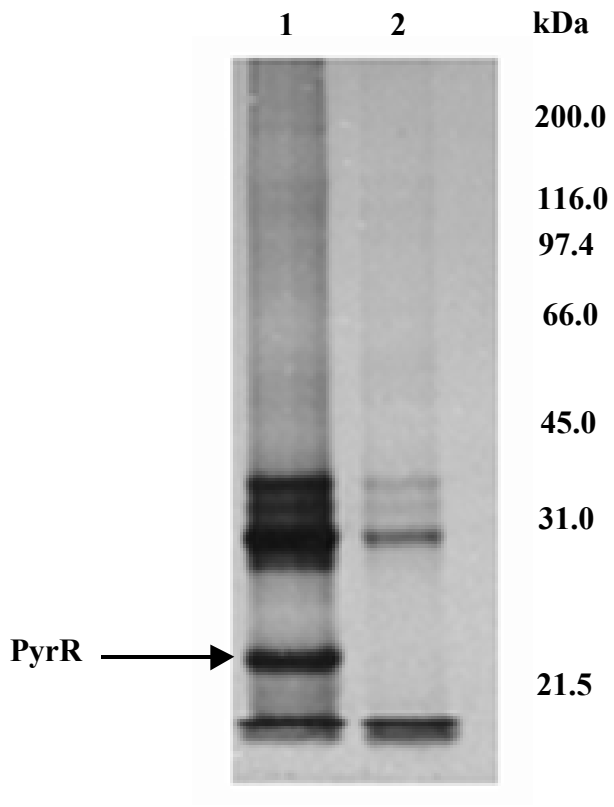

Fig. 36. Autoradiogram of SDS-12% PAGE from *in vitro* transcription and translation analysis (Zubay, 1973) to determine apparent subunit size of the PyrR protein from *P. aeruginosa*. Lanes: 1, expression of the *pyrR* gene cloned in the same orientation as the *lac* promoter on the vector (pMVP1); 2, expression of the *pyrR* gene cloned in an orientation opposite to the *lac* promoter, (pMVP2, control). The molecular masses of the protein markers are shown alongside.

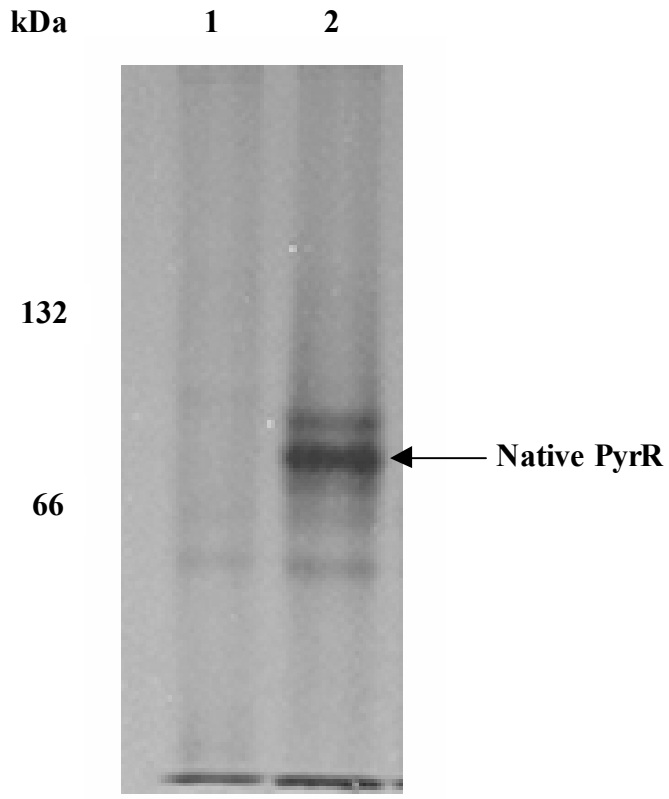

Fig. 37. Autoradiogram of native-10% PAGE from *in vitro* transcription and translation analysis (Zubay, 1973) to determine apparent native size of the PyrR protein from *P. aeruginosa*. Lanes: 1, expression of the *pyrR* gene cloned in an orientation opposite to the *lac* promoter on the vector (pMVP2, control); 2, expression of the *pyrR* gene cloned in the same orientation as the *lac* promoter, (pMVP1). The molecular masses of the protein markers are shown alongside.

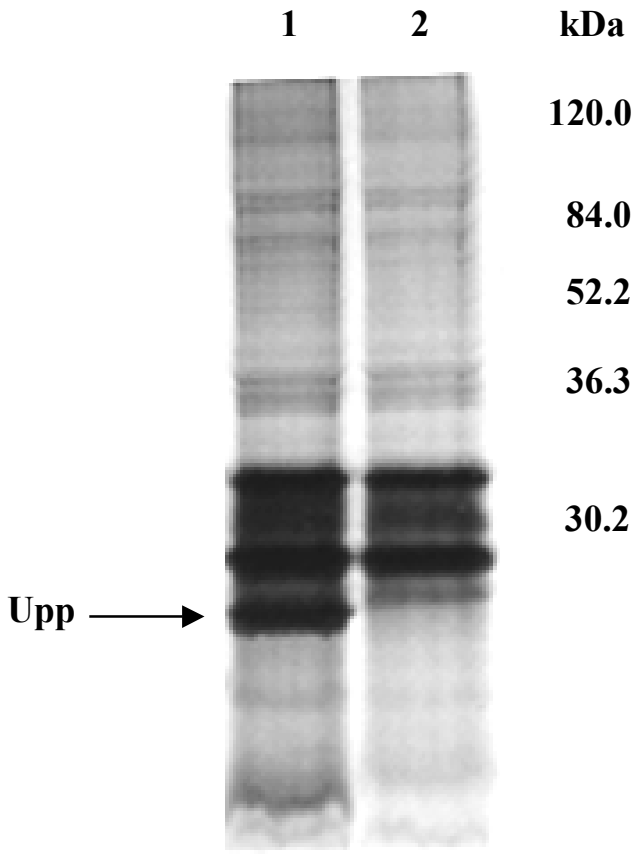

Fig. 38. Autoradiogram of SDS-12% PAGE from *in vitro* transcription and translation analysis (Zubay, 1973) to determine apparent subunit size of the Upp protein from *P. aeruginosa*. Lanes: 1, expression of the *upp* gene cloned in the same orientation as the *lac* promoter on the vector (pMVP5); 2, expression of the *upp* gene cloned in an orientation opposite to the *lac* promoter, (pMVP6, control). The molecular masses of the protein markers are shown alongside.

protein. Plasmid pMVP6 (Fig. 19) containing the *upp* gene cloned in an orientation opposite to the *lac* promoter was used as a negative control. Results showed that the Upp protein electrophoresed at approximately 28 kDa (Fig. 38).

Insertional inactivation of *pyrR* by cassette mutagenesis.

To determine the effect of PyrR on the expression of pyrimidine genes, the *pyrR* gene on the *P. aeruginosa* chromosome was inactivated by gene replacement, using a gentamicin cassette. Mating experiments were performed and a *P. aeruginosa pyrR* deletion strain, MVP7401 was isolated. The pyrimidine enzymes encoded by *pyrB*, *pyrC*, *pyrD*, *pyrE* and *pyrF* were assayed in *P. aeruginosa* AK903 and in the isogenic *pyrR* mutant strain, MVP7401. Results seen in Table 5 showed that inactivation of the *pyrR* gene caused approximately a two-fold decrease in expression of the *pyrBC'*, *pyrD* and *pyrE* genes, and about a three-fold decrease in the expression of *pyrF* compared to expression of these genes in the isogenic wild type strain. Expression of *pyrC* was the least affected, being reduced only 20% by inactivation of *pyrR*. The decrease in expression of the *pyr* genes suggested that PyrR was a positive regulator of the expression of the downstream pyrimidine biosynthetic genes. The role of PyrR as an activator is unique to *Pseudomonas*, as the well characterized PyrR protein from *B. subtilis* is a mRNA-binding attenuation protein. Interestingly, a polar effect was observed for expression of the *pyrBC'* genes, since inactivation of the *pyrR* gene did not completely diminish *pyrBC'* expression. Primer extension and complementation studies in *P. putida* showed the presence of a second transcription-start site located about 67-69

bp upstream of the *pyrBC'* translational start and a putative promoter region that resulted in the extension of a minor transcript. In addition, a *P. putida pyrR* mutant harboring the *pyrR* gene on a plasmid restored parental gene expression levels in all except the *pyrBC'* genes (Kumar, 2000). The low ATCase activity observed in the *P. aeruginosa pyrR* mutant suggested the presence of two promoters governing expression of the *P. aeruginosa pyrRBC'* operon. The stronger P_1 promoter located 67 bp upstream of the PyrR translational start generates the major transcript as a single *pyrRBC'* message while the minor *pyrBC'* transcript is generated from the second P_2 promoter located upstream of the *pyrBC'* genes (Fig. 39).

Table 5. Specific activities of the pyrimidine biosynthetic enzymes in *P. aeruginosa* wild type and *pyrR* mutant.

Enzyme	**Specific Activity (μmol min^{-1} mg protein^{-1})**	
	AK903 (*pyrR*$^{+}$)	MVP7401 (*pyrR*$^{-}$)
Aspartate transcarbamoylase (*pyrB*)	107.8	40.3
Dihydroorotase (*pyrC*)	152.3	126.4
Dihydroorotate dehydrogenase (*pyrD*)	32.0	16.3
Orotate phosphoribosyltransferase (*pyrE*)	22.8	12.5
OMP decarboxylase (*pyrF*)	18.4	6.6

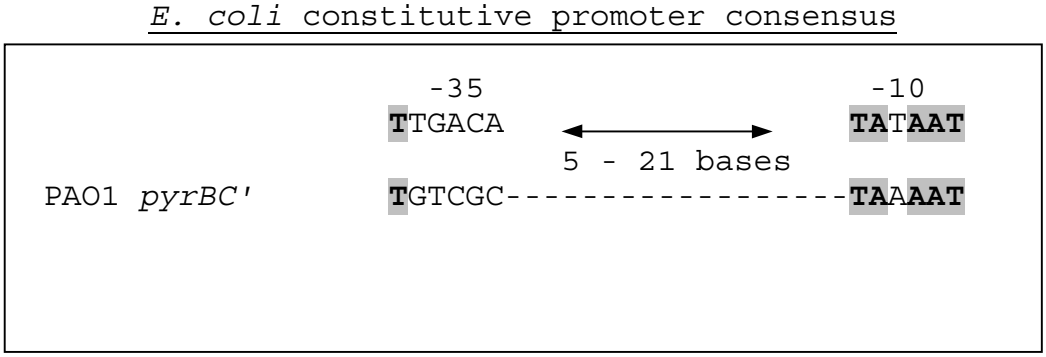

Fig. 39. *Pseudomonas pyrBC'* promoter (P_2) sequence.

Autoregulation by PyrR.

Computer analysis of the *pyrR* promoter region revealed a potential RNA secondary structure formation suggestive of autoregulation (Fig. 32). To determine if PyrR is under autogenous control, the DNA upstream of the *pyrR* coding sequence was cloned into the reporter gene vector, pQF50. The resulting *pyrR*::*lacZ* transcriptional fusion plasmid, pMVP50 was electroporated into *P. aeruginosa pyrR* mutant strain, MVP7401 and assayed for β-galactosidase activity against its isogenic wild type strain as described in Materials and Methods. Results indicated an upto three-fold increase in β-galactosidase activity in the *pyrR* mutant strain compared to the wild type strain (Table. 4, Fig. 33). In the absence of the PyrR protein there was a higher level of *pyrR* expression, with PyrR negatively regulating its own expression. The scattered distribution of the *pyr* genes throughout the genome suggested that the *P. aeruginosa* PyrR was more likely to be a DNA binding protein. The approximate location of these *pyr* genes in the *P. aeruginosa* genome are *pyrBC'* (20'), *pyrC* (35'), $pyrC_3$ (74'), *pyrD* (40'), *pyrE* (9') and *pyrF* (50'). The *pyr* genes in *B. subtilis* are arranged in an operon and expressed from a single message, a situation more conducive to regulation by an RNA binding protein. Results from the above *pyrR*::*lacZ* transcriptional fusion assay suggested that PyrR binds DNA. The decrease in β-galactosidase expression, seen in the wild type compared to the *pyrR* mutant should be possible only if the PyrR bound to the DNA fragment.

Purification of PyrR.

To prove the PyrR proteins ability to bind DNA, the protein was purified by classic chromatographic methods, for testing both autoregulation and DNA binding to the downstream *pyr* genes. For affinity chromatography, the *P. aeruginosa pyrR* was fused to the glutathione S-transferase (GST) gene from *Schistosoma japonicum*, and cloned into the expression vector pGEX-2T which has a thrombin protease recognition site for cleaving the PyrR protein from the fusion product. The resulting plasmid, pMVP10, was sequenced to ensure in frame translation of PyrR from the GST protein tag. Sequence data showed that PyrR was translated in frame as a fusion from the GST protein, and that the first methionine codon of the PyrR protein was replaced with a glycine residue. The plasmid pMVP10 was transformed in *E. coli* BL21, a protease deficient host strain commonly used for high-level expression of recombinant proteins (Studier & Moffatt, 1986), and expression of the fusion protein was induced with IPTG. To determine the IPTG concentration at which optimal expression could be achieved, 50 ml cultures of *E. coli* BL21 harboring pMVP10 were induced with IPTG varying from 0.1 mM to 0.9 mM, and analyzed by SDS-PAGE (Fig. 40). Results showed that 0.1 mM IPTG was sufficient for maximal expression of the GST protein, since the intensity of the band which corresponded to the GST protein did not increase at IPTG concentrations greater than 0.1 mM. An induction time course study was performed to determine the length of time that allowed for maximum yield of the fusion protein. A 50 ml culture of *E. coli* BL21 harboring pGEX-2T was induced with 0.1 mM IPTG and 1 ml aliquots were removed at 1 h intervals for up to 6 h, and the samples were analyzed by SDS-PAGE (Fig. 41).

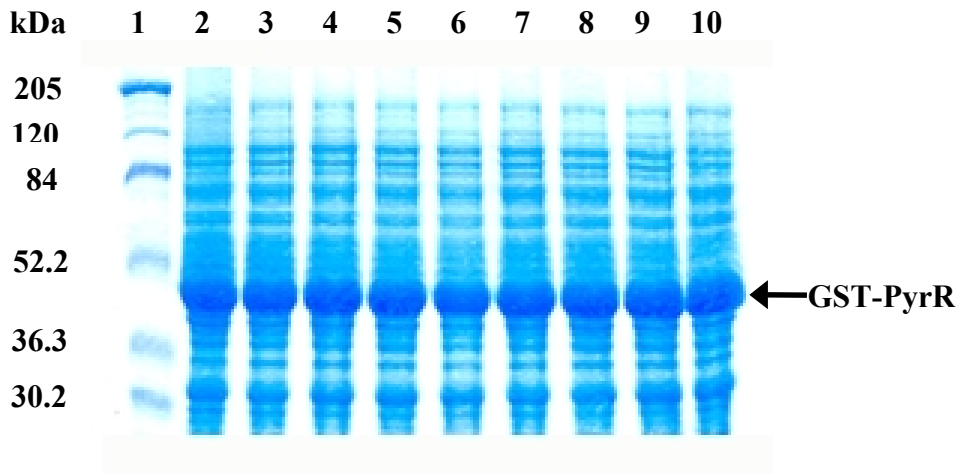

Fig. 40. SDS-12% PAGE analysis of samples obtained from the induction study to determine optimum IPTG concentration for expression of pMVP10 in *E. coli* BL21. All inductions were performed for 4 h. Lanes: 1, molecular mass marker (myosin, 205 kDa; β-galactosidase, 120 kDa; bovine serum albumin, 84 kDa; ovalbumin, 52.2 kDa; carbonic anhydrase, 36.3 kDa; and soybean trypsin inhibitor, 30.2 kDa); 2, 0.1 mM IPTG; 3, 0.2 mM IPTG; 4, 0.3 mM IPTG; 5, 0.4 mM IPTG; 6, 0.5 mM IPTG; 7, 0.6 mM IPTG; 8, 0.7 mM IPTG; 9, 0.8 mM IPTG; 10, 0.9 mM IPTG.

Results showed that an induction time of 4 h was sufficient for optimal expression of the GST::PyrR fusion protein. All subsequent cultures for protein expression were therefore induced with 0.1 mM IPTG for 4 h. Most of the contaminating cellular proteins were removed from the clarified lysate by ammonium sulfate fractionation. A step gradient fractionation was performed to determine the percent saturation at which the fusion protein was precipitated (Fig. 42), most of the GST::PyrR fusion precipitated between 30 and 40% saturation. These two fractions were pooled and used for batch purification using glutathione Sepharose 4B as the affinity matrix. SDS-PAGE analysis of the fractions obtained throughout the affinity chromatography purification procedure is shown in Fig. 43. Eluates 1, 2 and 3 shown in lanes 8, 9 and 10 respectively contained the GST::PyrR fusion, however these fractions also contained contaminating proteins. This indicated that some non-specific proteins bound to the glutathione Sepharose 4B matrix. Anion exchange chromatography was employed to remove these contaminating proteins, however before further purification, the eluate fractions were pooled and treated with thrombin protease to cleave PyrR from the GST tag. To determine the optimal cleavage time with thrombin, a time course study was performed. A 200 µl aliquot of the GST::PyrR fusion was incubated with 50 units of thrombin protease at 4°C, and 20 µl samples were removed at 1 h intervals for up to 8 h and analyzed by SDS-PAGE (Fig. 44). Results showed that an 8 h incubation did not allow for complete cleavage. Based on this information, a cleavage time of ~16 h (overnight) was adopted for the purification

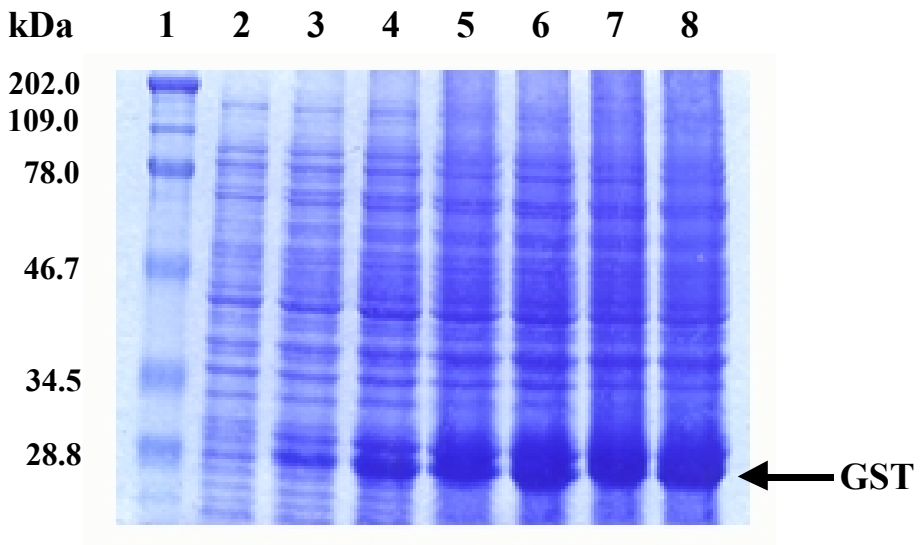

Fig. 41. SDS-12% PAGE analysis of samples obtained from the time-course IPTG induction study. The cells were induced with 0.1 mM IPTG. Lanes: 1, molecular mass marker (myosin, 202 kDa; β-galactosidase, 109 kDa; bovine serum albumin, 78 kDa; ovalbumin, 46.7 kDa; carbonic anhydrase, 34.5 kDa; and soybean trypsin inhibitor, 28.8 kDa); 2, uninduced cells (0 h); 3, 1 h induction; 4, 2 h induction; 5, 3 h induction; 6, 4 h induction; 7, 5 h induction; 8, 6 h induction.

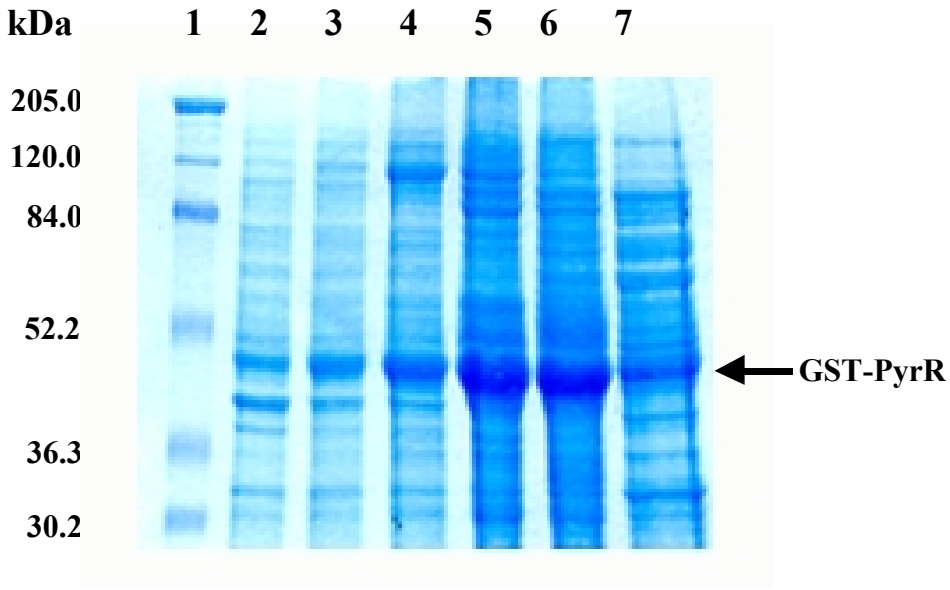

Fig. 42. SDS-12% PAGE analysis of samples obtained from the ammonium sulfate fractionation of pMVP10 expressed in *E. coli* BL21. Lanes: 1, molecular mass marker (myosin, 205 kDa; β-galactosidase, 120 kDa; bovine serum albumin, 84 kDa; ovalbumin, 52.2 kDa; carbonic anhydrase, 36.3 kDa; and soybean trypsin inhibitor, 30.2 kDa); 2, 20% saturation; 3, 25% saturation; 4, 30% saturation; 5, 35% saturation; 6, 40% saturation; 7, 45% saturation.

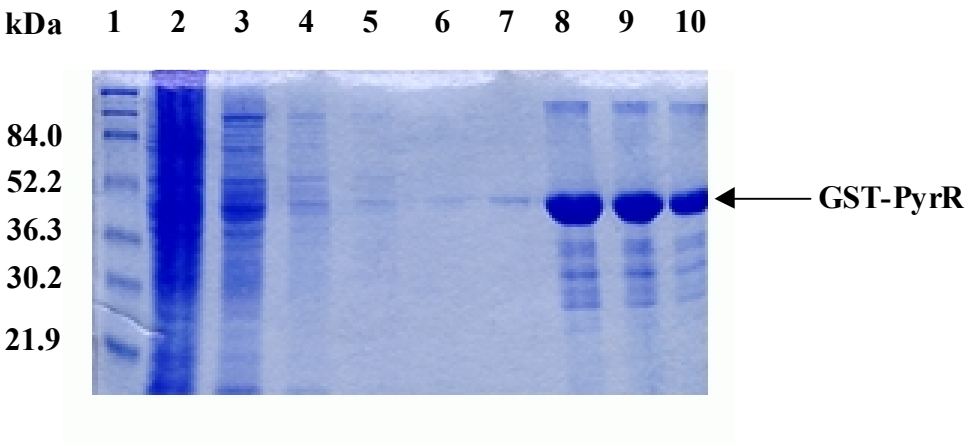

Fig. 43. SDS-12% PAGE analysis of the fractions collected during affinity chromatography purification of *P. aeruginosa* PyrR. Washes were with 5 ml of 1X PBS, pH 7.3 and fusion protein was eluted with 2 ml of 10 mM reduced glutathione. Lanes: 1, molecular mass marker (bovine serum albumin, 84 kDa; ovalbumin, 52.2 kDa; carbonic anhydrase, 36.3 kDa; soybean trypsin inhibitor, 30.2 kDa; and lysozyme, 21.9 kDa); 2, flow through; 3, wash 1; 4, wash 2; 5, wash 3; 6, wash 4; 7, wash 5; 8, eluate 1; 9, eluate 2; 10, eluate 3. The proteins were visualized by Coomassie blue staining.

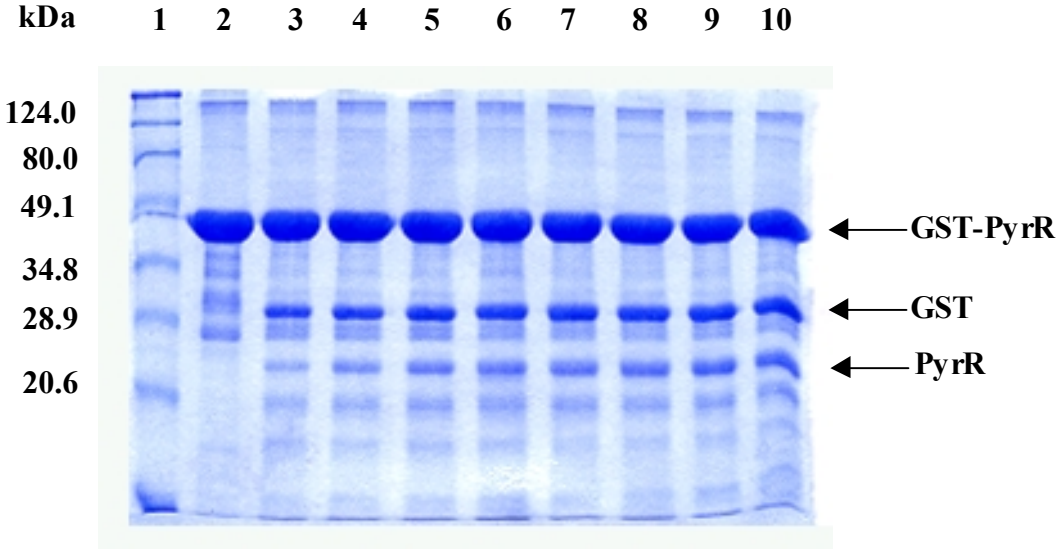

Fig. 44. SDS-12% PAGE of samples obtained from time course cleavage of *P. aeruginosa* PyrR from the GST tag. The fusion protein was incubated with 50 units of thrombin protease. Lanes: 1, molecular mass standards (β-galactosidase, 124 kDa; bovine serum albumin, 80 kDa; ovalbumin, 49.1 kDa; carbonic anhydrase, 34.8 kDa; soybean trypsin inhibitor, 28.9 kDa; and lysozyme, 20.6 kDa); 2, uncleaved sample (0 h incubation with thrombin); 3, after 1 h incubation; 4, after 2 h incubation; 5, after 3 h incubation; 6, after 4 h incubation; 7, after 5 h incubation; 8, after 6 h incubation; 9, after 7 h incubation; 10, after 8 h incubation. Proteins were visualized by Coomassie blue staining.

procedure. The thrombin treated fraction was subjected to anion-exchange chromatography on DEAE Sepharose for the next step in the purification. Results from Figure 45 showed that the bulk of the GST protein eluted in the 0 M NaCl (lane 1), the 0.1 M NaCl fraction contained most of the uncleaved GST::PyrR fusion, the remainder of the GST and about 50% of the PyrR protein. The remainder of the PyrR protein eluted with 0.2 M NaCl however this fraction also contained small amounts of the GST and fusion proteins.

Western blot analysis.

To establish that the purified protein which corresponded to an apparent molecular mass of 21 kDa was the *P. aeruginosa* PyrR protein, a Western blot analysis was performed with polyclonal antibodies raised against the *B. subtilis* PyrR protein (kindly provided by Dr. R. L. Switzer, University of Illinois). These antibodies cross-reacted with crude extract from wild type *P. aeruginosa* (data not shown), with pure PyrR protein and with the GST::PyrR fusion protein from *P. aeruginosa* (Fig. 46), which suggested that these two proteins bore similar antigenic epitopes. The same antibodies did not react with the negative control, *E. coli* JM109 crude extract.

Purification of the Upp protein.

Prior to the affinity chromatography step, the majority of the contaminating cellular proteins from the clarified lysate were removed by ammonium sulfate fractionation. A step gradient fractionation was performed to determine the percent saturation at which the

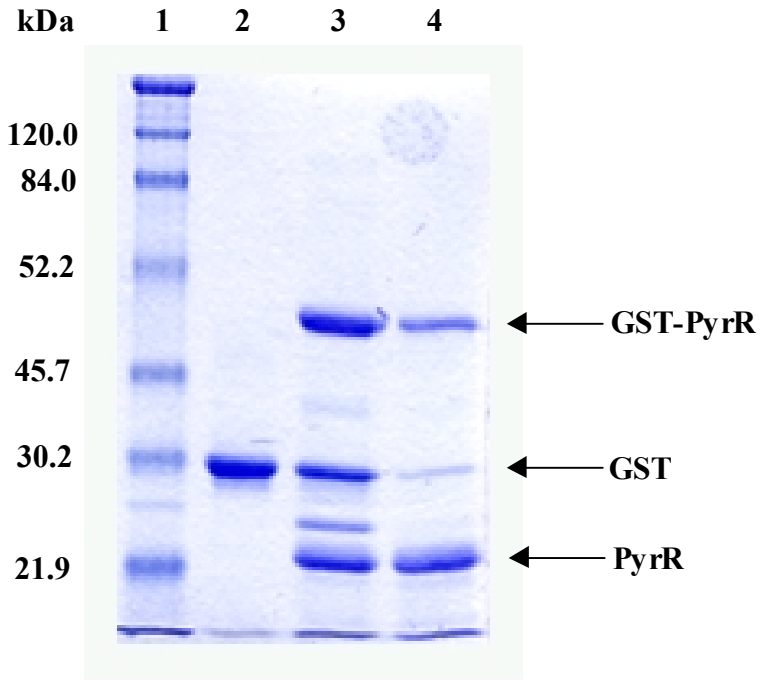

Fig. 45. SDS-15% PAGE analysis of the fractions collected during the DEAE anion exchange chromatography purification of *P. aeruginosa* PyrR. Lanes: 1, molecular mass marker (β-galactosidase, 120 kDa; bovine serum albumin, 84 kDa; ovalbumin, 52.2 kDa; carbonic anhydrase, 36.3 kDa; soybean trypsin inhibitor, 30.2 kDa; and lysozyme, 21.9 kDa); 2, 0 M NaCl elution; 3, 0.1 M NaCl elution; 4, 0.2 M NaCl elution. The proteins were visualized by Coomassie Blue staining.

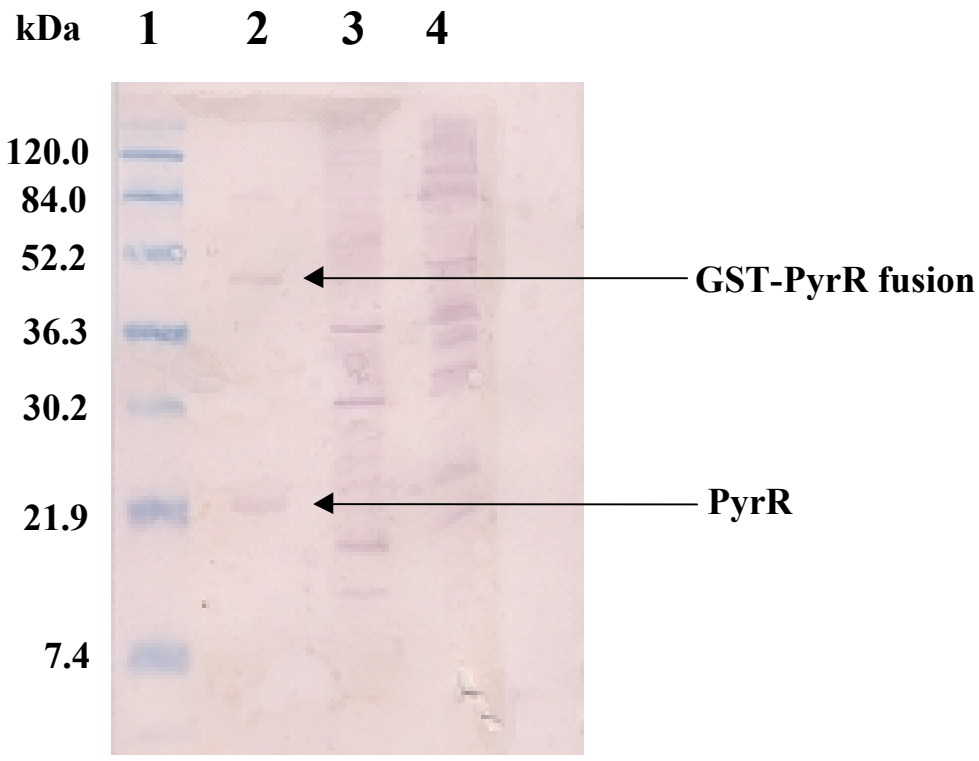

Fig. 46. Western blot with antibodies raised against PyrR from *Bacillus subtilis*. PyrR antiserum (1:1000) was probed against 10 μg of total protein. Lanes: 1, molecular mass marker (*β*-galactosidase, 120 kDa; bovine serum albumin, 84 kDa; ovalbumin, 52.2 kDa; carbonic anhydrase, 36.3 kDa; soybean trypsin inhibitor, 30.2 kDa; and lysozyme, 21.9 kDa; aprotinin, 7.4 kDa); 2, purified *P. aeruginosa* PyrR; 3, wild type *B. subtilis* crude extract; 4, *E. coli* JM109 crude extract.

GST-Upp fusion protein precipitated (Fig. 47), most of the GST-Upp fusion appeared to precipitate between 20 and 40% saturation. These three fractions were pooled and used for batch purification using glutathione Sepharose 4B as the affinity matrix. The eluate which contained the GST-Upp fusion protein was cleaved with thrombin protease, and the cleaved sample was subjected to a second round of batch purification to remove the GST tag. SDS-PAGE analysis (Fig. 48) showed that affinity chromatography sufficiently removed all contaminating proteins leaving only purified Upp protein.

RNA-binding electrophoretic mobility shift assay (EMSA).

Switzer and co-workers have shown using a RNA-binding EMSA that the *B. subtilis* PyrR protein binds to the *pyr* mRNA. To determine if the *P. aeruginosa* could be an RNA-binding protein, a RNA-binding EMSA using purified *P. aeruginosa* PyrR protein with mRNA isolated from *B. subtilis* was performed by Heather Savacool-Bonner of Dr. R.L. Switzer's research group, University of Illinois (data not shown). The results showed that the *P. aeruginosa* PyrR did not bind to the *pyr* mRNA from *B. subtilis*, suggesting that it was not likely to be a RNA-binding protein since all other RNA-binding PyrR proteins have the conserved residues shown by Switzer and co-workers be involved in binding RNA.

DNA-binding EMSA.

Data from *pyr* enzyme assays in a *pyrR* cassette deletion mutant, PyrR sequence analysis and data obtained from *pyrR*::*lacZ* transcriptional fusion assays all

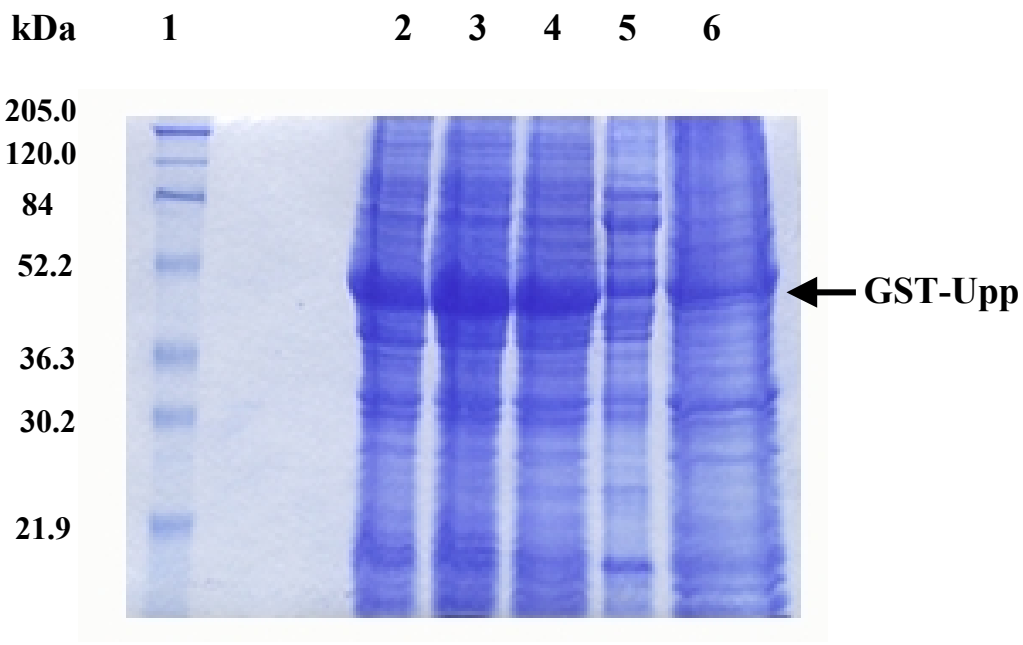

Fig. 47. SDS-12% PAGE analysis of samples obtained from the ammonium sulfate fractionation of pMVP11 expressed in *E. coli* BL21. Lanes: 1, molecular mass marker (myosin, 205 kDa; β-galactosidase, 120 kDa; bovine serum albumin, 84 kDa; ovalbumin, 52.2 kDa; carbonic anhydrase, 36.3 kDa; and soybean trypsin inhibitor, 30.2 kDa; lysozyme, 21.9 kDa); 2, 20% saturation; 3, 25% saturation; 4, 30% saturation; 5, 40% saturation; 6, 50% saturation.

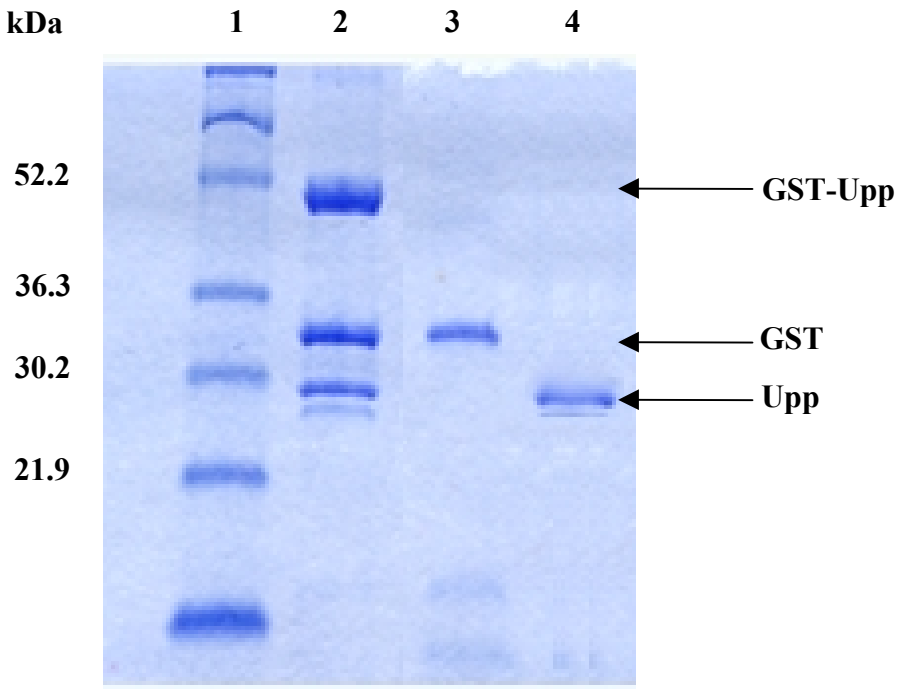

Fig. 48. SDS-12% PAGE analysis of fractions obtained during affinity chromatography purification of *P. aeruginosa* Upp. The fusion protein was eluted with 2 ml of 10 mM reduced glutathione. Lanes: 1, molecular mass marker (ovalbumin, 52.2 kDa; carbonic anhydrase, 36.3 kDa; soybean trypsin inhibitor, 30.2 kDa; and lysozyme, 21.9 kDa); 2, Eluate after first round of batch purification treated with thrombin protease showing incomplete cleavage; 3, Eluate after second round of batch purification showing GST tag; 4, Supernatant from second round of batch purification showing purified Upp protein.

suggest PyrR to be a DNA-binding regulatory protein. To test this, a DNA-binding EMSA was performed with purified PyrR protein using end-labeled DNA fragments containing the promoter regions of the *pyrR*, *pyrD*, *pyrE* and *pyrF* genes. The *in vitro* assays were carried out in the absence and presence of orotate, OMP, UMP and PRPP, which were considered to be potential ligands for the following reasons: (i) orotate is a key intermediate in the pyrimidine pathway and the substrate for *pyrE* encoded OPRTase, another control point in the biosynthetic pathway. (ii) OMP is the product of the OPRTase reaction but also serves as a substrate for OPRTase acting in reverse. This reverse reaction has been shown to be favored in *E. coli* and *S. typhimurium* (Jensen, 1982), although this equilibrium has not been studied in *P. aeruginosa*, it could be assumed to be the same in *Pseudomonas*. Therefore, OMP could serve as a signal molecule to indicate high pyrimidine levels, (iii) UMP is the product of the biosynthetic pathway and shown to act as a co-repressing molecule in *B. subtilis*. When pyrimidine levels are high, UMP binds to the *B. subtilis* PyrR enabling it to bind to the mRNA and decrease expression of the *pyr* genes; no decrease in expression was observed in the absence of UMP binding. The binding of UMP to the *B. subtilis* PyrR has been shown by crystal structure data to involve four key residues; Arg-138 (♦), Thr-156 (•), Thr-41 and Val-162 (Φ). The presence of the latter two of these residues in the *P. aeruginosa* PyrR sequence (Fig. 34) suggested that UMP might also be a ligand for the *P. aeruginosa* PyrR protein, and (iv) a conserved PRPP binding domain identified in the *B. subtilis* PyrR sequence was also present in the *P. aeruginosa* PyrR sequence. In addition, PRPP has been shown to antagonize the RNA-binding capability of the *B. subtilis* PyrR protein.

Results from the EMSA of purified PyrR with the upstream promoter region of the *pyrR* gene (Fig. 49), showed that the PyrR protein bound to the DNA containing the upstream sequence of the *pyrR* gene in the absence of any ligands (lane 2), and in the presence of 0.1 mM orotate (lane 3) or 0.1 mM UMP (lane 5). This was indicated by the retarded electrophoretic mobility of the DNA/protein complex compared to the mobility of the free DNA probe (lane 1). In other words either, orotate and UMP were not ligands for PyrR, or they bound to PyrR but did not affect or promote its ability to bind DNA. The addition of 0.1 mM OMP (lane 4) or 0.1 mM PRPP (lane 6) to the binding reaction obstructed PyrR from binding to the *pyrR* DNA, establishing both PRPP and OMP as ligands for the *P. aeruginosa* PyrR protein. An EMSA using DNA fragments containing the promoter regions of the biosynthetic genes, *pyrD*, *pyrE* and *pyrF* showed the PyrR protein bound to all three genes (Figs. 50, 51, 52), respectively under the same conditions as for the *pyrR* gene. A DNA/protein complex was formed in the absence of any ligands and in the presence of orotate or UMP, and the formation of the DNA/protein complex was prevented in the presence of OMP or PRPP.

Since PyrR has been determined to be an activator protein for the *pyrD*, *pyrE* and *pyrF* genes and a repressor protein for autoregulation, it was thought that the PyrR protein would have a greater affinity for the *pyr* genes than for its own DNA. To determine the binding specificity of PyrR to its own DNA *versus* the DNA of the downstream *pyr* genes, EMSA assays were performed with the DNA concentration held constant at 5,000 cpm and varying the PyrR concentration from 0.1 μg to 5 μg (Figs. 55, 56). The intensity of the bands were measured with a video densitometer using a

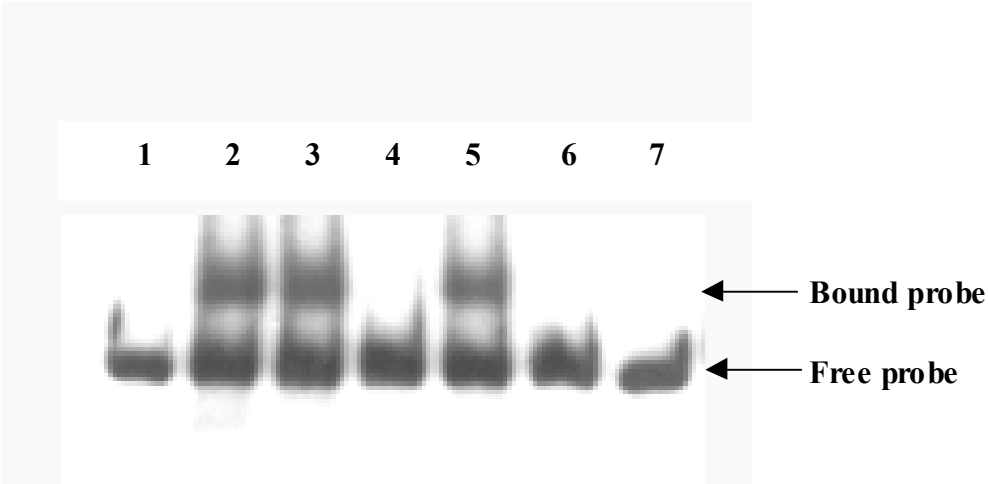

Fig. 49. Autoradiograph of a 4% polyacrylamide gel showing the DNA-binding EMSA of purified PyrR with the *pyrR* promoter fragment used as the end-labeled probe. All reactions were carried out using 5,000 cpm of DNA and 13 nM purified PyrR protein. Lanes: 1, DNA probe without protein; 2, DNA probe and PyrR; 3, DNA probe, PyrR and 0.1 mM orotate; 4, DNA probe, PyrR and 0.1 mM OMP; 5, DNA probe, PyrR and 0.1 mM UMP; 6, DNA probe, PyrR and 0.1 mM PRPP; 7, DNA probe without protein.

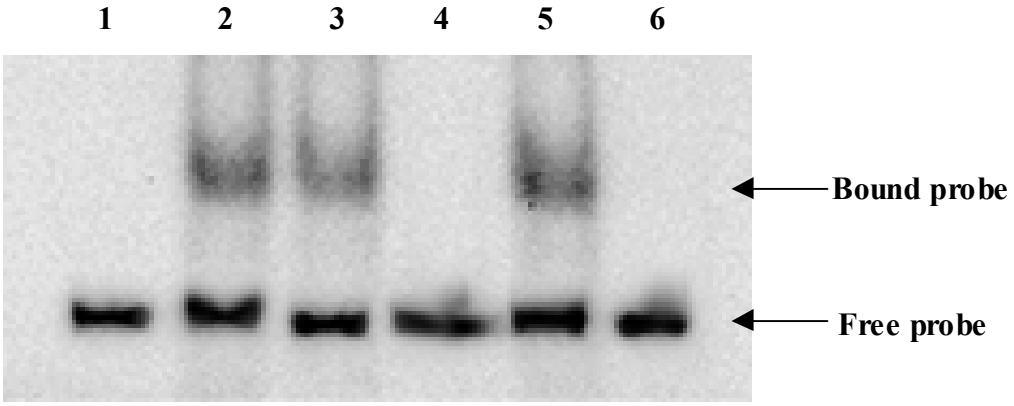

Fig. 50. Autoradiograph of a 4% polyacrylamide gel showing the DNA-binding EMSA of purified PyrR with the *pyrD* promoter fragment used as the end-labeled probe. All reactions were carried out using 5,000 cpm of DNA and 13 nM purified PyrR protein. Lanes: 1, DNA probe without protein; 2, DNA probe and PyrR; 3, DNA probe, PyrR and 0.1 mM orotate; 4, DNA probe, PyrR and 0.1 mM OMP; 5, DNA probe, PyrR and 0.1 mM UMP; 6, DNA probe, PyrR and 0.1 mM PRPP.

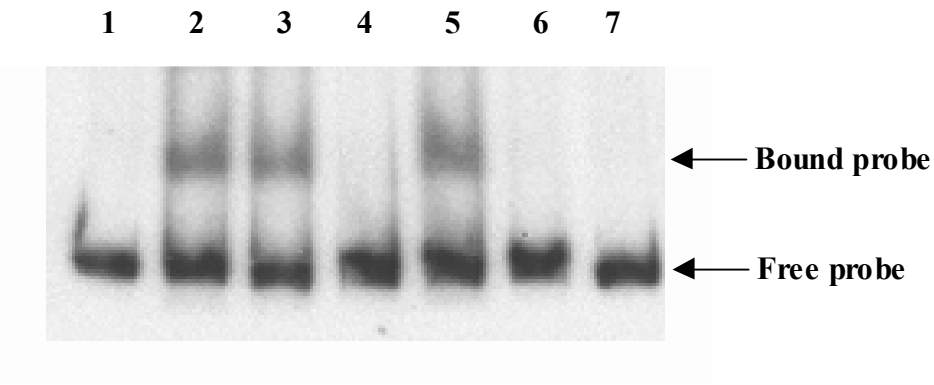

Fig. 51. Autoradiograph of a 4% polyacrylamide gel showing the DNA-binding EMSA of purified PyrR with the *pyrE* promoter fragment used as the end-labeled probe. All reactions were carried out using 5,000 cpm of DNA and 13 nM purified PyrR protein. Lanes: 1, DNA probe without protein; 2, DNA probe and PyrR; 3, DNA probe, PyrR and 0.1 mM orotate; 4, DNA probe, PyrR and 0.1 mM OMP; 5, DNA probe, PyrR and 0.1 mM UMP; 6, DNA probe, PyrR and 0.1 mM PRPP; 7, DNA probe without protein.

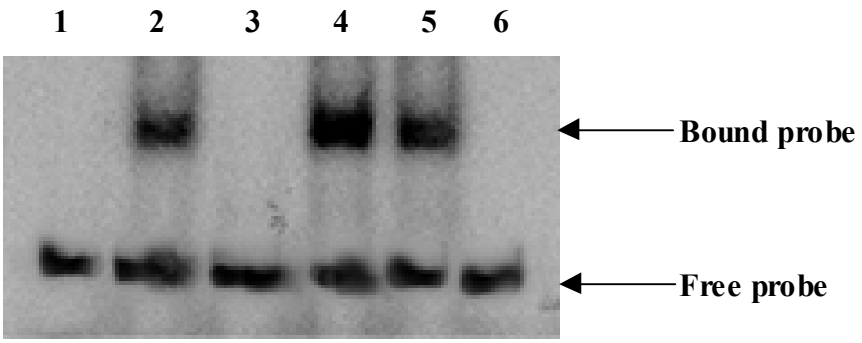

Fig. 52. Autoradiograph of a 4% polyacrylamide gel showing the DNA-binding EMSA of purified PyrR with the *pyrF* promoter fragment used as the end-labeled probe. All reactions were carried out using 5,000 cpm of DNA and 13 nM purified PyrR protein. Lanes: 1, DNA probe, PyrR and 0.1 mM PRPP; 2, DNA probe, PyrR and 0.1 mM UMP; 3, DNA probe, PyrR and 0.1 mM OMP; 4, DNA probe, PyrR and 0.1 mM orotate; 5, DNA probe and PyrR; 6, DNA probe without protein.

NIH Image Version 1.61 program by Wayne Rasband. The apparent dissociation constants (K_d) were graphically determined based on the varying intensities of the shifted bands (Fig. 57, 58). An apparent K_d of 6.8 nM was determined for PyrR binding to *pyrE* DNA compared to an apparent K_d value of 9.6 nM for binding of PyrR to *pyrR* DNA. Hence a lower concentration of PyrR was required for binding to the *pyrE* DNA. This suggested that the PyrR protein had a greater affinity for *pyrE*, which also represented its affinity for the other two downstream genes, *pyrD* and *pyrF*, compared to its affinity for binding to *pyrR* for autoregulation. The binding specificities of OMP and PRPP were also determined by similar EMSA binding studies. The DNA and PyrR concentrations were held constant while the concentration of ligand was varied from 0.03 mM to 1 mM. Results showed that OMP had a greater affinity for PyrR than for PRPP, since the lowest concentration of 0.03 mM OMP prevented PyrR from binding to *pyrR* DNA (data not shown) it can be assumed that the K_d for OMP is less than 30 μM. A K_d of 35 μM was determined for PRPP to PyrR (Fig. 59). The intracellular concentration of PRPP is 9.0 μM (Traut, 1994), suggesting that PRPP only binds to PyrR when PRPP levels are high. High intracellular PRPP levels are indicative of high purines and consequently high pyrimidine levels, therefore the binding of PRPP to PyrR would prevent it from binding to the downstream genes to activate their expression. Since the maximum concentration of PyrR protein used in these EMSA assays was only 13 nM, saturation of binding was not achieved, therefore only the relative K_d values could be reported here.

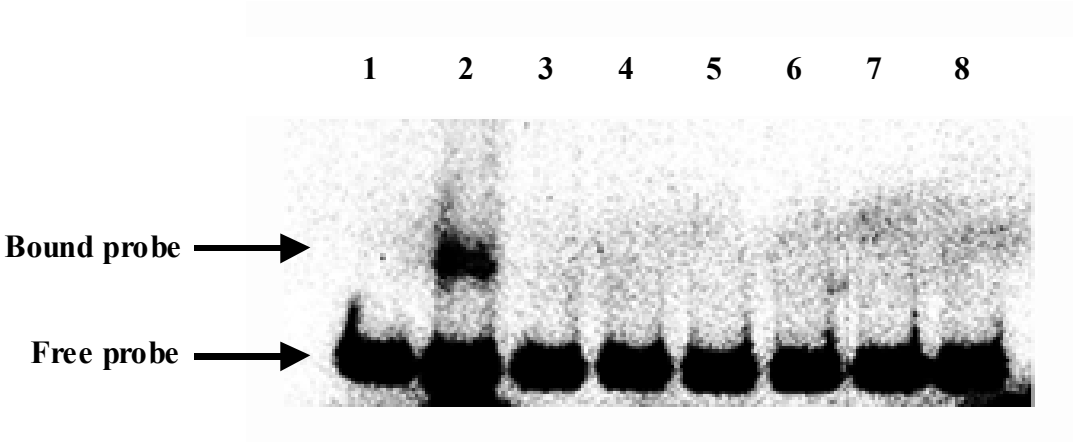

Fig. 53. Autoradiograph of competitive binding EMSA of purified PyrR to *pyrR* end-labeled DNA (5,000 cpm) in the presence of orotate *versus* PRPP. The concentration of PyrR and PRPP was held constant at 6.5 nM and 0.1 mM respectively. The orotate concentration was varied as stated. Lanes: 1, DNA probe only; 2, DNA probe and PyrR; 3, DNA probe, PyrR, PRPP and 1 mM orotate; 4, DNA probe, PyrR, PRPP and 0.5 mM orotate; 5, DNA probe, PyrR, PRPP and 0.25 mM orotate; 6, DNA probe, PyrR, PRPP and 0.125 mM orotate; 7, DNA probe, PyrR, PRPP and 0.06 mM orotate; 8, DNA probe, PyrR, PRPP and 0.03 mM orotate.

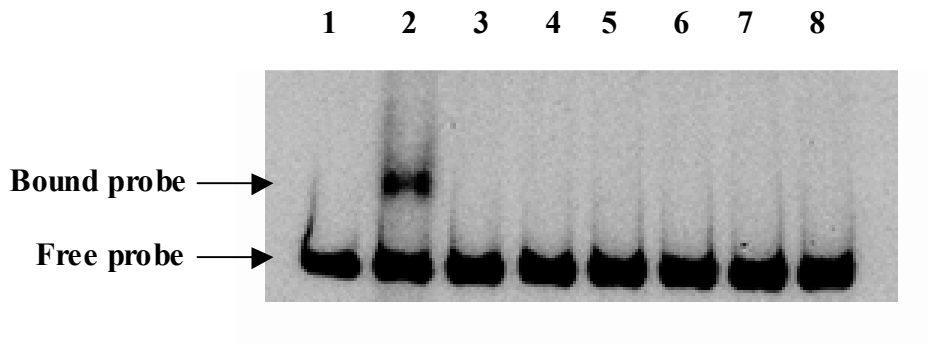

Fig. 54. Autoradiograph of competitive binding EMSA of purified PyrR to *pyrR* end-labeled DNA (5,000 cpm) in the presence of UMP *versus* PRPP. The concentration of PyrR and PRPP was held constant at 6.5 nM and 0.1 mM respectively. The UMP concentration was varied as stated. Lanes: 1, DNA probe only; 2, DNA probe and PyrR; 3, DNA probe, PyrR, PRPP and 1 mM UMP; 4, DNA probe, PyrR, PRPP and 0.5 mM UMP; 5, DNA probe, PyrR, PRPP and 0.25 mM UMP; 6, DNA probe, PyrR, PRPP and 0.125 mM UMP; 7, DNA probe, PyrR, PRPP and 0.06 mM UMP; 8, DNA probe, PyrR, PRPP and 0.03 mM UMP.

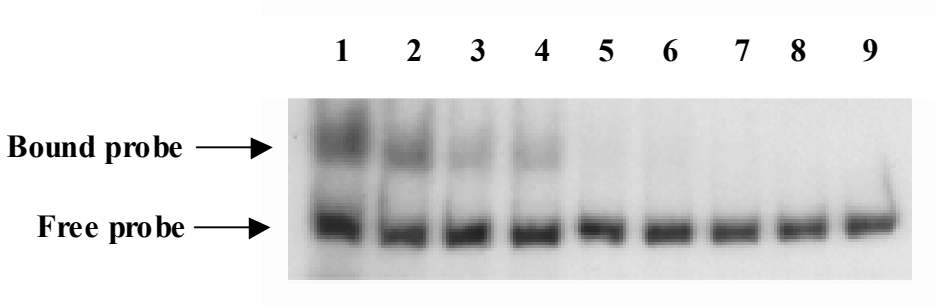

Fig. 55. Autoradiograph of EMSA for specificity of binding of purified PyrR to *pyrR* using 5,000 cpm of end-labeled DNA. Lanes: 1, 13 nM PyrR; 2, 10.4 nM PyrR; 3, 7.8 nM PyrR; 4, 5.2 nM PyrR; 5, 2.6 nM PyrR; 6, 1.3 nM PyrR; 7, 0.65 nM PyrR; 8, 0.26 nM PyrR; 9, no protein.

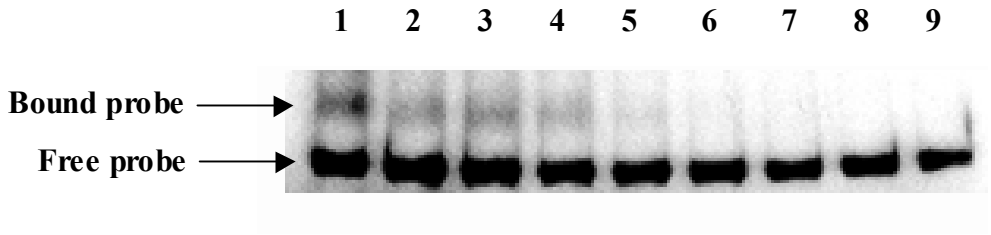

Fig. 56. Autoradiograph of EMSA for specificity of binding of purified PyrR to *pyrE* using 5,000 cpm of end-labeled DNA. Lanes: 1, 13 nM PyrR; 2, 10.4 nM PyrR; 3, 7.8 nM PyrR; 4, 5.2 nM PyrR; 5, 2.6 nM PyrR; 6, 1.3 nM PyrR; 7, 0.65 nM PyrR; 8, 0.26 nM PyrR; 9, no protein.

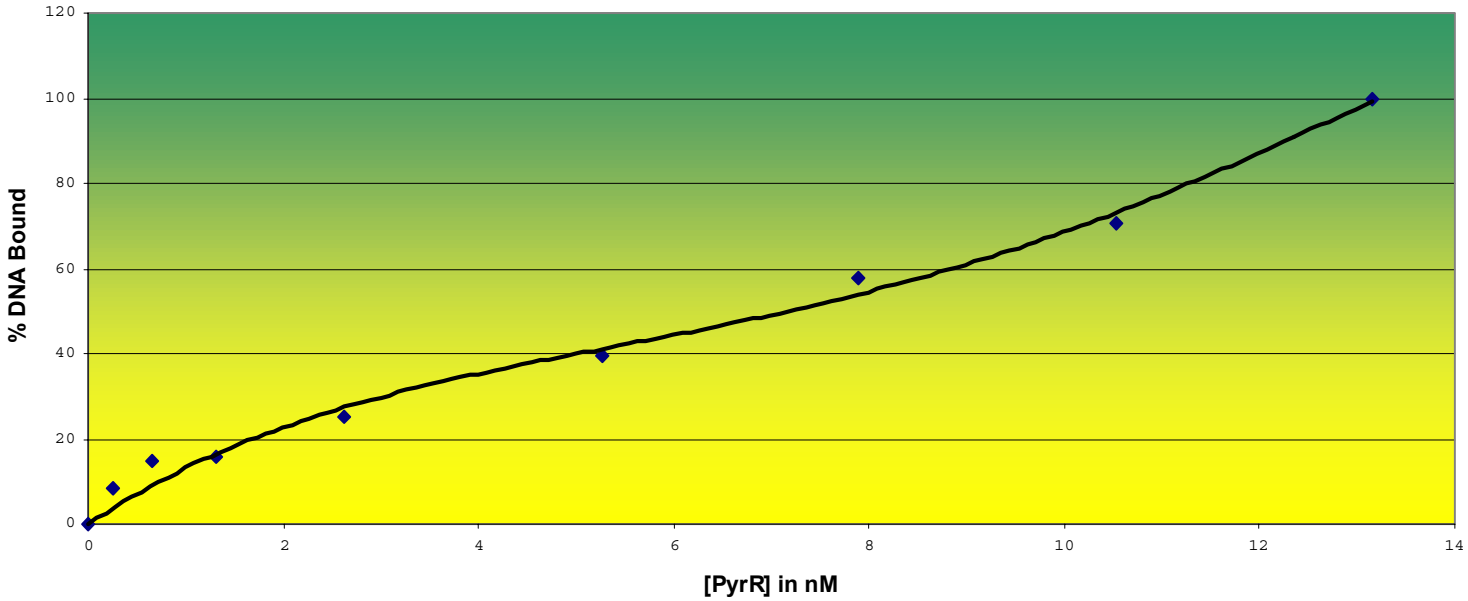

Fig. 57. Determination of the dissociation constant (K_d) for PyrR on *pyrE* DNA by EMSA using purified PyrR protein.

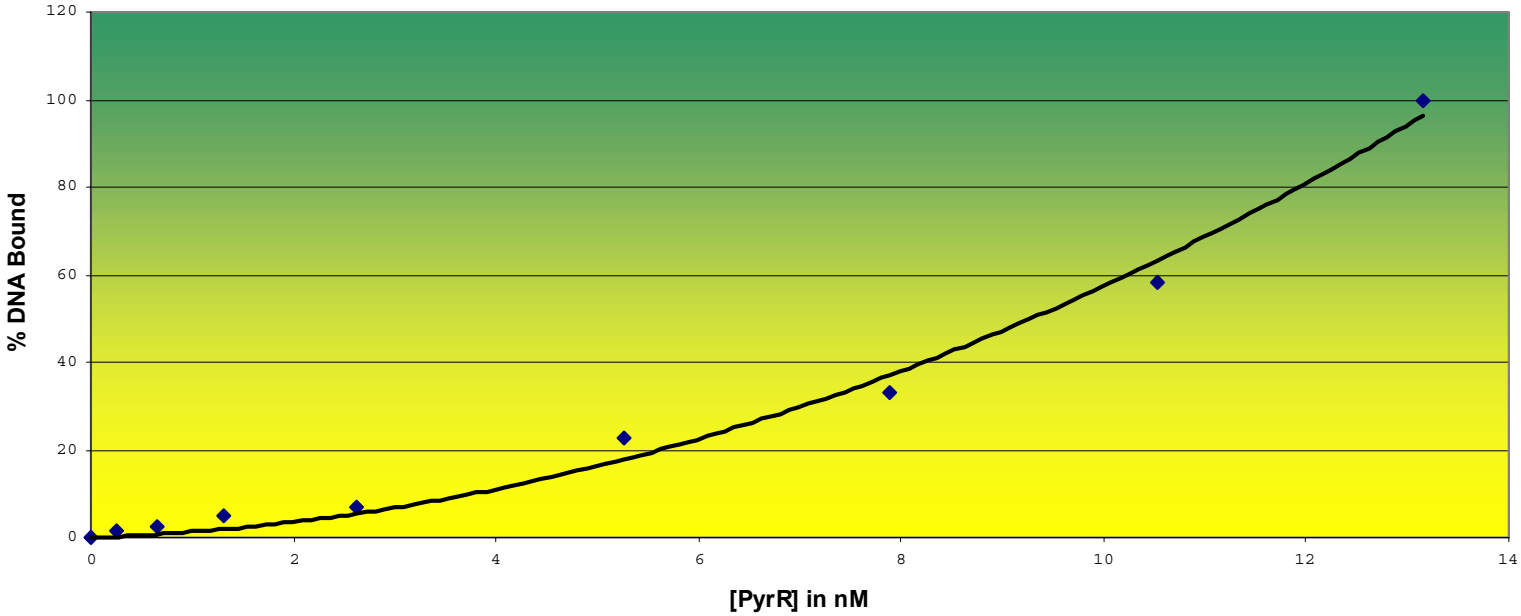

Fig. 58. Graphical representation of the dissociation constant (K_d) for PyrR on *pyrR* DNA.

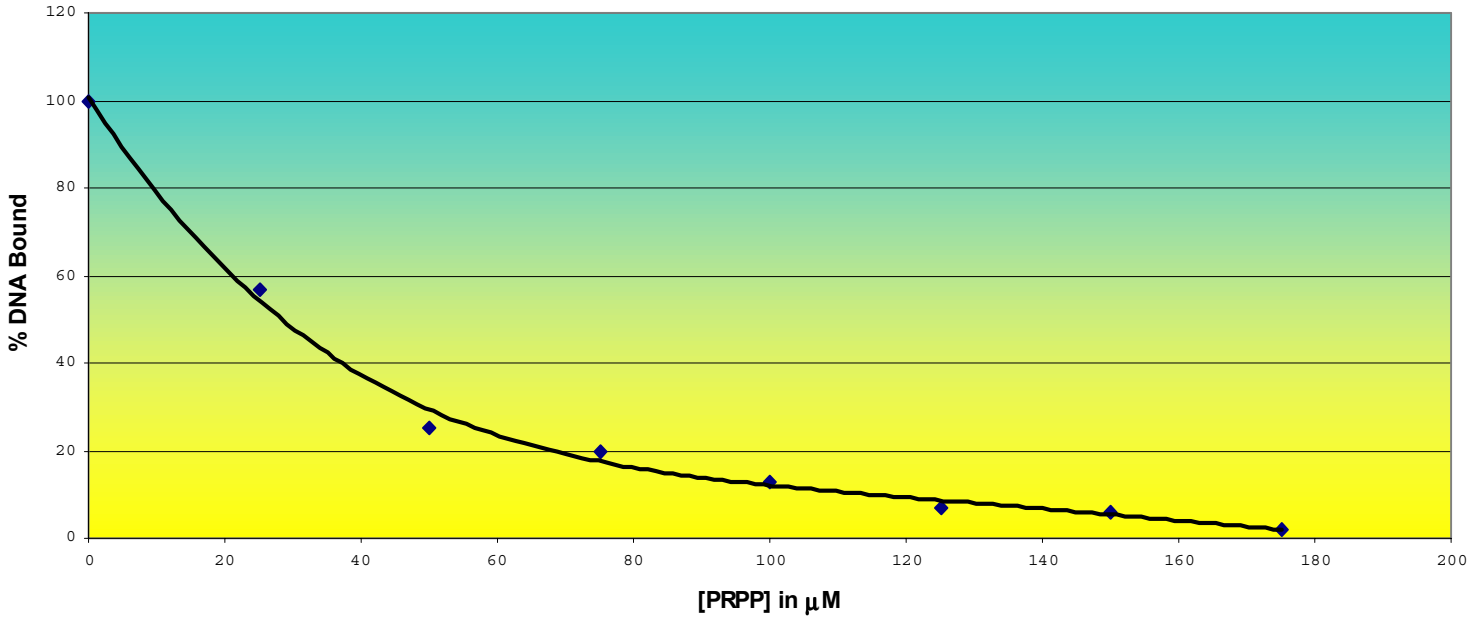

Fig. 59. Graphical representation of the dissociation constant (K_d) for PRPP on PyrR.

Gel Filtration Chromatography.

The native molecular weight of the purified *Pseudomonas* PyrR was determined by gel filtration chromatography in the absence or presence of the ligands OMP and PRPP. In general, two peaks were resolved by HPLC and a possible third peak was detected but not fully resolved. A fourth peak corresponding to the GST-PyrR fusion present in the purified PyrR preparation was also detected (Fig. 60). From a standard curve (Fig. 61), the two resolved peaks corresponded to molecular masses averaging 20 kDa and 80 kDa. Given the subunit size of the *Pseudomonas* PyrR was 20 kDa, the 80 kDa peak would represent a tetrameric aggregated form of the native protein. In *B. subtilis*, the more aggregated hexameric form of the PyrR protein is favored in the presence of UMP and the less aggregated dimeric form in the presence of PRPP. To test if such was also the case with the *Pseudomonas* protein, the purified protein was pre-incubated with OMP and PRPP prior to loading on to the gel filtration column. Figures 62 and 63 showed that in *Pseudomonas*, the more aggregated tetrameric form was favored in the presence of PRPP. The addition of OMP, did not shift the equilibrium and thus did not affect the molecular state of PyrR (data not shown).

Uracil phosphoribosyltransferase (UPRTase) assay.

UPRTase assays were performed as described in Materials and Methods and analyzed by HPLC. Figures 64 and 65 present uracil and orotate standards respectively. It can be seen from the figures that optimal uracil detection is at 254 nm and orotate at 280 nm. Since orotate is considered a key intermediate in pyrimidine regulation (Jensen,

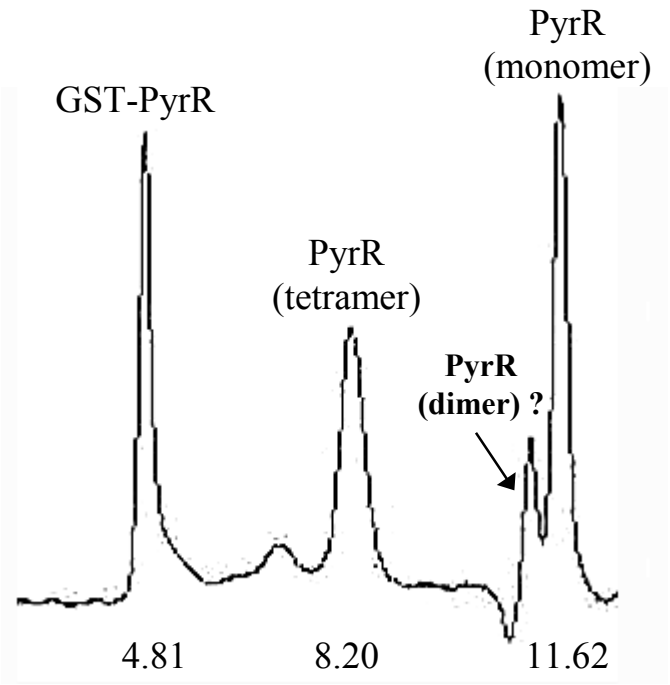

Fig. 60. Chromatogram from gel filtration analysis of purified PyrR protein. Retention times in minutes are shown below the peaks of interest.

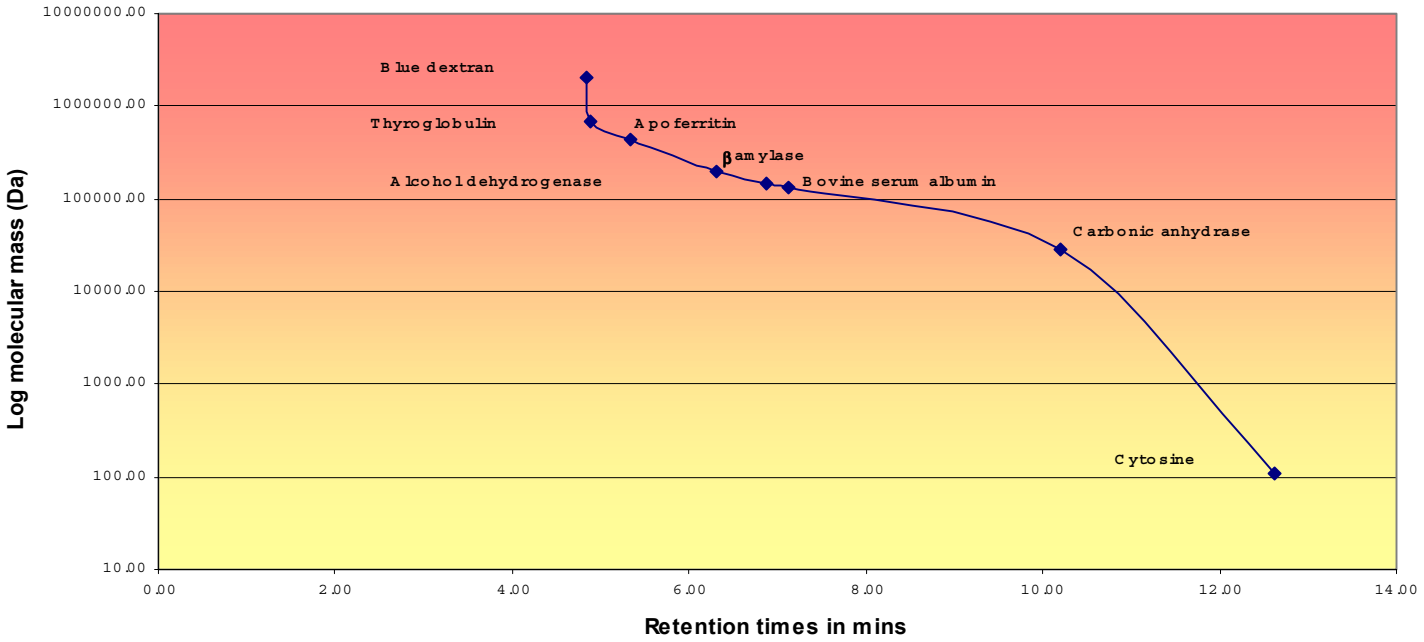

Fig. 61. Gel filtration standard curve.

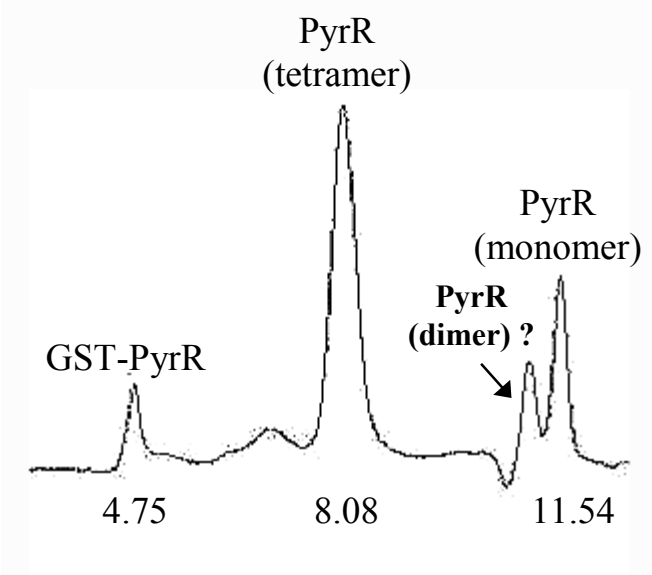

Fig. 62. Chromatogram from gel filtration analysis of purified PyrR protein pre-incubated with 0.1 mM PRPP. Retention times in minutes are shown below the peaks of interest.

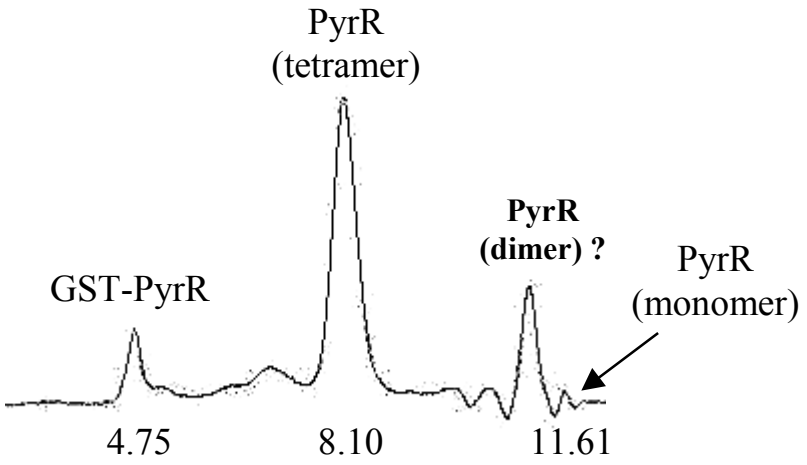

Fig. 63. Chromatogram from gel filtration analysis of purified PyrR protein pre-incubated with 2 mM PRPP. Retention times in minutes are shown below the peaks of interest.

1982), wild type *Pseudomonas* cells were grown with glucose as carbon source (Fig. 66), in the absence and presence of excess orotate (Fig. 67), and with succinate as carbon source (Fig. 68). Chromatograms showed that UPRTase activity in *Pseudomonas* was enhanced when cells were grown in the presence of excess exogenous orotate (Table 6). However, UPRTase activity decreased when the cells were grown in succinate as the carbon source.

The alignment of the *P. aeruginosa* PyrR with UPRTases from *Pseudomonas*, *E. coli* and *B. subtilis* (Fig. 70) showed some homology between PyrR and the Upp proteins from these organisms. Since the *B. subtilis* PyrR protein has UPRTase activity, the *Pseudomonas* PyrR protein was tested for UPRTase activity. Also, since PRPP and Mg^{2+} act as stabilizing substrates for UPRTase in *E. coli*, the purified *Pseudomonas* PyrR protein was pre-incubated with PRPP and Mg^{2+} prior to assaying for UPRTase activity. Despite sharing sequence homology with the Upp proteins, UPRTase activity was not detected with the purified PyrR protein (Fig. 69).

Orotate phosphoribosyltransferase (OPRTase) assays.

OPRTase assays were performed as described in Materials and Methods using the same samples used for the UPRTase assays mentioned above. The assay was analyzed by HPLC and the formation of the reaction product, OMP was detected at 280 nm. Figures 71 and 72 present the UMP and OMP standards at 254 nm and 280 nm, respectively. Chromatograms from the assay (Figs. 73, 74, 75) showed no change in OPRTase activities in wild type cells regardless of growth conditions. In *B. subtilis*,

UMP is the signal molecule for pyrimidine regulation and hence the PyrR protein from *B. subtilis* displays nominal UPRTase activity. Since the *Pseudomonas* PyrR protein did not display UPRTase activity it was tested for OPRTase function, considering that in *Pseudomonas*, orotate is a key regulatory intermediate (Jensen, 1982). When aligned with various OPRTases, the *Pseudomonas* PyrR protein showed nominal sequence similarity (Fig. 77), yet it contained the OMP binding domain. Despite this, as can be seen from Figure 76, the *Pseudomonas* pyrR protein did not have any detectable OPRTase activity.

Table 6. HPLC assay data for UPRTase and OPRTase activity in *P. aeruginosa* wild type cells grown under varying conditions.

Strain	**Genotype**	**Growth Conditions**	**Specific Activity[a] (μmol/min/mg protein)**	
			UPRTase	OPRTase
PAO1	Wild type	Glucose	46.9	33.8
PAO1	Wild type	Glucose + 1mM orotate	60.9	28.8
PAO1	Wild type	Succinate	21.1	20.0

[a] Specific activities were calculated based on the peak area of the product formed; UMP for UPRTase and OMP for OPRTase.

Orotate decarboxylase assays.

Very few organisms that have the ability to deacrboxylate orotate to uracil have been identified. In *Neurospora crassa*, the enzyme isoorotate decarboxylase (IDCase) removes the CO_2 from isoorotate to yield uracil, and this reaction is the final step of a recently identified thymidine salvage pathway (Smiley *et al*., 1999*)*. A similar reaction is also found to occur in two strains of the *Mycobacterium* (Vitols *et al*., 1967) that can utilize orotate as sole nitrogen source by decarboxylating it to uracil before the ring is broken for nitrogen source (Vogels and Van der Drift, 1976). To date, an orotate decarboxylase has never been shown to be present in *Pseudomonas*.

A glance at Fig. 1 (*de novo* pathway) clearly shows that orotate cannot satisfy the pyrimidine requirement of *pyrE* or *pyrF* mutants. One way to test for an orotate decarboxylase would be to see if a *pyrE* or *pyrF* mutant could grow on orotate. To that end, a recruited strain of a *pyrE* deletion mutant (MVP7404) was isolated as follows: 100 µl of a PAO8017 (crc^-, $pyrE^-$) culture was plated on *Pseudomonas* minimal medium, with glucose as the carbon source and orotate as the pyrimidine source. The plate was incubated at 37°C until isolated colonies appeared (~ 5 days incubation). A colony was inoculated into *Pseudomonas* minimal broth with glucose and orotate and incubated with shaking at 37°C. If the culture reached an OD_{600} ~0.6 within 16 hr of incubation, this meant that the cell had 'recruited' the ability to use orotate as a pyrimidine source, indicating that an orotate decarboxylase enzyme may be present in *Pseudomonas*. To that end, orotate decarboxylase assays were performed as described in Materials and Methods and analyzed by HPLC. The recruited *pyrE* mutant (MVP7404) was grown

under the conditions listed in Table 7. Results showed a 5-fold conversion of orotate to uracil when the cells were grown in excess exogenous orotate compared to the same cell in the absence of exogenous orotate. To further prove that uracil was indeed produced from decarboxylating the orotate, the same reaction assays were analyzed for UPRTase activity by the addition of PRPP and Mg^{2+} *in vitro*, and the product UMP was quantitated (Table 8). Calculated specific activities showed that uracil was made when orotate was added to the reaction mix. This was reflected by the 5-fold increase in UPRTase activity observed when compared to the control reaction mixture. The finding of this orotate decarboxylase enzyme was novel in *Pseudomonas* and of great importance as this diversion could serve as an alternate pathway to rapidly make pyrimidines.

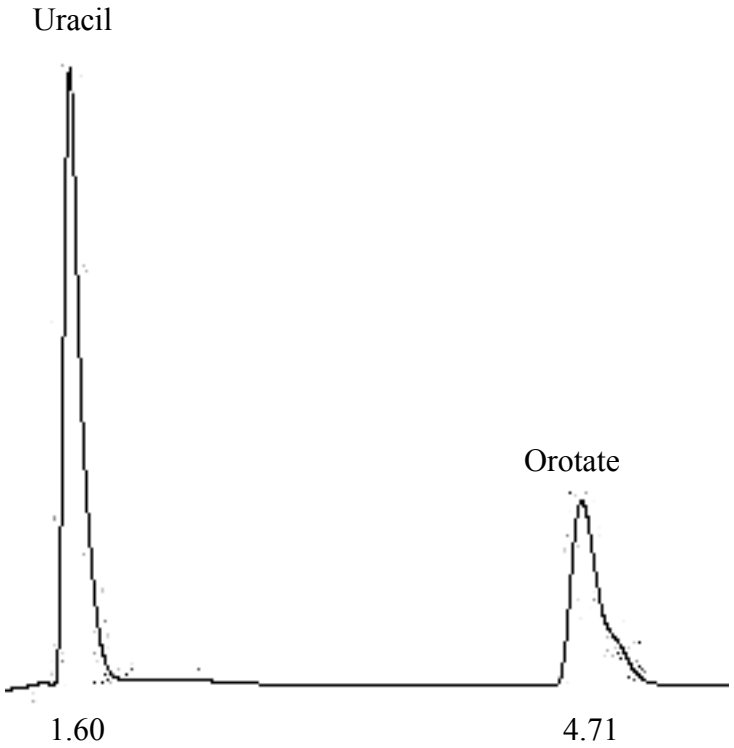

Fig. 64. Chromatogram of 0.1 mM uracil and 0.1 mM orotate standards detected at 254 nm. Retention times are given in minutes.

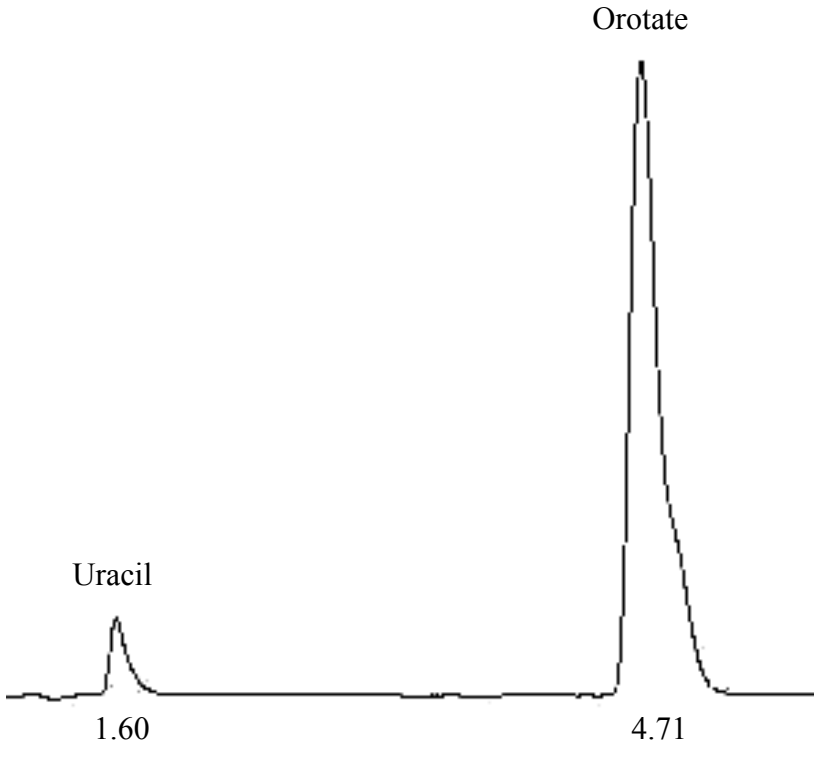

Fig. 65. Chromatogram of 0.1 mM uracil and 0.1 mM orotate standards detected at 280 nm. Retention times are given in minutes.

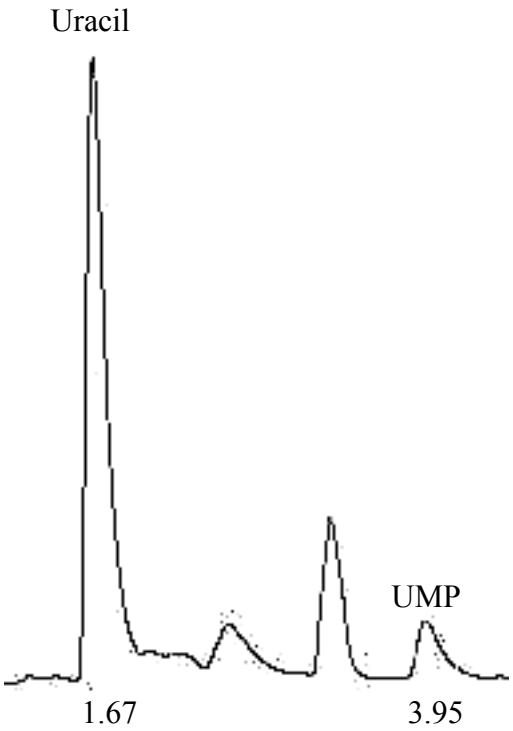

Fig. 66. Chromatogram of UPRTase activity in wild type *P. aeruginosa* grown in *Pseudomonas* minimal medium with glucose.

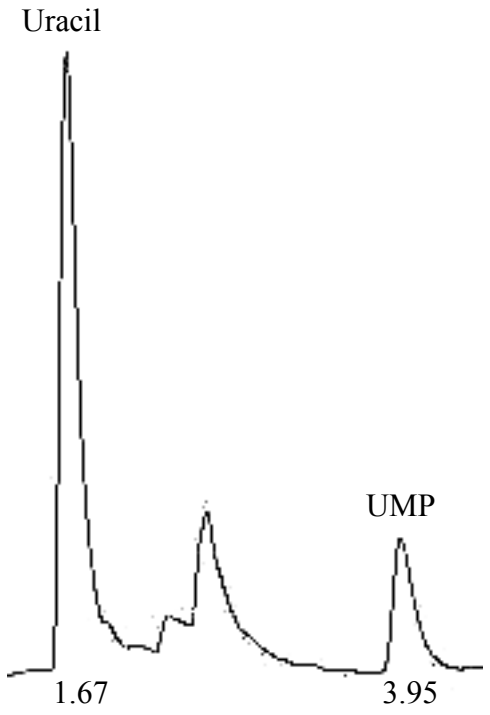

Fig. 67. Chromatogram of UPRTase activity in wild type *P. aeruginosa* grown in *Pseudomonas* minimal medium with glucose and orotate.

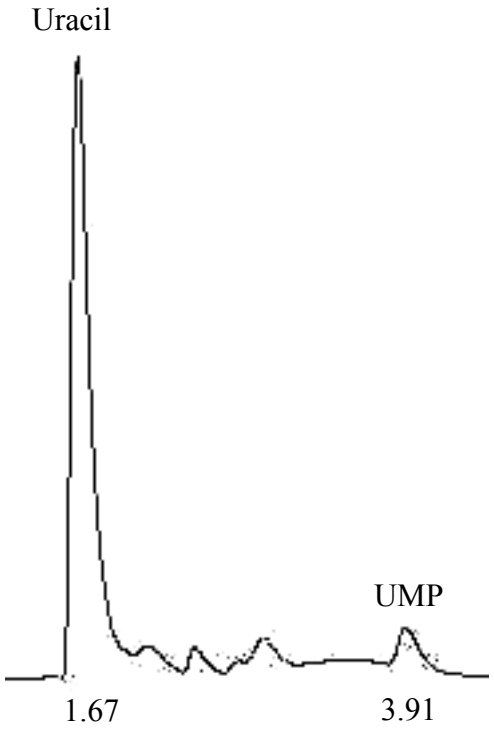

Fig. 68. Chromatogram of UPRTase assay in wild type *P. aeruginosa* grown in *Pseudomonas* minimal medium with succinate.

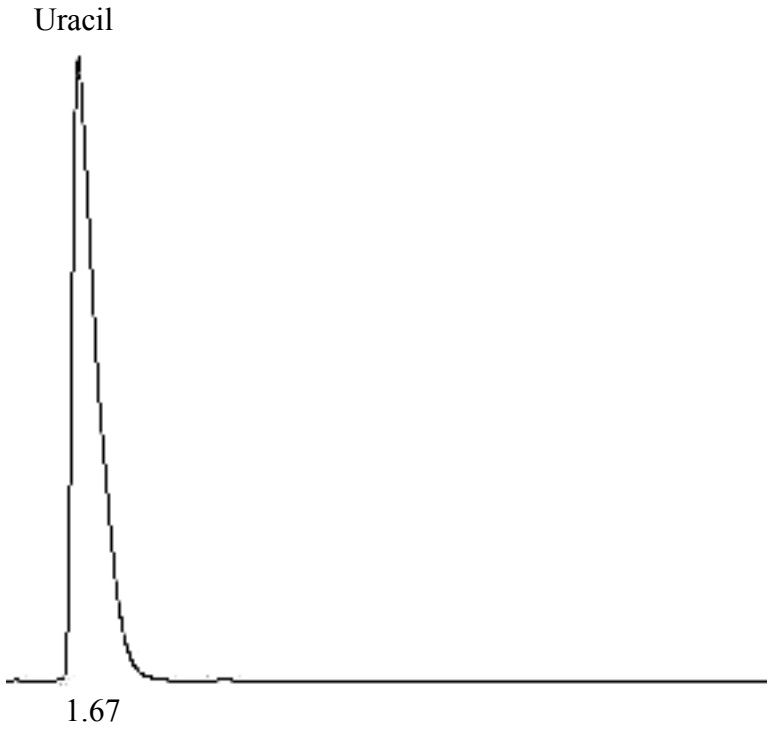

Fig.69 . Chromatogram of UPRTase assay of *P. aeruginosa* purified PyrR protein.

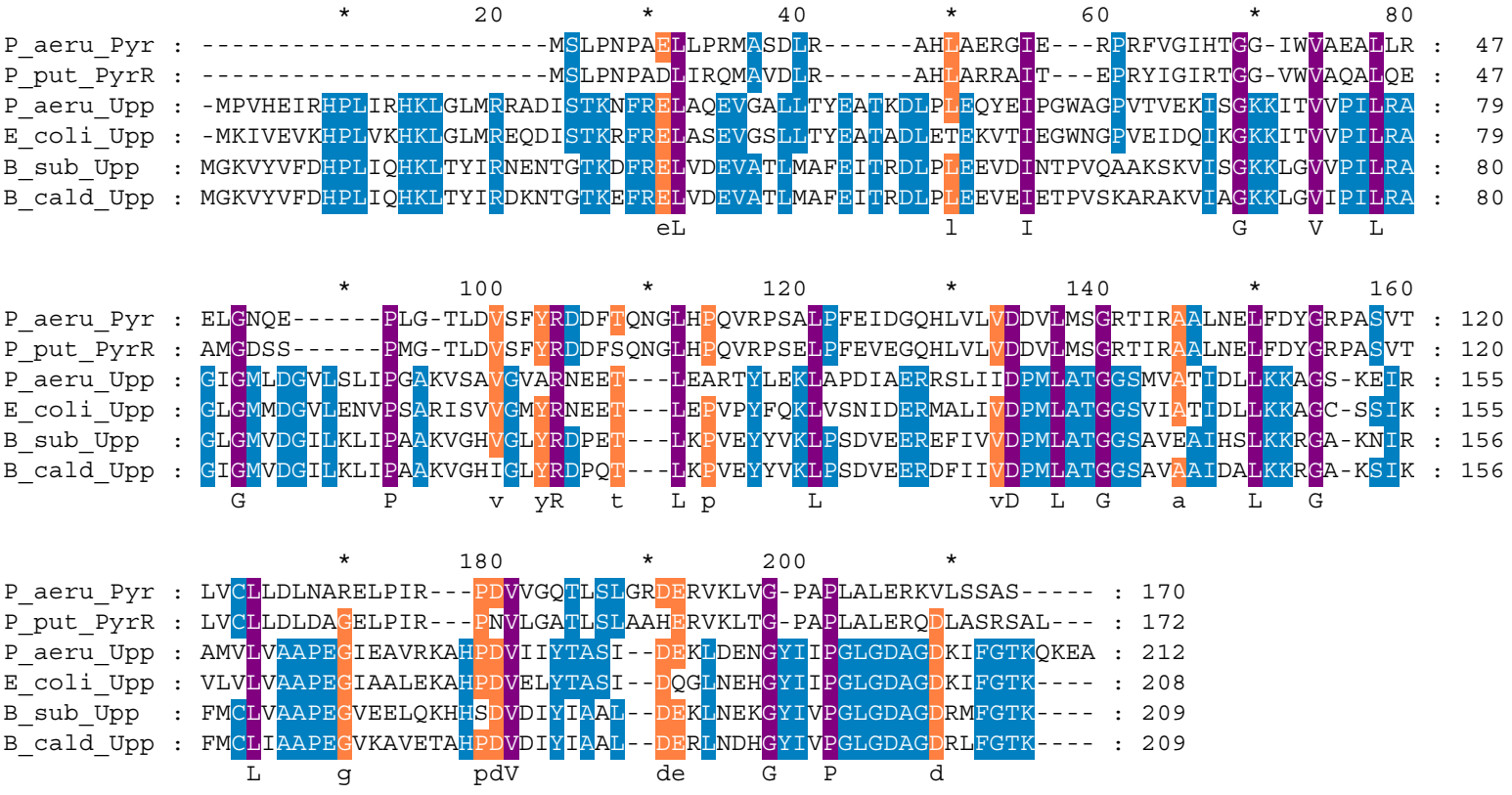

Fig. 70. Sequence alignment of the *Pseudomonas* PyrR protein with various Upp proteins.

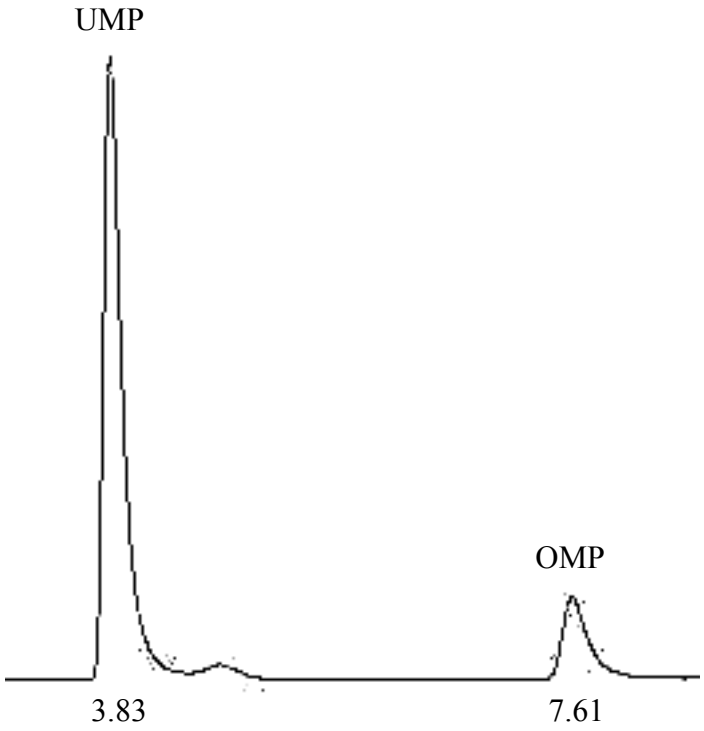

Fig. 71. Chromatogram of 0.1 mM UMP and 0.1 mM OMP standards detected at 254 nm. Retention times are given in minutes.

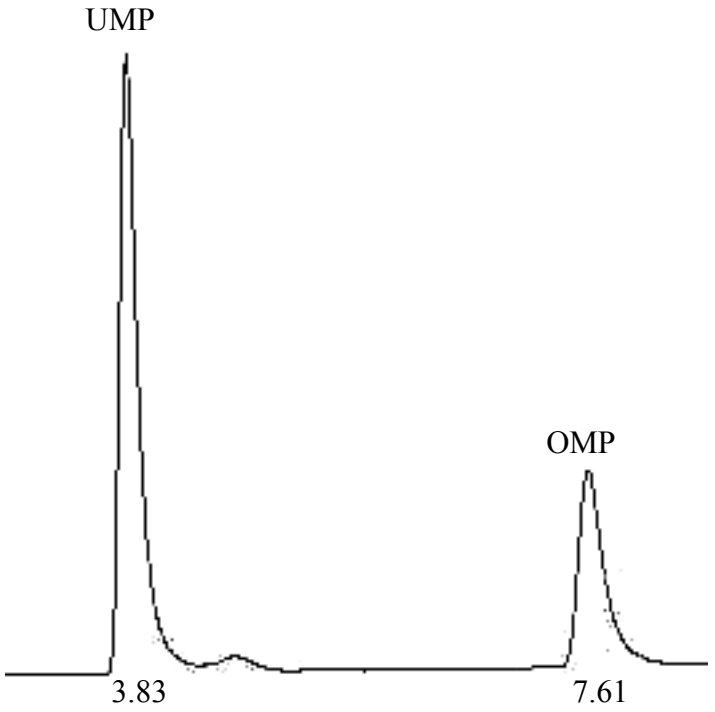

Fig. 72. Chromatogram of 0.1 mM UMP and 0.1 mM OMP standards detected at 280 nm. Retention times are given in minutes.

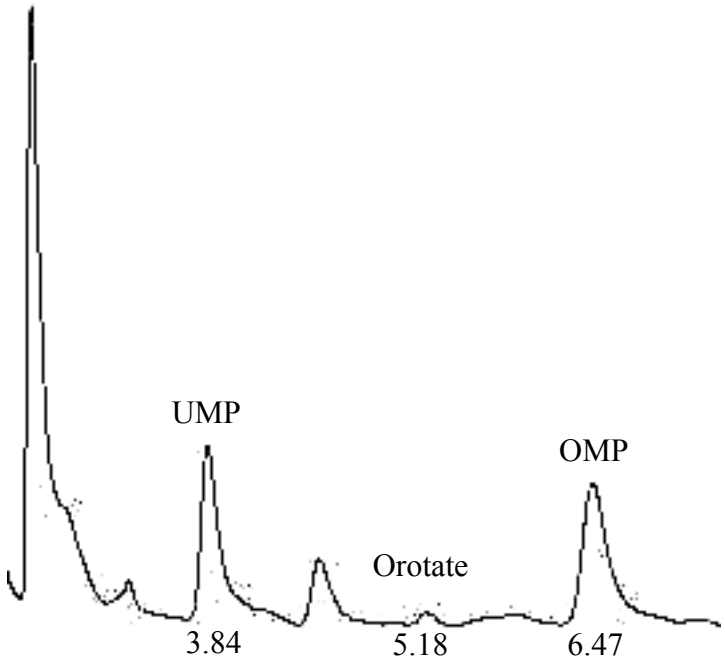

Fig. 73. Chromatogram of OPRTase activity in wild type *P. aeruginosa* grown in *Pseudomonas* minimal medium with glucose.

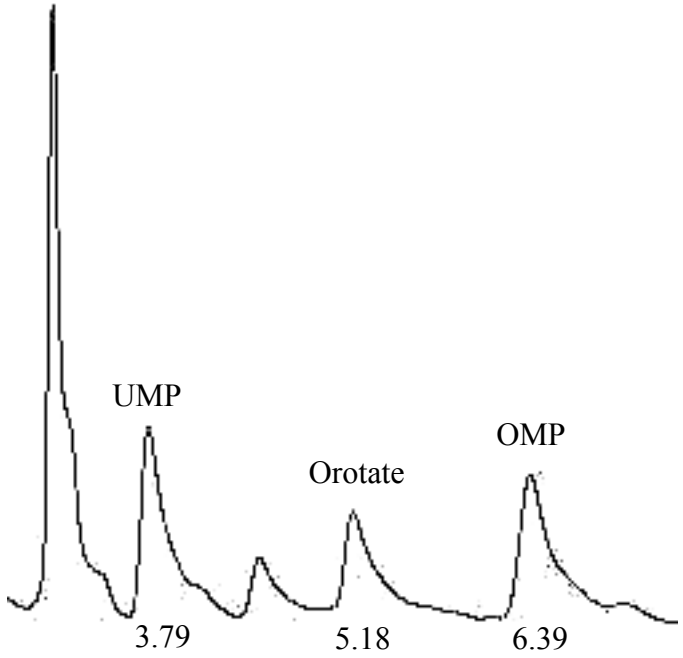

Fig.74 . Chromatogram of OPRTase activity in wild type *P. aeruginosa* grown in *Pseudomonas* mimimal medium with glucose and orotate.

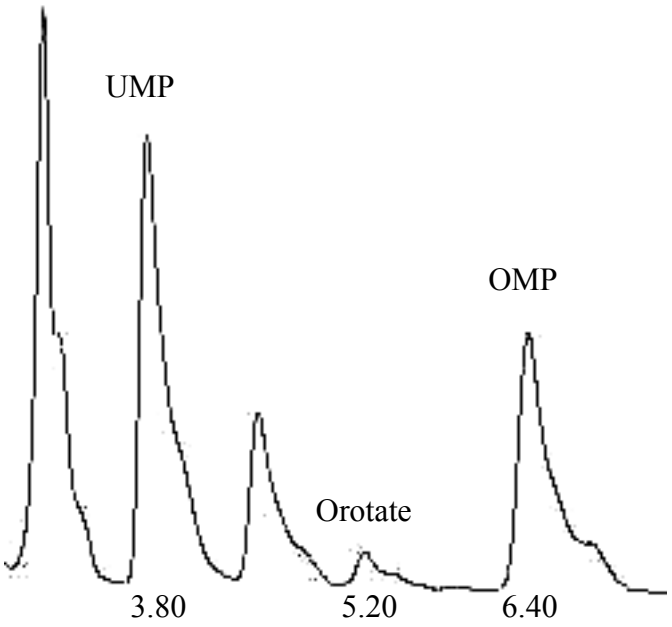

Fig. 75. Chromatogram of OPRTase activity in wild type *P. aeruginosa* grown in *Pseudomonas* minimal medium with succinate.

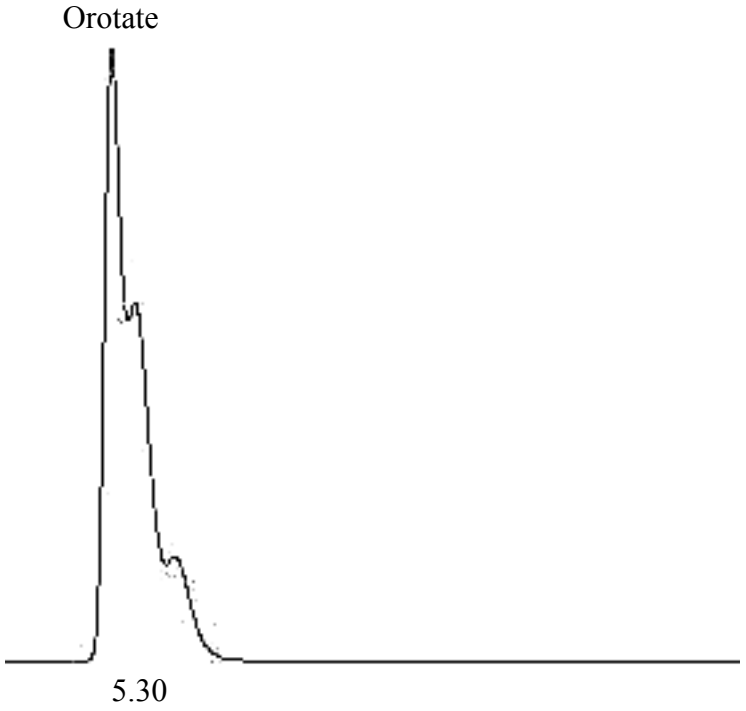

Fig. 76. Chromatogram of OPRTase activity in *P. aeruginosa* purified PyrR protein.

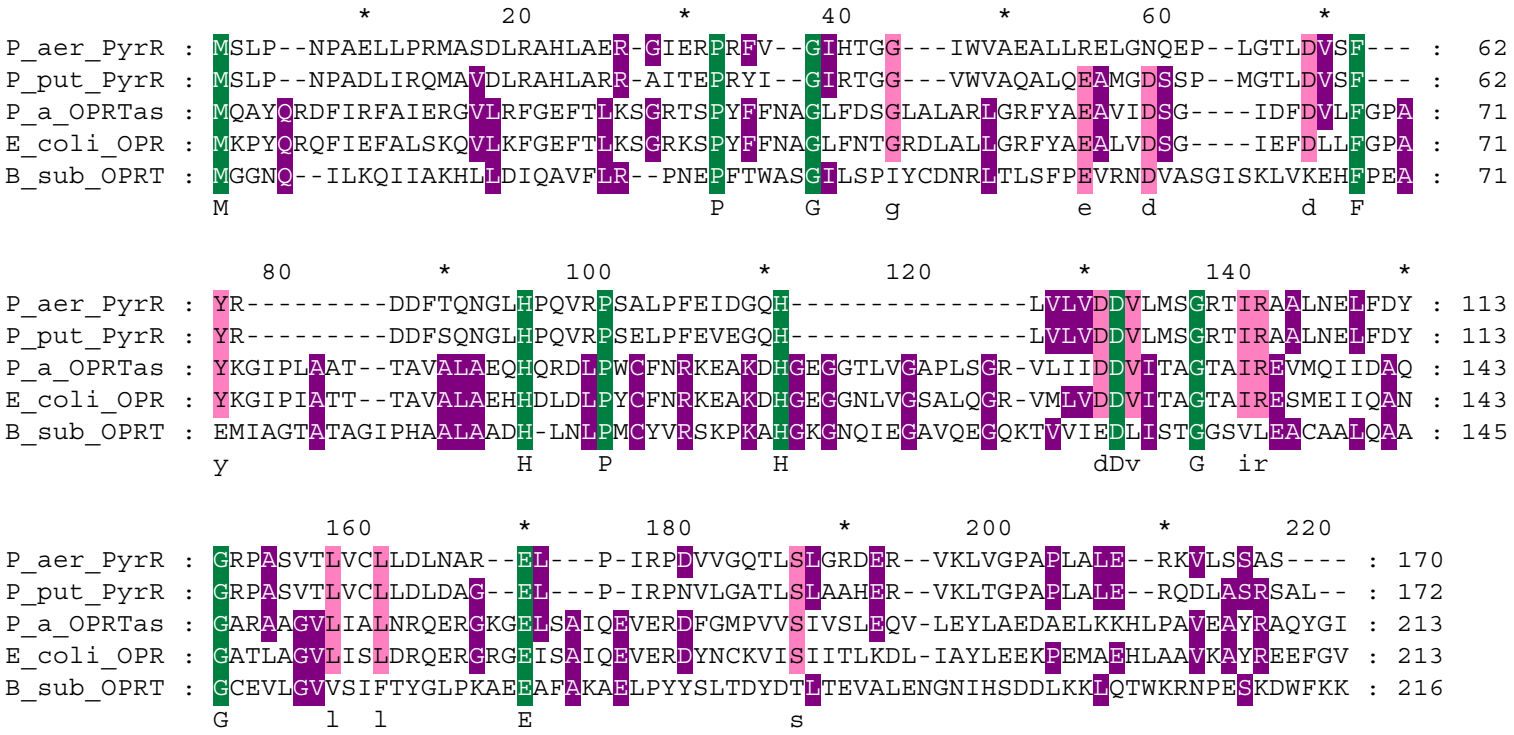

Fig. 77. Sequence alignment of the *Pseudomonas* PyrR proteins with various OPRTases.

Table 7. Orotate decarboxylase assay data from the recruited *P. aeruginosa crc, pyrE* mutant (MVP7404) grown with glucose as the carbon source in the absence and presence of exogenous orotate.

Strain	**Genotype**	**Growth Conditions**	**Specific Activity[a] (μmol min^{-1} mg $protein^{-1}$)**
MVP7404	*crc*$^-$, *pyrE*$^-$	Glucose	30.3
MVP7404	*crc*$^-$, *pyrE*$^-$	Glucose + 1mM orotate	153.3

[a] Specific activities were calculated from the peak areas of the uracil product formed.

Table 8. Orotate decarboxylase and UPRTase assay data from the recruited *P. aeruginosa crc*, *pyrE* mutant (MVP7404) grown with glucose and exogenous orotate.

Strain	**Genotype**	**Specific Activity (μmol min^{-1} mg $protein^{-1}$)[a]**			
PAO8017	*crc*$^-$, *pyrE*$^-$	-$MgCl_2$	+$MgCl_2$	+PRPP	+$MgCl_2$ +PRPP
Orotate Decarboxylase		160.0	143.0	200.0	180.0
UPRTase		43.3	50.0	100.0	240.0

[a] Specific activities were calculated from the peak areas of the products formed; uracil for orotate decarboxylase and UMP for UPRTase.

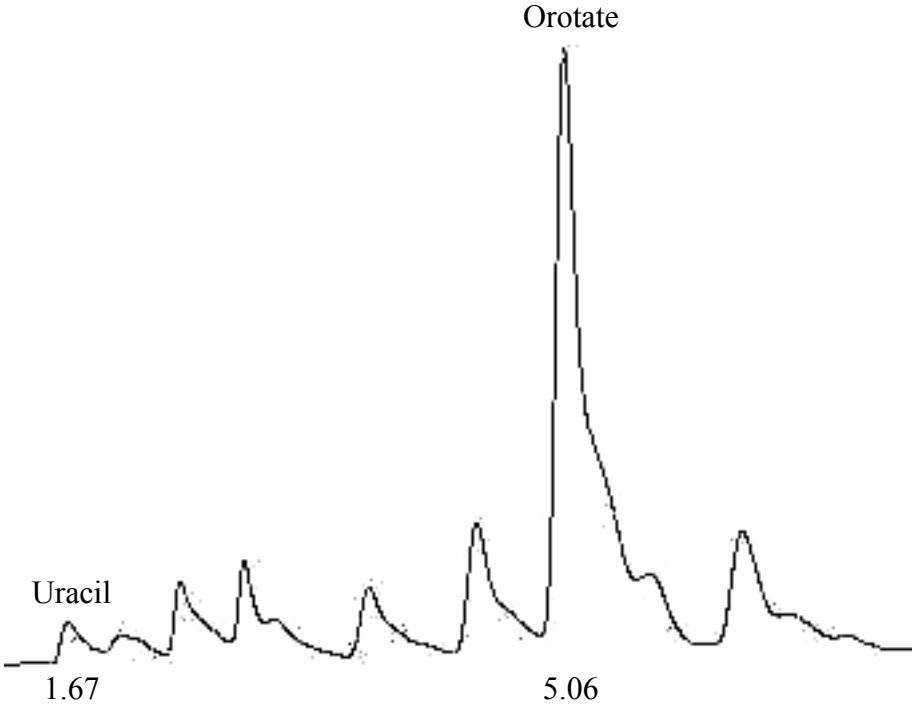

Fig. 78. Chromatogram from an orotate decarboxylase assay of wild type *P. aeruginosa* grown in *Pseudomonas* minimal medium with glucose as the carbon source. Retention times in minutes are shown below the peaks of interest.

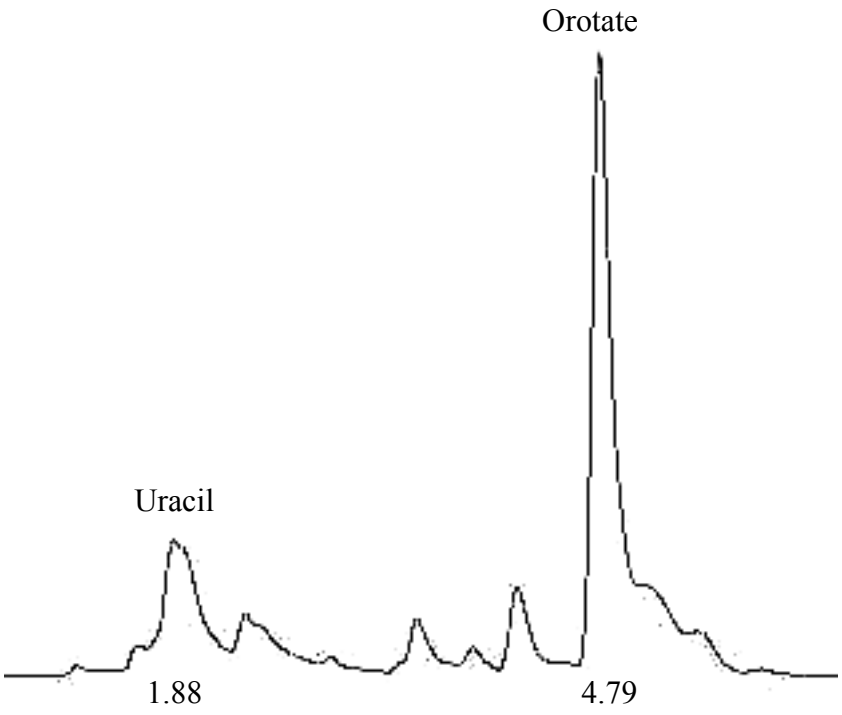

Fig. 79. Chromatogram from an orotate decarboxylase assay of the recruited *P. aeruginosa crc*, *pyrE* mutant (MVP7404) grown in *Pseudomonas* minimal medium with glucose as the carbon source. Retention times in minutes are shown below the peaks of interest.

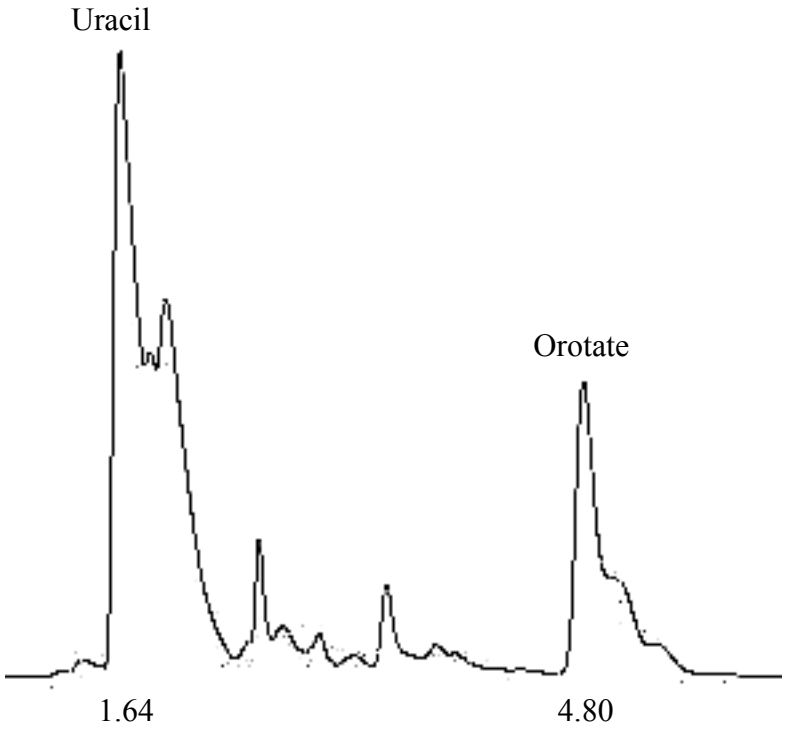

Fig. 80. Chromatogram from an orotate decarboxylase assay of the recruited *P. aeruginosa crc*, *pyrE* mutant (MVP7404) grown in *Pseudomonas* minimal medium with glucose as the carbon source and supplemented with exogenous orotate. Retention times in minutes are shown below the peaks of interest.

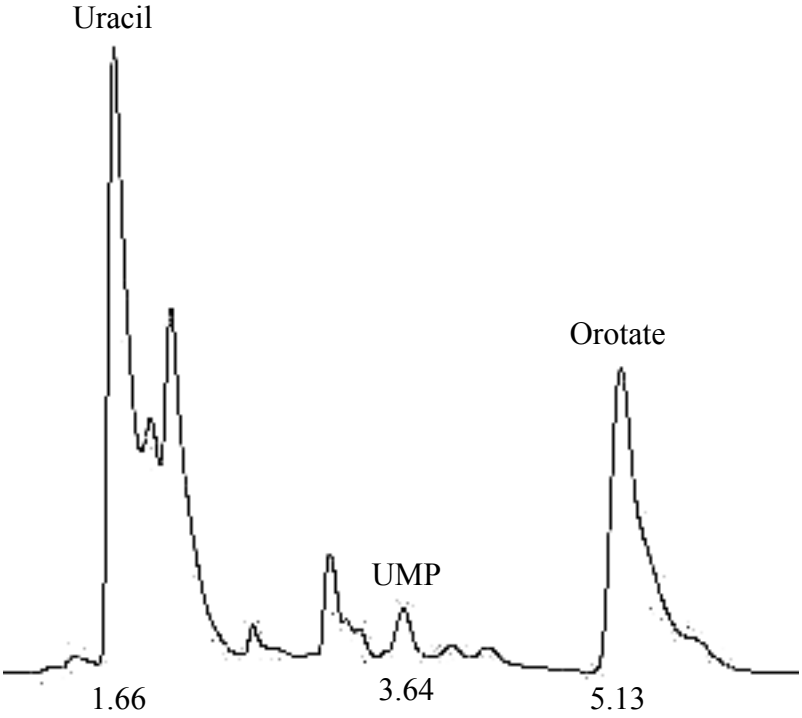

Fig. 81. Chromatogram from an orotate decarboxylase assay, with the addition of $MgCl_2$ in the reaction mix, of the recruited *P. aeruginosa crc*, *pyrE* mutant (MVP7404) grown in *Pseudomonas* minimal medium with glucose as the carbon source and supplemented with exogenous orotate. Retention times in minutes are shown below the peaks of interest.

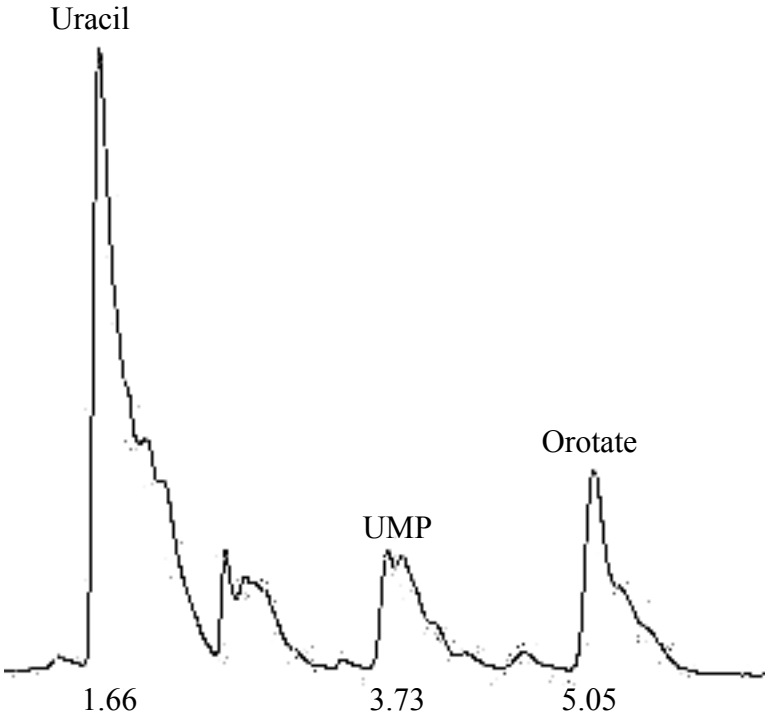

Fig. 82. Chromatogram from an orotate decarboxylase assay, with the addition of PRPP in the reaction mix, of the recruited *P. aeruginosa crc*, *pyrE* mutant (MVP7404) grown in *Pseudomonas* minimal medium with glucose as the carbon source and supplemented with exogenous orotate. Retention times in minutes are shown below the peaks of interest.

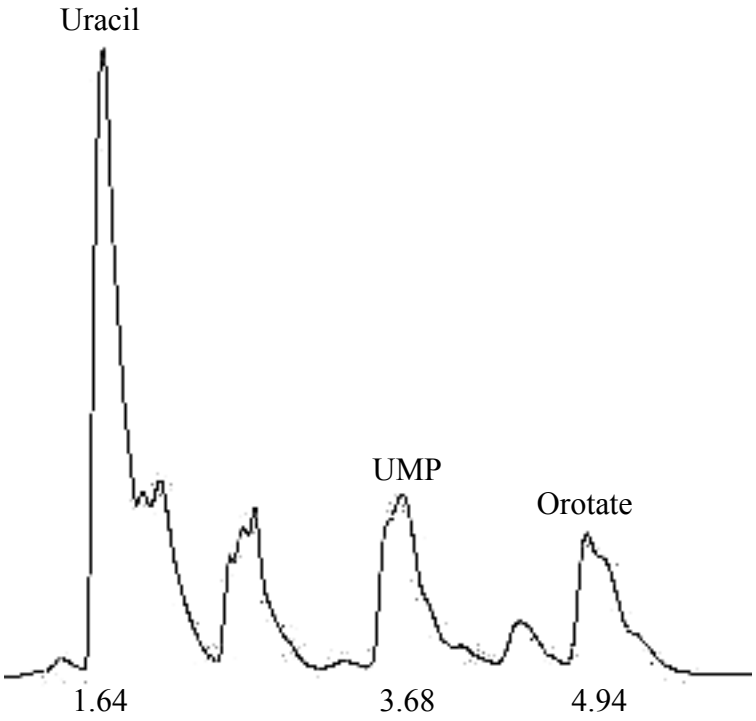

Fig. 83. Chromatogram from an orotate decarboxylase assay, with the addition of $MgCl_2$ and PRPP in the reaction mix, of the recruited *P. aeruginosa crc*, *pyrE* mutant (MVP7404) grown in *Pseudomonas* minimal medium with glucose as the carbon source and supplemented with exogenous orotate. Retention times in minutes are shown below the peaks of interest.

5-fluoroorotate (5-FOA) plate assays.

When 5-FOA enters the cell and, the sequential action of the *pyrE* and *pyrF* encoded enzymes, OPRTase and OMP decarboxylase respectively converts it to 5-FUMP. 5-FUMP is toxic to the cell because it is ultimately incorporated into RNA as 5-FUTP, the fluoro-analog of the ribonucleotide, UTP. The presence of the fluoro group causes mistranslation by the ribosome and thus kills the cell, creating a zone of killing. The presence of a zone of killing was therefore indicative of 5-FOA entry into the cell and its conversion to the toxic fluoronucleotide. However, the absence of a zone of killing suggested that either, the entry of 5-FOA into the cell was prevented, or 5-FOA entered the cell but could not be metabolized to the toxic nucleotide level. Plate assay results of *P. aeruginosa* wild type cells using 0.2% glucose as the carbon and energy source showed a zone of killing (Fig. 84a). However, when 10 mM succinate was used as the carbon and energy source, a zone of killing was not observed (Fig. 84b). This suggested that in the presence of succinate, wild type cells either did not allow entry of orotate into the cell or could not metabolize the fluoroorotate, once in the cell. Phibbs and co-workers have shown the existence of catabolite repression control in *Pseudomonas*. This catabolite repression control involves the *crc* encoded Crc protein, for which succinate has been shown to be the strongest repressing metabolite. The 5-FOA plate assays described above were repeated using a *P. aeruginosa crc* mutant strain (PAO8023), to determine if Crc played a role in the entry of orotate and its metabolism by the cell. A zone of killing was observed when either glucose or succinate, was used as

A

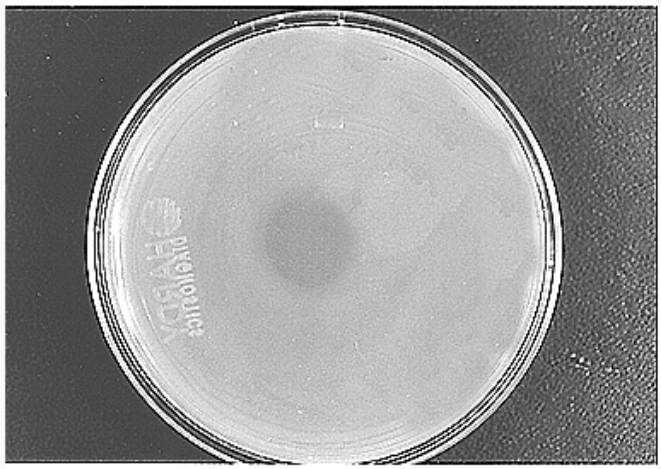

B

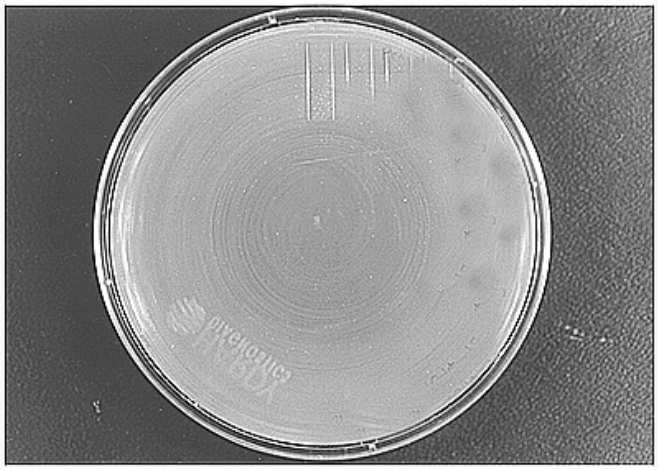

Fig. 84. Effect of 5-Fluoroorotate on *P. aeruginosa*, AK903 grown in minimal medium with glucose (A) or succinate (B). Zone of killing observed in glucose, not in succinate.

A

B

Fig. 85. Effect of 5-Fluoroorotate on *P. aeruginosa crc* mutant, PAO8023 grown in minimal medium with glucose (A) or succinate (B). Zone of killing observed in both glucose and succinate.

carbon and energy source (Figs. 85a, b), this suggested that in the absence of the Crc protein, succinate no longer affected the uptake or metabolism of orotate by *P. aeruginosa*.

Orotate as a pyrimidine source.

The ability of a pyrimidine auxotroph to utilize uracil or orotate as a pyrimidine source was tested by growing *P. aeruginosa pyrD*$^-$ strain (PAO0114) on glucose or succinate minimal (Table 9). A glance at Table 9 shows that uracil satisfied the pyrimidine requirement when either glucose or succinate was used as the carbon source, while orotate satisfied the pyrimidine requirement in glucose, but not in succinate. This suggested that orotate utilization as sole pyrimidine source (transport or metabolism) prevented by succinate.

Isolation of *out* mutants.

The transport of succinate into the cell has been shown in *E. coli*, *S. typhimurium* (Baker *et al*., 1996), and *Sinorhizobium meliloti* (Yurgel *et al*., 2000) to be via the DctA protein, a high-affinity permease that is part of the dicarboxylate transport (Dct) system. The study in *S. meliloti* (Yurgel *et al*., 2000) recently established that the Dct transport system also enables the entry of orotate, a monocarboxylate, into the cell. Mutants isolated based on their resistance to 5-FOA, known as *out* mutants, because of their inability to utilize orotate as sole pyrimidine source have been mapped to the *dctA* locus (Baker *et al*. 1996). Figure 86 show that the *P. aeruginosa* DctA sequence has amino

Table 9. The ability of a *P. aeruginosa pyrD* mutant to utilize succinate as a carbon and energy source and orotate as a pyrmidine source.

Carbon source	**Pyrimidine source**	**Absorbance at 600 nm** PAO 0114 (*pyrD*$^-$)
Glucose	Uracil	1.557
Glucose	Orotate	1.344
Succinate	Uracil	1.326
Succinate	Orotate	0.066

mutants were isolated using *P. aeruginosa* wild type cells (MVP7402) and a *P. aeruginosa pyrD* auxotroph (MVP7403). Mutants isolated from wild type cells were tested for their ability to use succinate as a carbon and energy source, and the mutants isolated from the *pyrD*$^-$ strain were tested for the ability to use orotate as the pyrimidine source (Table. 9). Results showed that the mutant strains, MVP7402 and MVP7403 were able to grow on succinate as the carbon source, though not as well as on glucose. This suggested that although the Dct system is the primary mode of transport for succinate, there is an alternative mechanism by which the cell could acquire succinate. In addition, orotate could not satisfy the pyrimidine requirement in the mutants isolated from the *pyrD*$^-$ auxotroph (MVP7403), which suggested that the Dct system was present in *Pseudomonas* and was the only mode by which orotate could enter the cell.

Quantitative radiolabel orotate assay.

In *E. coli* and *S. typhimurium* succinate was found to compete with orotate for entry into the cell (Baker et al. 1996). In order to test this in *P. aeruginosa*, a competitive radiolabeled orotate entry assay was performed. The percent of radiolabeled orotate entering resting cells was measured in wild type grown in glucose or succinate as the both in the absence and presence of exogenous orotate. As Fig. 87 shows, there was no difference in the amount of orotate entering the cells when grown in glucose or succinate alone. However, approximately 3 times more radiolabeled orotate entered the wild type cells grown in succinate in the presence of 1 mM exogenous orotate compared to those grown in glucose and orotate (Fig. 87). This suggested that expression of the *dctA* gene

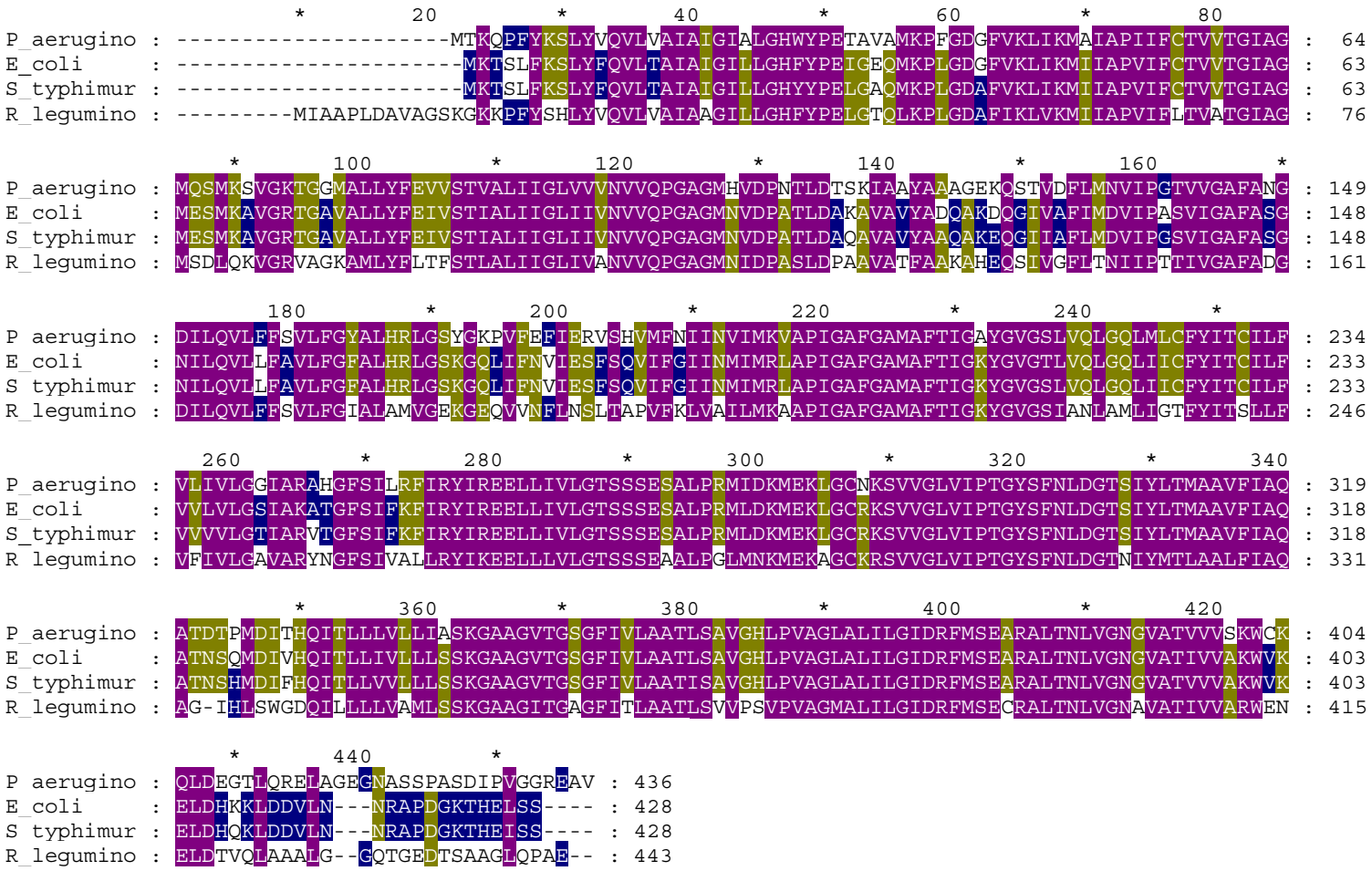

Fig. 86. Sequence alignment of the *P. aeruginosa* DctA protein with various other DctA proteins.

Table 10. The ability of *P. aeruginosa out* mutants (DctA$^-$) to utilize succinate as a carbon and energy source and orotate as a pyrimidine source.

Carbon source	**Pyrimidine source**	**Strain**	
		MVP7402 (DctA$^-$ isolated from wild type)	**MVP7403** (DctA$^-$ isolated from *pyrD* auxotroph)
Glucose	-	+ + +	Not tested
Succinate	-	+ +	Not tested
Glucose	Uracil	Not tested	+ + +
Succinate	Uracil	Not tested	+
Glucose	Orotate	Not tested	-
Succinate	Orotate	Not tested	-

acid similarity and identity to other DctA sequences including that of *E. coli*. To ascertain the presence of a functional Dct transport system in *Pseudomonas*, *out* (DctA$^-$) in *P. aeruginosa* was induced by orotate in the presence of succinate as the carbon source. This finding was unique to the *P. aeruginosa* DctA transport system. Previous data from 5-fluoroorotate plate assays showed that the Crc protein had an effect on either (i) the entry of orotate or (ii) the metabolism of orotate, in cells grown in succinate. To determine if this effect by the Crc protein was at the level of orotate entry or orotate metabolism, the same radiolabeled orotate assay was repeated using the *crc, pyrE* mutant strain (PAO8023). Fig. 87 shows that the Crc protein affect the ability of orotate to enter the cell when either glucose or succinate was the carbon source. Therefore, it is thought that Crc affects the metabolism of orotate once in the cell, rather than its entry into the cell as the previously suggested by the 5-FOA plate assays where a zone of killing was observed in a *crc* mutant and no zone of killing observed in the isogenic wild type strain.

Effect of Crc on pyrimidine gene expression.

The Crc protein is a global regulator known to regulate a number of biosynthetic and catabolic pathways in *Pseudomonas* (Collier *et al*., 1996). To determine if Crc played a role in pyrimidine metabolism, the *pyr* genes were assayed in a *P. aeruginosa* wild type and compared to those in an isogenic *crc*$^-$ mutant. Cells were grown in succinate, in the absence and presence of orotate (Table 11). There was a decrease in *pyrE* expression for wild type cells grown in excess of orotate compared to those grown without orotate while *pyrE* expression in the *crc* mutant cells was not affected by orotate.

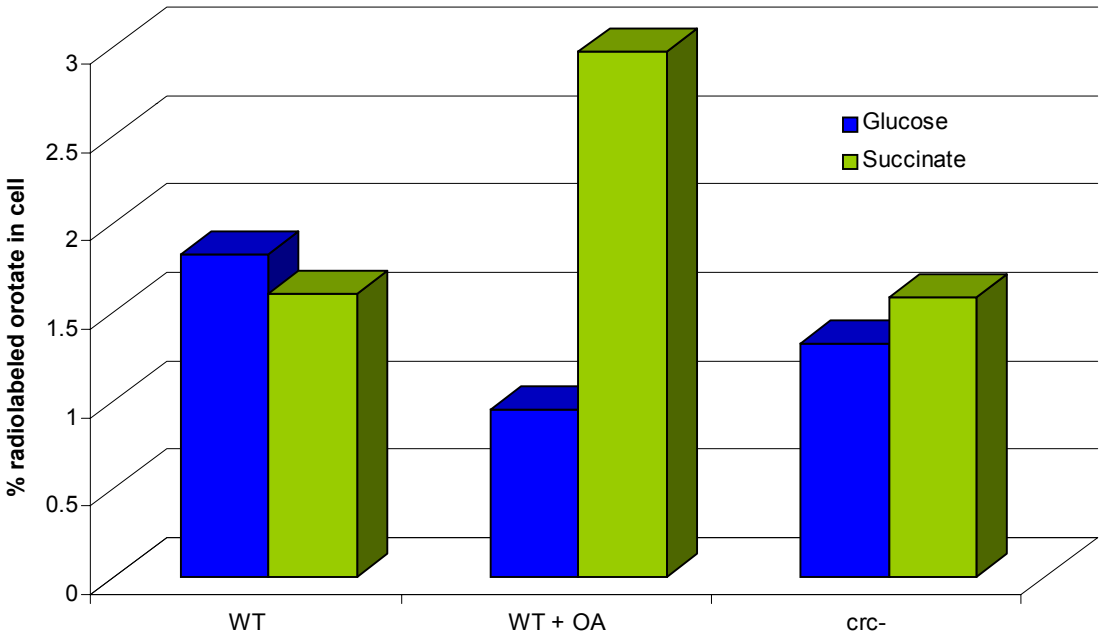

Fig. 87. Effect of excess orotate in growth medium on entry of radiolabeled orotate into *P. aeruginosa* wild type cells grown in glucose or succinate minimal medium in the presence and absence of orotate and *P. aeruginosa crc* mutant cells grown in glucose or succinate minimal medium.

This suggess that Crc affects *pyrE* expression only under conditions of high orotate. A similar result was obtained for a *crc* mutant strain harboring the *crc* gene on a plasmid (Table 11). Here, there was a four-fold decrease in *pyrE* expression under the same high levels of orotate. This effect was not observed for the expression of the other *pyr* genes tested, which suggests that Crc played a role only in the metabolism of orotate because of *pyrE* expression. Moreover, when the cells grown in glucose (Table 12), this effect by Crc was not observed on expression of *pyrE*. This suggests that Crc only comes into play when succinate is used as the carbon and energy source.

Effect of Crc on *pyrR* gene expression.

To determine if the Crc protein affected expression of the *pyrR* gene at the level of transcription, the *pyrR*::*lacZ* transcriptional fusion, pMVP50 was assayed for β-galactosidase activity in wild type *P. aeruginosa* and its isogenic *crc* mutant, PAO8020 (Table 13 and Fig. 88). The level of β-galactosidase activity was the same in the *P. aeruginosa* wild type strain and the isogenic *crc* mutant strain. Thus, the Crc protein did not effect transcription of the *pyrR* message most likely because the Crc protein did not bind to DNA.

Although no effect was observed by Crc at the level of transcription, the expression of BkdR, a transcriptional activator protein of the branched-chain keto acid dehydrogenase (BCKAD) operon, is negatively regulated by Crc (Hester et al., 2000a, b). This suggests that the mechanism of regulation of *bkdR* occurs at the posttranscriptional level. It was therefore important to ascertain if the same phenomenon applied for *pyrR*.

Accordingly, a *pyrR*::*lacZ* translational fusion, pMVP52 was expressed in a *P. aeruginosa* wild type strain and a *crc* mutant strain and assayed for β-galactosidase activity (Table 14 and Fig. 89) to determine if this was also the case for the expression of PyrR. When both strains were grown in glucose, there was no change in the amount of PyrR expressed. However, when the cells were grown in succinate, there was a two-fold increase in PyrR in the *crc* mutant (Fig. 89). This suggested that Crc acted posttranscriptionally in regulating PyrR levels when succinate is the carbon source. The Crc protein shares sequence similarity with exonucleases, and although it does not appear to have endo- or exonuclease activity, it has been shown to possess all the necessary structural features to cleave a phosphodiester bond (MacGregor *et al.,* 1996). Therefore, it is possible that the Crc protein exerts its effect by acting on secondary RNA structure (i.e. dsRNA) thereby affecting the translational efficiency or the stability (i.e. half-life) of functional mRNA (Hester *et al*., 2000b). The *pyrR* promoter readily forms a stable stem loop structure sequesters the Shine-Dalgarno sequence and AUG start codon, so that it is probable that the Crc protein cleaves the mRNA at the Shine-Dalgarno sequence thus disrupting the ribosomal binding site. This would then cause a decrease in amount of PyrR protein translated.

Table 11. Pyrimidine gene expression in *P. aeruginosa* a wild type, in a *crc* mutant and in a *crc* mutant harboring the crc^+ gene on a plasmid. Cells were grown in succinate as the carbon and energy source in the presence and absence of exogenous orotate.

Strain	**Genotype**	**Growth Conditions**	**Specific Activity (μmol min^{-1} mg $protein^{-1}$)**				
			ATCase	**DHOase**	**DHO dehydrogenase**	**OPRTase**	**OMP decarboxylase**
PAO1	Wild type	Succinate	474.0	556.0	14.0	16.0	11.0
PAO1	Wild type	Succinate + 1mM Orotate	714.0	375.0	8.0	7.0	10.0
PAO8020	*crc*$^-$	Succinate	476.0	571.0	12.0	8.0	11.0
PAO8020	*crc*$^-$	Succinate + 1mM Orotate	444.0	500.0	9.0	5.0	22.0
PAO8020	*crc*$^-$ (*crc*$^+$)	Succinate	410.0	42.0	18.0	175.0	35.0
PAO8020	*crc*$^-$ (*crc*$^+$)	Succinate + 1mM Orotate	365.0	84.0	27.0	40.0	35.0

Table 12. Pyrimidine gene expression in *P. aeruginosa* a wild type, in a *crc* mutant and in a *crc* mutant harboring the crc^+ gene on a plasmid. Cells were grown in glucose as the carbon and energy source in the presence and absence of exogenous orotate.

Strain	**Genotype**	**Growth Conditions**	**Specific Activity (μmol min^{-1} mg $protein^{-1}$)**		
			ATCase	DHOase	OPRTase
PAO1	Wild type	Glucose	450.0	75.0	30.0
PAO1	Wild type	Glucose + 1mM Orotate	419.3	80.6	116.1
PAO8020	crc^-	Glucose	354.8	112.9	77.4
PAO8020	crc^-	Glucose + 1mM Orotate	333.3	104.2	362.5
PAO8020	crc^- (crc^+)	Glucose	250.0	66.7	176.6
PAO8020	crc^- (crc^+)	Glucose + 1mM Orotate	450.0	166.7	218.3

Table 13. *β*-galactosidase activity measurements of *pyrR*::*lacZ* reporter gene fusions in wild type strain AK903 and *crc* deletion strain PAO8020 under different conditions of growth.

Plasmid	**Strain**	**Genotype**	**Specific Activity (units of *β*-galactosidase[a])**			
			Glucose	Glucose + 1mM Orotate	Succinate	Succinate + 1mM Orotate
pyrR::*lacZ*	AK903	Wild type	330.5	330.2	319.8	353.3
pyrR::*lacZ*	PAO 8020	*crc* $^{-}$	284.0	308.5	369.1	404.3

[a] One unit of *β*-galactosidase hydrolyzed 1 nmol of *o*-nitrophenol min^{-1} mg of $protein^{-1}$.

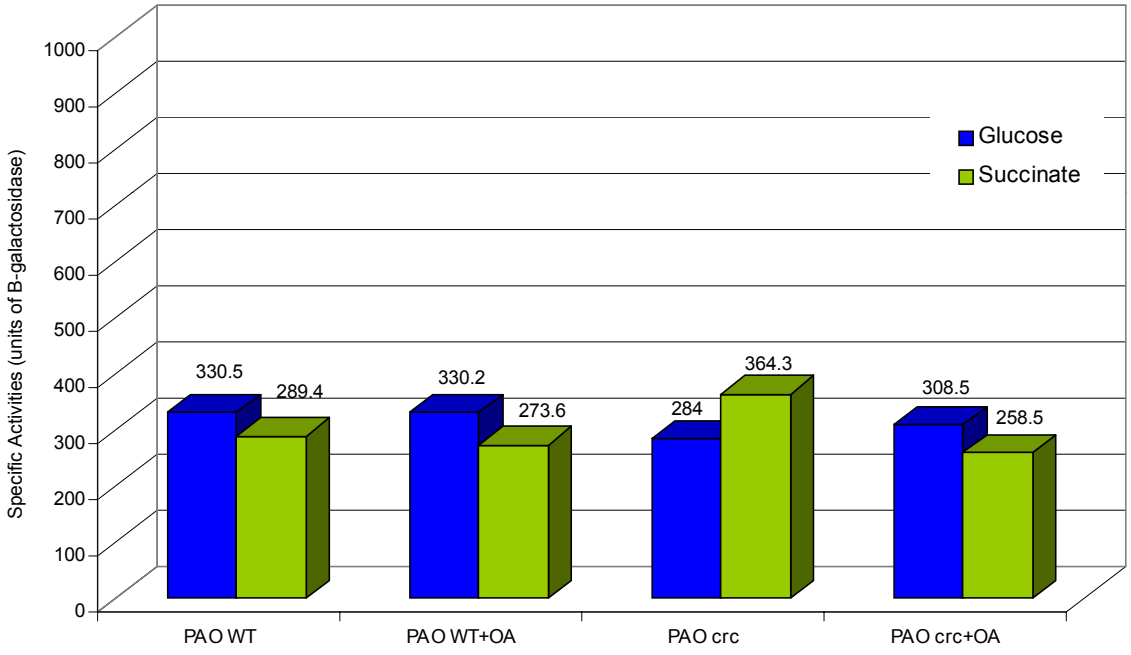

Fig. 88. Graphical representation of the *pyrR*::*lacZ* transcriptional fusion data from Table 13.

Table 14. *β*-galactosidase activity measurements of *pyrR*::*lacZ* translational gene fusions in wild type strain AK903 and *crc* deletion strain PAO 8020 under different conditions of growth.

Plasmid	Strain	**Genotype**	**Specific Activity (units of *β*-galactosidase[a])**			
			Glucose	Glucose + 1mM Orotate	Succinate	Succinate + 1mM Orotate
pyrR::*lacZ*	AK903	Wild type	258.0	258.2	321.9	300.1
pyrR::*lacZ*	PAO 8020	*crc* $^{-}$	295.4	314.8	606.5	603.8

[a] One unit of *β*-galactosidase hydrolyzed 1 nmol of *o*-nitrophenol min^{-1} mg of $protein^{-1}$.

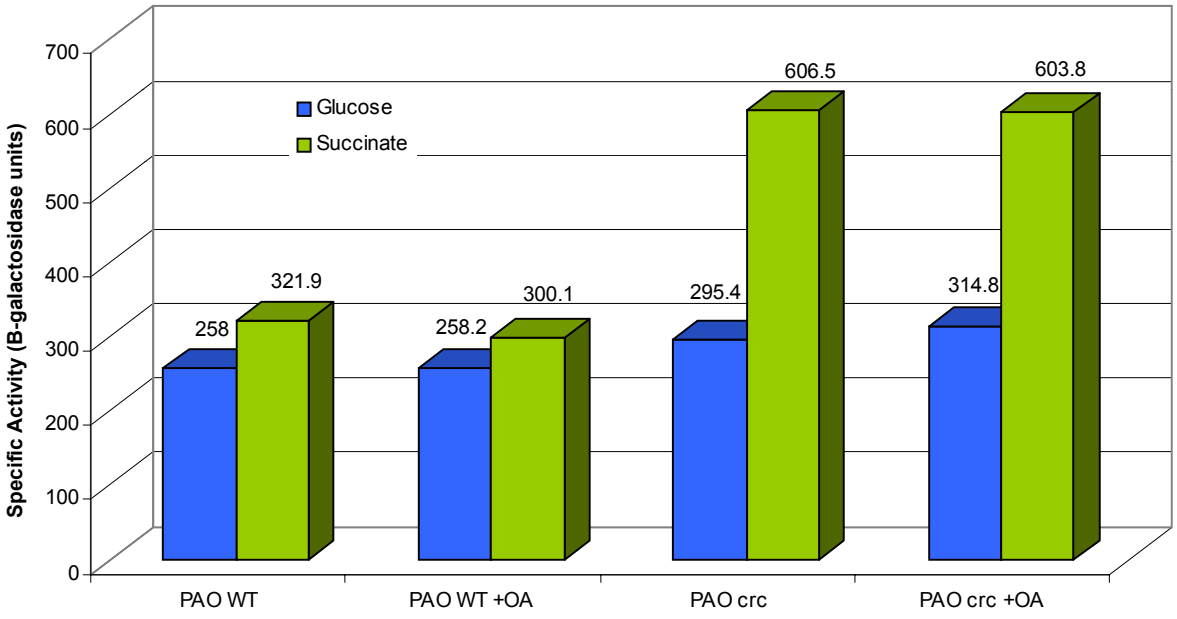

Fig. 89. Graphical representation of the *pyrR*::*lacZ* translational fusion data from Table 14.

CONCLUSIONS

Based on data from this study, the following mechanism of action by the PyrR and Crc proteins is proposed. The mechanistic pathway begins with the PyrR protein being expressed at low levels, which is achieved by having the Shine-Dalgarno sequence sequestered within a stable stem-loop formation. Such a secondary structure has been shown to down-regulate translation of a protein by 10-100 fold (Yarchuk *et al*., 1992). The PyrR protein represses its own expression by binding to the DNA upstream of the *pyrR* coding sequence. In this instance, basal level expression of the *pyrBC′* genes is observed through activity of only the P_2 promoter. The presence of the P_2 promoter ensures continual expression of the *pyrBC′* genes, guaranteeing continual formation of carbamoylaspartate, which is then converted to dihydroorotate by the action of ATCase. Dihydroorotate has been shown to be a starting compound for the synthesis of pyoverdin, an important siderophore in *Pseudomonas* (Maksimova *et al*., 1993) and an obligate requirement for pathogenicity.

As the flow through the biosynthetic pathway continues and the cellular levels of pyrimidines increase, there is an accumulation of endogenous orotate brought about by the activation of the *pyrD* gene by PyrR. As pointed out by Jensen (1982), the flux through the pathway is dependent upon the accumulation of orotate within the cell (Jensen, 1982). In *Pseudomonas*, orotate accumulation occurs under several physiological conditions. For example, (i) the *pyrE* and *crc* genes share the same promoter region. Phibbs and co-workers (2000a) have shown that the Crc protein is

constitutively expressed and that this expression is greater in cells grown in succinate. (ii) Wang *et al*. (1999) have determined the dissociation constants of the substrates for OPRTase to be 280 μM for orotate and 33 μM for PRPP. This suggests that intracellular levels of orotate must to reach at least 280 μM in order to be converted to OMP. (iii) Tom West and co-workers have shown that orotate induces expression of *pyrC*. Such an induction would also increase endogenous levels of dihydroorotate.

We believe that flow through the pyrimidine biosynthetic pathway is also dependent on the ratio of unbound PyrR versus PyrR bound by OMP which can no longer bind DNA. When pyrimidine levels are limited, PyrR is made in a form that activates expression of the downstream *pyr* genes, *pyrD*, *pyrE*, and *pyrF* (monomeric state). When the concentration of PyrR is high, the protein dimerizes and acts as a repressor for autoregulation. Sequence alignment of the DNA fragments used as probes for EMSA, revealed a 9 bp conserved sequence ATGSSCSCC that could be the putative regulatory element for binding of PyrR (Fig. 90). This 9 bp consensus is appropriately located upstream of the -10 and -35 promoter elements of the *pyrD*, *pyrE* and *pyrF* genes (Fig. 90). This positioning is characteristic of activator binding sites. This same consensus sequence was also identified in the region upstream of the *pyrR* gene (Fig. 90). Interestingly, the sequence is present as an imperfect inverted repeat, separated by 11 bp, moreover, it is situated within the -10 and -35 *pyrR* promoter elements, which is trademark of repressor binding sites. This inverted repeat being separated by 11 bp represents one turn of the helix suggesting that the PyrR protein binds to the *pyrR* repression site as a dimer, but binds to the activation sites as a monomer. However, this

consensus was not identified in the DNA sequence upstream of the *pyrC* gene (encoding dihydroorotase) suggesting that perhaps *pyrC* expression is under a different form of regulation, one that is not mediated by PyrR.

In the absence of ligands, equilibrium for the native state of PyrR is predominantly between the monomeric and dimeric forms, ensuring continued activation of the pathway, therefore PyrR must be made at low levels. The *P. aeruginosa* PyrR protein was found to shift between a monomeric, (dimeric) and tetrameric molecular state. The tetrameric state is favored in high PRPP concentrations and under such cellular conditions PRPP binds to PyrR causing a conformational shift to the aggregated tetrameric state. It is possible that this conformational shift either obstructs the DNA binding domain or the DNA binding domain is no longer accessible. The role of PyrR when bound by PRPP (PyrR in its tetrameric form) is yet unclear and is currently under investigation. However, this study has shown that PyrR in this aggregated form does not bind to DNA. Though the presence of OMP did not shift the PyrR equilibrium, the *pyrF* gene product, OMP decarboxylase has been shown to be a very proficient enzyme (Harris et al., 2000). Moreover, the dissociation constant of OMP for OPRTase is 3 μM (Wang et al., 1999) compared to 280 μM for orotate. It is therefore very likely that high levels of pyrimidines would lead to accumulation of OMP. When OMP accumulates, it binds to PyrR and abolishes the DNA binding capability of the PyrR protein thereby preventing further activation of the downstream *pyr* genes. However, it is proposed that the biosynthetic pathway will be turned on again when the ratio of unbound PyrR exceeds that of OMP bound PyrR. This situation would only arise when pyrimidines availability

is limited. It must be noted that PyrR bound by OMP also prevents autoregulation. The consequent increase in expression of PyrR further facilitates the change in ratio of unbound to OMP bound protein, in order to activate the pathway again.

In *Pseudomonas*, succinate is the preferred carbon source thus the cells have a faster growth rate. Phibbs and co-workers (2000b) have also shown that expression of the Crc protein is greater when cells are grown in succinate as the carbon source, this leads to an increase in Crc bound orotate and therefore a decrease in levels of PyrR. Moreover, expression of the DctA transport protein is induced in the presence of high levels of exogenous orotate when succinate is used as the carbon source. This induction of the Dct transport system by orotate is novel as such a phenomenon has not been reported in other organisms. In addition, when pyrimidine levels are high, the Crc protein bound by orotate, cleaves the secondary structure of the *pyrRBC'* mRNA such that the ribosomal binding site is disrupted (Fig. 91). This results in a decrease in translation of PyrR and since the PyrR protein is an activator for *pyrD*, *pyrE* and *pyrF*, expression of these genes also decreases causing a reduction in the pyrimidine pools.

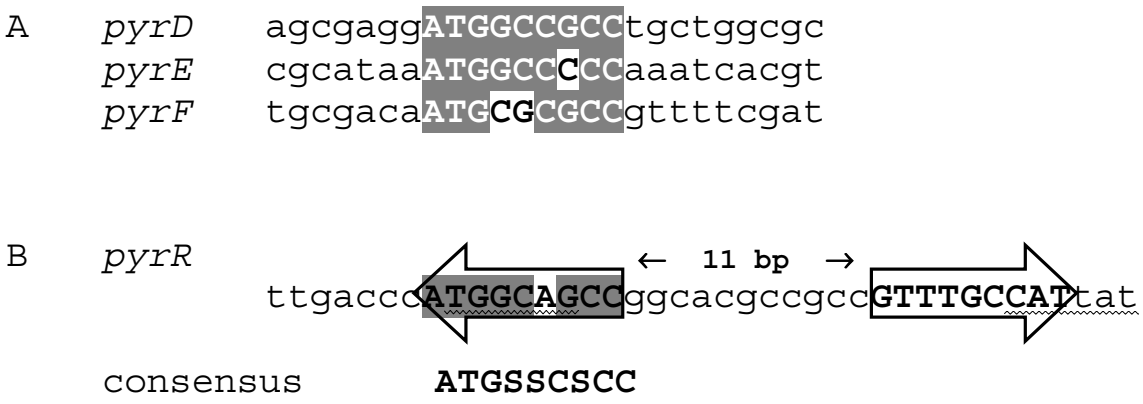

Fig. 90. Alignment of potential regulatory sequence elements identified upstream of the genes regulated by the PyrR protein. The most conserved nucleotide positions are shaded. A consensus deduced from these elements is indicated using the GCG code for the degenerated nucleotide positions. (A) Activation sequence for the *pyrD*, *pyrE* and *pyrF* genes. (B) Repression sequence for the *pyrR* gene. An imperfect inverted repeat sequence separated by 11 bp is shown within the block arrows. The *pyrR* –10 and –35 promoter regions are underlined.

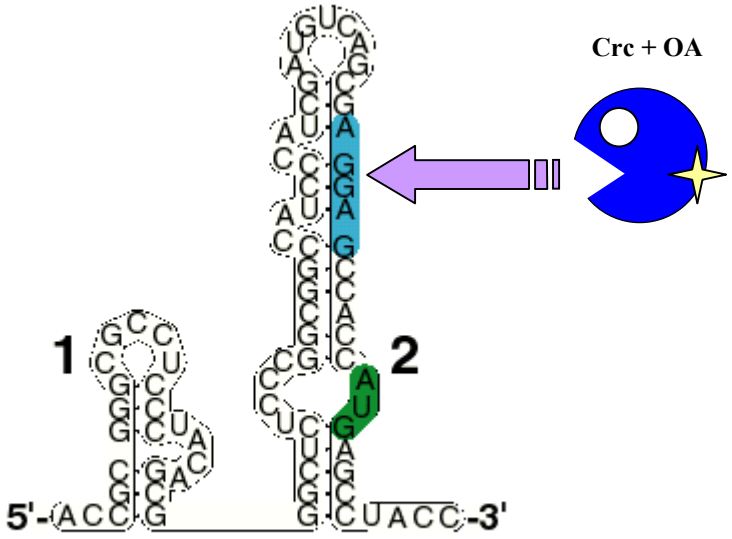

Fig. 91. The action of Crc on *pyrR* mRNA, causing disruption of the ribosomal binding site of PyrR.

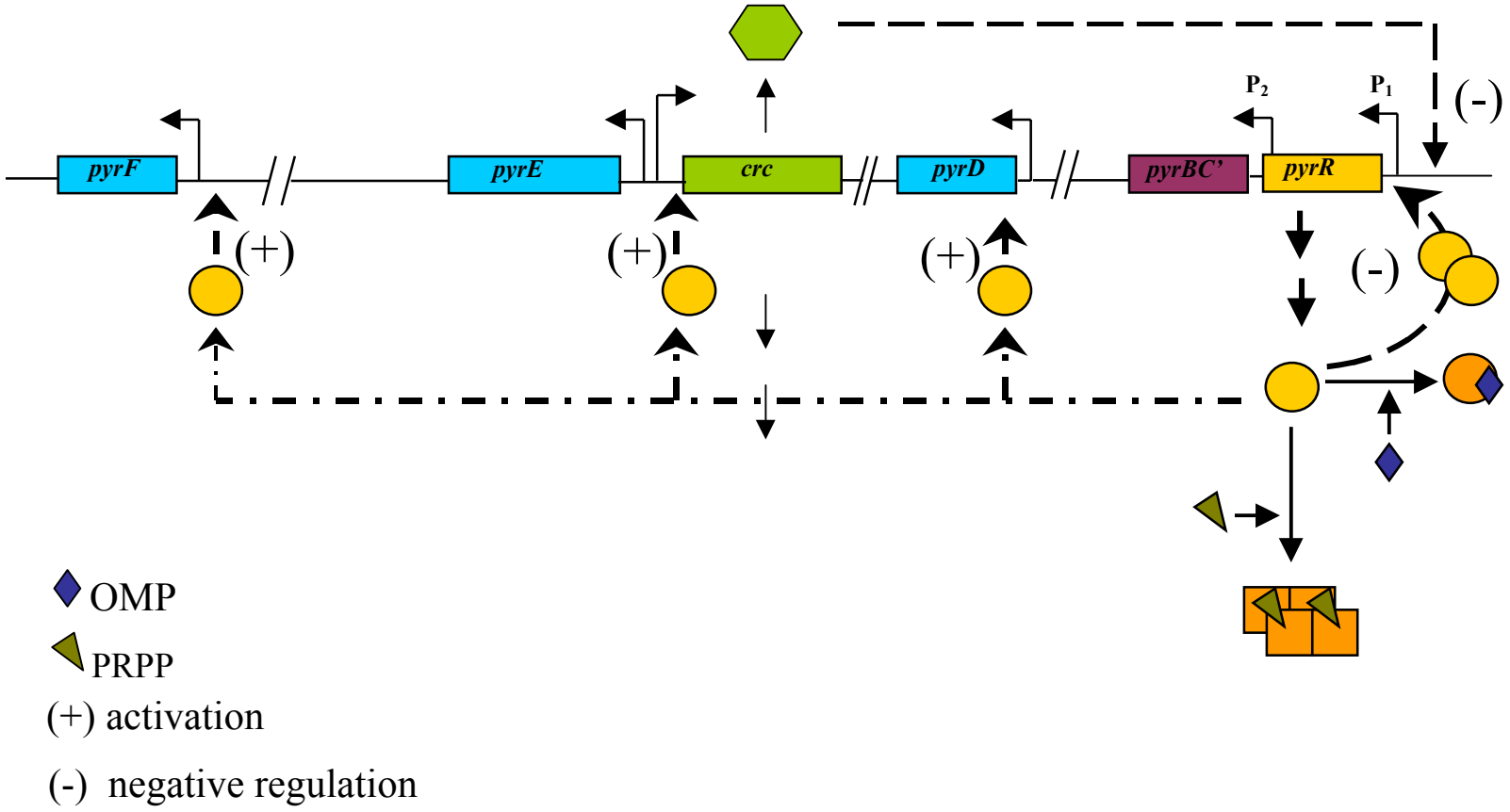

Fig. 92. Overall mechanism of pyrimidine regulation by PyrR and Crc in *P. aeruginosa*.

REFERENCES

Abdelal, A., Kessler, D. P. & Ingraham, J. L. (1969). Arginine-auxotrophic phenotype resulting from a mutation in the *pyrA* gene of *Escherichia coli*. *J Bacteriol* **97,** 466-468.

Abdelal, A. T., Bussey, L. & Vickers, L. (1983). Carbamoylphosphate synthetase from *Pseudomonas aeruginosa*: subunit composition, kinetic analysis and regulation. *Eur J Biochem* **129**, 697-702.

Altschul, S. F., Gish, W., Miller, W., Myers, E. W. & Lipman, D. J. (1990). Basic local alignment search tool. *J Mol Biol* **215,** 403-410.

Anderson, P. M. & Meister, A. (1965). Evidence of an activated form of carbon dioxide in the reaction catalyzed by *Escherichia coli* carbamoylphosphate synthetase. *Biochemistry* **4**, 2803-2809.

Ausubel, F. M., Brent, R., Kingston, R. E., Moore, D., Seidman, J. G., Smith, J. A., Struhl, K., Albright, L. M., Coen, D. M., Varki, A. & Chanda, V. B. (1993). *Current Protocols in Molecular Biology*. New York: Greene Publishing Associates and Wiley Interscience.

Baker, K. E., Ditullio, K. P., Neuhard, J. & Kelln, **R. A. (1996).** Utilization of orotate as a pyrimidine source by *Salmonella typhimurium* and *Escherichia coli* requires the dicarboxylate transport protein encoded by *dctA*. *J Bacteriol* **178,** 7099-7105.

Beck, D. E. (1995). The pyrimidine salvage pathway in prokaryotes: Labyrinths of enzymatic diversity. Ph.D. Dissertation (Molecular Biology), University of North Texas.

Beckwith, J. R., Pardee, A. B., Austrian, R. & Jacob, F. (1962). Coordination of the synthesis of the enzymes in the pyrimidine pathway of *E. coli*. *J Mol Biol* **5**, 618-634.

Bertani, G. (1951). Studies on lysogenesis. I. The mode of phage liberation by lysogenic *Escherichia coli*. *J Bacteriol* **62,** 293-300.

Bollag, D. M. & Edelstein, S. J. (1991). *Protein Methods*. pp71-160. New York: Wiley Interscience.

Bolotin, A., Mauger, S., Malarme, K., Ehrlich, S. D. & Sorokin, A. (1999). Low-redundancy sequencing of the entire *Lactococcus lactis* IL1403 genome, *Antonie Van Leeuwenhoek* **76**, 27-76.

Bradford, M. M. (1976). A rapid and sensitive method for the quantification of microgram quantities of protein utilizing the principle of protein-dye binding. *Anal Biochem* **72,** 248-254.

Caroline, D. F. (1969). Pyrimidine synthesis in *Neurospora crassa*: gene-enzyme relationships. *J Bacteriol* **100**, 1371-1377.

Chu, C. P. & West, T. P. (1990). Pyrimidine biosynthetic pathway of *Pseudomonas fluorescens*. *J Gen Microbiol* **136,** 875-880.

Collier, D. N., Hager, P. W. & Phibbs, Jr., P. V. (1996). Catabolite repression control in the pseudomonads. *Res Microbiol* **147,** 551-561.

Condon, S., Collins, J. K. & O'Donovan, G. A. (1976). Regulation of arginine and pyrimidine biosynthesis in *Pseudomonas putida*. *J Gen Microbiol* **92,** 375-383.

Conway, T. (1992). The Entner-Doudoroff pathway: History, physiology and molecular biology. *FEMS Microbiol Rev* **103,** 1-28.

Dagert, M. & Ehrich, S. D. (1979). Prolonged incubation in calcium chloride improves the competence of *Escherichia coli*. *Gene* **6**, 23-28.

De Lorenzo, V. & Timmis, K. N. (1994). Analysis and construction of stable phenotypes in Gram negative bacteria with Tn5 and Tn10-derived transposons. *Meth Enzymol* **235,** 386-405.

Deretic, V., Konyecsni, W. M., Mohr, C. D., Martin, D. W. & Hibler, N. S. (1989). Common denominators of promoter control in *Pseudomonas* and other bacteria. *Biotechnology* **7,** 1249-1254.

De Rijk, P. & De Wachter, R. (1997). Rna Viz, a program for the visualization of RNA secondary structure. *Nucleic Acids Res* **25,** 4679-4684.

Elagöz, A., Abdi, A., Hubert, J. C. & Kammerer, B. (1996). Structure and organization of the pyrimidine biosynthesis pathway genes in *Lactobacillus plantarum*: A PCR strategy for sequencing without cloning. *Gene* **182**, 37-43.

Ellis, K. J. & Morrison, J. F. (1982). Buffers of constant ionic strength for studying pH-dependent processes. *Meth Enzymol* **87,** 405-426.

Entner, N. & Doudoroff, M. (1952). Glucose and gluconic acid oxidation in *Pseudomonas saccharophila*. *J Biol Chem* **196,** 853-862.

Farin, F. & Clarke, P. H. (1978). Positive regulation of amidase synthesis in *Pseudomonas aeruginosa*. *J Bacteriol* **135,** 379-392.

Farinha, M. A. & Kropinski, A. M. (1990a). Construction of broad-host-range plasmid vectors for easy visible selection and analysis of promoters. *J Bacteriol* **172,** 3496-3499.

Farinha, M. A. & Kropinski, A. M. (1990b). High efficiency electroporation of *Pseudomonas aeruginosa* using frozen cell suspensions. *FEMS Microbiol Lett* **58,** 221-225.

Fleischmann, R. D., Adams, M. D., White, O., Clayton, R. A., Kirkness, E. F., Kerlavage, A. R., Bult, C. J., Tomb, J. F., Dougherty, B. A. & Merrick, J. M. (1995). Whole-genome random sequencing and assembly of *Haemophilus influenzae* Rd. *Science* **269**, 496-512.

Foltermann, K. F., Wild, J. R., Zink, D. L. & O'Donovan, G. A. (1981). Regulatory variance of aspartate transcarbamoylase among strains of *Yersinia enterocolitica*-like organisms. *Curr Microbiol* **6**, 43-47.

Gambello, J. R., & Iglewski, B. H. (1991). Cloning and characterization of the *Pseudomonas aeruginosa lasR* gene, a transcriptional activator of elastase expression. *J Bacteriol* **173,** 3000-3009.

Gerhart, J. C. Pardee, A. B. (1962). The enzymology of control by feedback inhibition. *J Biol Chem* **237**, 891-896.

Gerhart, J. C. & Pardee, A. B. (1964). Aspartate transcarbamoylase, an enzyme designed for feedback inhibition. *Fed Proc* **23**, 727-735.

Ghim, S. Y., & Neuhard, J. (1994). The pyrimidine biosynthetic operon of the thermophilic *Bacillus caldolyticus* includes genes for uracil phosphoribosyltransferase and uracil permease. *J Bacteriol* **176,** 3698-3707.

Goldberg, J. B. (2000). *Pseudomonas*: Global bacteria. *Trends Microbiol* **8,** 55-57.

Grogan, D. W. & Gunsalus, R. P. (1993). *Sulfolobus acidocaldarius* synthesizes UMP via a standard *de novo* pathway: Results of a biochemical-genetic study. *J Bacteriol* **175**, 1500-1507.

Hager, S. E. & Jones, M. E. (1967). A glutamine dependent enzyme for the synthesis of carbamoylphosphate for pyrimidine biosynthesis in fetal rat liver. *J Biol Chem* **242**, 5674-5680.

Hames, B. D. (1981). In *Gel Electrophoresis of Proteins. A Practical Approach*, p 290. Edited by B. D. Hames & D. Rickwood. London: IRL Press Limited.

Harris, P., Navarro Poulsen, J. C., Jensen, K. F. & Larsen, S. (2000). Structural basis for the catalytic mechanism of a proficient enzyme: orotidine 5'-monophosphate decarboxylase. *Biochemistry* **39,** 4217-4224.

Hayward, W. S. & Belser, W. L. (1965). Regulation of pyrimidine biosynthesis in *Serratia marcescens*. *Proc Natl Acad Sci USA* **53**, 1483-1489.

Hester, K. L., Lehman, J., Najar, F., Song, L., Roe, B. A., MacGregor, C. H., Hager, P. W., Phibbs. Jr., P. V. & Sokatch, J. R. (2000a). Crc is involved in catabolite repression control of the *bkd* operons of *Pseudomonas putida* and *Pseudomonas aeruginosa*. *J Bacteriol* **182,** 1144-1149.

Hester, K. L., Madhusudhan, K. T. & Sokatch, J. R. (2000b). Catabolite repression control by Crc in 2xYT medium is mediated by posttranscriptional regulation of *bkdR* expression in *Pseudomonas putida*. *J Bacteriol* **182,** 1150-1153.

Higgins, D. G., Thompson, J. D. & Gibson, T. J. (1996). Using CLUSTAL for multiple alignments. *Methods Enzymol* **266,** 383-402.

Huff, J. P., Grant, B. J., penning, C. A. & Sullivan, K. F. (1990). Optimization of transformation of *Escherichia coli* with plasmid DNA. *Biotechniques* **9,** 570-577.

Hutson, J. Y. & Downing, M. (1968). Pyrimidine biosynthesis in *Lactobacillus leichmannii*. *J Bacteriol* **96**, 1249-1254.

Hylemon, P. B. & Phibbs, Jr., P. V. (1972). Independent regulation of hexose catabolizing enzymes and glucose transport activity in *Pseudomonas aeruginosa*. *Biochem Biophys Res Commun* **48,** 1041-8.

Isaac, J. H. & Holloway, B. W. (1968). Control of pyrimidine biosynthesis in *Pseudomonas aeruginosa*. *J Bacteriol* **96,** 1732-1741.

Jensen, K. F. (1982). Metabolism of 5-phosphoribosyl-1- pyrophosphate (PRPP) in *Escherichia coli* and *Salmonella typhimurium*. In *Metabolism of Nucleotides, Nucleosides and Nucleobases in Microorganisms*, pp. 1-25. Edited by A. Munch-Petersen. London: Academic Press.

Jones, M. E. (1980). Pyrimidine nucleotide biosynthesis in animals: genes, enzymes and regulation of UMP biosynthesis. *Ann Rev Biochem* **49**, 253-279.

Kalman, S. M., Duffield, P. H. & Brozowski, T. (1966). Purification and properties of a bacterial carbamoylphosphate synthetase. *J Biol Chem* **241**, 1871-1877.

Kafer, C. & Thornburg, R. W. (1999). Pyrimidine metabolism in plants. *Paths to Pyrimidines* **5,** 7-19.

Kaneko, T., Sato, S., Kotani, H., Tanaka, A., Asamizu, E., Nakamuru, Y., Miyajima, N., Hirosawa, M., Sugiura, M., Sasamoto, S., Kimura, T., Hosouchi, T., Matsuno, A., Muraki, A., Nakazaki, N., Naruo, K., Okomura, S., Shimpo, S., Takeuchi, C.,

Wada, T., Watanabe, A., Yamuda, M., Yasuda, M. & Tabata, S. (1996). Sequence analysis of the genome of the unicellular cyanobacterium *Synechocystis* sp. strain PCC6803. II. Sequence determination of the entire genome and assignment of potential protein-coding regions. *DNA Res* **3,** 109-136.

Koch, C. & Høiby, N. (1993). Pathogenesis of cystic fibrosis. *Lancet* **341,**1065-1069.

Kumar, A. P. (2000). Structure-function studies on aspartate transcarbamoylase and regulation of pyrimidine biosynthesis by a positive activator protein, PyrR in *Pseudomonas putida*. Ph.D. Dissertation (Molecular Biology). University of North Texas.

Lacroute, F. (1968). Regulation of pyrimidine biosynthesis in *Saccharomyces cerevisiae*. *J Bacteriol* **95**, 824-832.

Laemmli, U. K. (1970). Cleavage of structural proteins during the assembly of the head of bacteriophage T4. *Nature* **227,** 680-685.

Long, C. & Koshland, Jr., D. E. (1978). Cytidine triphosphate synthetase. *Methods Enzymol* **51,** 79-83.

Long, C. W. & Pardee, A. B. (1967). Cytidine triphosphate synthetase of *Escherichia coli* B. I. Purification and kinetics. *J Biol Chem* **242,** 4715-4721.

Lu, Y., Turner, R. J. & Switzer, R. L. (1995). Roles of three transcriptional attenuators of the *Bacillus subtilis* pyrimidine biosynthetic operon in the regulation of its expression. *J Bacteriol* **177,** 1315-1325.

Lu, Y. & Switzer, R. L. (1996). Evidence that the *Bacillus subtilis* pyrimidine regulatory protein PyrR acts by binding to *pyr* mRNA at three sites *in vivo*. *J Bacteriol* **178,** 5806-5809.

MacGregor, C. H., Wolff, J. A., Arora, S. K. & Phibbs, Jr., P. V. (1991). Cloning of a catabolite repression control (*crc*) gene from *Pseudomonas aeruginosa*, expression of the gene in *Escherichia coli*, and identification of the gene product in *Pseudomonas aeruginosa*. *J Bacteriol* **173,** 7204-7212.

MacGregor, C. H., Wolff, J. A., Arora, S. K., Hylemon, P. B. & Phibbs, Jr., **P. V. (1992).** Catabolite repression control in *Pseudomonas aeruginosa*. In *Pseudomonas Molecular Biology and Biotechnology*, pp. 198-206. Edited by E. Galli, S. Silver, & B. Witholt. Washington, DC: American Society for Microbiology.

MacGregor, C. H., Arora, S. K., Hager, P. W., Dail, M. B. & Phibbs, Jr., P. V. (1996). The nucleotide sequence of *Pseudomonas aeruginosa pyrE-crc-rph* region and purification of the *crc* gene product. *J Bacteriol* **178,** 5627-5635.

Maksimova, N. P., Blazhevich, O. V. & Fomichev, I. K. (1993). The role of pyrimidines in the biosynthesis of the fluorescing pigment pyoverdin Pm in *Pseudomonas putida* M. Mol *Gen Mikrobiol Virusol* **5,** 22-26.

McCarthy, J. E. & Gualerzi, C. (1990). Translational control of prokaryotic gene expression. *Trend Genet* **6**, 78-85.

Merle, P. & Kadenbach, B. (1980). The subunit composition of mammalian cytochrome C oxidase. *Eur J Biochem* **105,** 449-507.

Miller, J. H. (1972). In *Experiments in Molecular Genetics*. p. 432. Cold Spring Harbor, NY: Cold Spring Harbor Laboratory Press.

Nakinishi, S., Ito, K. & Tatibana, M. (1968). Two types of carbamoylphosphate synthetase in rat liver: Chromatographic resolution and immunological distinction. *Biochem Biophys Res Comm* **33**, 774-781.

Navre, M. & Schachman, H. K. (1983). Synthesis of aspartate transcarbamoylase in *Escherichia coli*: Transcriptional regulation of the *pyrBI* operon. *Proc Natl Acad Sci USA* **80,** 1207-1211.

Neuhard, J. (1982). Utilization of preformed pyrimidine bases and nucleosides. In *Metabolism of Nucleotides, Nucleosides and Nucleobases in Microorganisms*, pp. 95-148. Edited by A. Munch-Peterson. London: Academic Press.

O'Donovan, G. A. & Neuhard, J. (1970). Pyrimidine metabolism in microorganisms. *Bacteriol Rev* **34**, 278-343.

O'Donovan, G. A. & Shanley, M. S. (1995). Pyrimidine metabolism in *Pseudomonas*. *Paths to Pyrimidines* **3,** 49-59.

Ohta, Y., Maeda, M. & Kudo, T. (2001). *Pseudomonas putida* CE2010 can degrade biphenyl by a mosaic pathway encoded by the *tod* operon and *cmtE*, which are identical to those of *P. putida* F1 except for a single base difference in the operator-promoter region of the *cmt* operon. *Microbiology* **147,** 31-41.

Opel, M. L., Arfin, S. M. & Hatfield, G. W. (2001). The effects of DNA supercoiling on the expression of operons of the *ilv* regulon of *Escherichia coli* suggest a physiological rationale for divergently transcribed operons. *Mol Microbiol* **39,** 1109-1115.

Ornston, L. N. & Stanier, R. Y. (1966). The conversion of catechol and protocatechuate to beta-ketoadipate by *Pseudomonas putida*. *J Biol Chem* **16,** 3776-3786.

Park, S. M., Lu, C. D. & Abdelal, A. T. (1997). Purification and characterization of an arginine regulatory protein, ArgR, from *Pseudomonas aeruginosa* and its interactions with the control regions for the *car*, *argF*, and *aru* operons. *J Bacteriol* **179**, 5309-5317.

Pedersen, S. S. (1992). Lung infection with alginate-producing, mucoid *Pseudomonas aeruginosa* in cystic fibrosis. *APMIS* **100,** 1-79.

Phillips, A. T. & Mulfinger, L. M. (1981). Cyclic adenosine 3', 5' monophosphate levels in *Pseudomonas putida* and *Pseudomonas aeruginosa* during induction and carbon catabolite repression of histidase synthesis. *J Bacteriol* **145,** 1286-1292.

Potter, A. A., & Loutit, J. S. (1982). Exonuclease activity from *Pseudomonas aeruginosa* which is missing in phenotypically restrictionless mutants. *J Bacteriol* **151,**1204-1209.

Prescott, L. M. & Jones, M. E. (1969). Modified methods for the determination of carbamoylaspartate. *Anal Biochem* **32**, 408-419.

Procter, W. D. (1998). Genetic and biochemical characterization of HexR, a negative regulator of carbohydrate utilization by the hex regulon of *Pseudomonas aeruginosa*. Ph.D. Dissertation, East Carolina University School of Medicine.

Quinn, C. L., Stephenson, B. T. & Switzer, R. L. (1991). Functional organization and nucleotide sequence of the *Bacillus subtilis* pyrimidine biosynthetic operon. *J Biol Chem* **266,** 9113-9127.

Ronald, S., Farinha, M. A., Allan, B. J. & Kropinski, A. M. (1992). Cloning and physical mapping of transcriptional regulatory (sigma) factors from *Pseudomonas aeruginosa*. In *Pseudomonas: Molecular Biology and Biotechnology*, pp249-258. Edited by E. Galli, S. Silver & B. Witholt. Washington, D. C: American Society for Microbiology.

Roof, W. D., Foltermann, K. F. & Wild, J. R. (1982). The organization and regulation of the *pyrBI* operon in *Escherichia coli* includes a *rho*-independent attenuator sequence. *Mol Gen Genet* **187,** 391-400.

Saiki, R. K., Gelfland, D. H., Stoffel, S., Scharf, S. J., Higuchi, R., Harn, G. T., Mullis, K. B. & Erlich, H. A. (1988). Primer-directed enzymatic amplification of DNA with a thermostable DNA polymerase. *Science* **239**, 487-491.

Sanger, F., Nicklen, S. & Coulson, A. R. (1977). DNA sequencing with chain-terminating inhibitors. *Proc Natl Acad Sci USA* **74,** 5463-5467.

Schneider, K. & Beck, C. F. (1986) Promoter-probe vectors for the analysis of divergently arranged promoters. *Gene* **42,** 37-48.

Schurr, M. J., Vickery, J. F., Kumar, A. P., Campbell, A. L., Cunin, R., Benjamin, R. C., Shanley, M. S. & O'Donovan, G. A. (1995). Aspartate transcarbamoylase genes of *Pseudomonas putida*: Requirement for an inactive dihydroorotase for assembly into the dodecameric holoenzyme. *J Bacteriol* **177,** 1751-1759.

Schwartz, M., & Neuhard, J. (1975). Control of expression of the *pyr* genes in *Salmonella typhimurium*: effects of variations in uridine and cytidine nucleotide pools. *J Bacteriol* **121,** 814-822.

Schweizer, H. P. (1993). Small broad-host-range gentamicin resistance gene cassettes for site-specific insertion and deletion mutagenesis. *Biotechniques* **15,** 831-833.

Siegel, L. S., Hylemon, P. B. & Phibbs, Jr., **P. V. (1977).** Cyclic adenosine 3', 5'-monophosphate levels and activities of adenylate cyclase and cyclic adenosine 3', 5'-monophosphate phosphodiesterase in *Pseudomonas* and *Bacteriodes*. *J Bacteriol* **129,** 87-96.

Simon, R., Priefer, U. & Puhler, A. (1983). A broad host range mobilization system for *in vivo* genetic engineering: transposon mutagenesis in Gram negative bacteria. *Bio/Technology* **1**, 784-791.

Smiley, J. A., Angelot, J. M., Cannon, R.C., Marshall, E. M. & Asch, D. K. (1999). Radioactivity-based and spectrophotometric assays for isoorotate decarboxylase: identification of the thymidine salvage pathway in lower eukaryotes. *Anal Biochem* **266,** 85-92.

Smith, D. B. & Johnson, K. S. (1988). Single-step purification of polypeptides expressed in *Escherichia coli* as fusions with glutathione S-transferase. *Gene* **67,** 31-40.

Smith, J. M., Kelln, R. A. & O'Donovan, G. A. (1980). Repression and derepression of the enzymes of the pyrimidine biosynthetic pathway in *Salmonella typhimurium*. *J Gen Microbiol* **121,** 27-38.

Smyth, P. F. & Clarke, P. H. (1975). Catabolite repression in *Pseudomonas aeruginosa* amidase: the effect of carbon sources on amidase synthesis. *J Gen Microbiol* **90,**91-99.

Sonnhammer, E. L. L. & Durbin, R. (1994). A workbench for large scale sequence homology analysis. *Comput Applic Biosci* **10,** 301-307.

Spiers, A. J., Buckling, A. & Rainey, P. B. (2000). The causes of *Pseudomonas* diversity. *Microbiology* **146,** 2345-2350.

Stanier, R. Y., Palleroni, N. J. & Doudoroff, M. (1966). The aerobic Pseudomonads: A taxonomic study. *J Gen Microbiol* **43,** 159-271.

Stibitz, S., Black, W. & Falkow, S. (1986). The construction of a cloning vector designed for gene replacement in *Bordetella pertussis*. *Gene* **50,** 133-140.

Studier, F. W. & Moffatt, B. A. (1986). Use of bacteriophage T7 RNA polymerase to direct selective high-level expression of cloned genes. *J Mol Biol* **189,** 113-130.

Swank, R. T. & Munkres, K. D. (1971). Molecular weight analysis of oligopeptides by electrophoresis in polyacrylamide gel with sodium dodecyl sulfate. *Anal Biochem* **39**, 462-477.

Switzer, R. L., Quinn, C. L. & Stephenson, B. T. (1991). Functional organization and nucleotide sequence of the *Bacillus subtilis* pyrimidine biosynthetic operon. *J Biol Chem* **266**, 9113-9127.

Switzer, R. L., Turner, R. J. & Lu, Y. (1999). Regulation of the *Bacillus subtilis* pyrimidine biosynthetic operon by transcriptional attenuation: Control of gene expression by an mRNA-binding protein. In *Progress in Nucleic Acid Research and Molecular Biology*, vol. 62, pp. 329-367. Edited by K. Moldaves. London: Academic Press.

Tomchick, D. R., Turner, R. J., Switzer, R. L. & Smith, J. L. (1998). Adaptation of an enzyme to regulatory function: Structure of *Bacillus subtilis* PyrR, a *pyr* RNA binding attenuation protein and uracil phosphoribosyltransferase. *Structure* **6,** 337-350.

Traut, T. W. (1994). Physiological concentrations of purines and pyrimidines. *Mol Cell Biochem* **140,** 1-22.

Turnbough, C. L., Hicks, K. L. & Donahue, J. P. (1983). Attenuation control of *pyrBI* operon expression in *Escherichia coli* K12. *Proc Natl Acad Sci USA* **80,** 368-372.

Turner, R. J., Lu, Y. & Switzer, R. L. (1994). Regulation of the *Bacillus subtilis* pyrimidine biosynthetic (*pyr*) gene cluster by an autogenous transcriptional attenuation mechanism. *J Bacteriol* **176,** 3708-3722.

Turner, R. J., Bonner, E. R., Grabner, G. K. & Switzer, R. L. (1998). Purification and characterization of *Bacillus subtilis* PyrR, a bifunctional *pyr* mRNA-binding attenuation protein/uracil phosphoribosyltransferase. *J Biol Chem* **273,** 5932-5938.

Van de Casteele, M., Chen, P., Roovers, M., Legrain, C. & Glansdorff, N. (1997). Structure and expression of a gene cluster from the extreme thermophile *Thermus aquaticus* strain Z05. *J Bacteriol* **179,** 3470-3481.

Vickrey, J. F. (1993). Isolation and characterization of the operon containing aspartate transcarbamoylase and dihydroorotase from *Pseudomonas aeruginosa*. Ph.D. Dissertation (Molecular Biology), University of North Texas.

Vitols, M. J., Shaposhnikov, V. N. & Shvachkin, Y. P. (1967). A new path of orotic acid catabolism in microorganisms. *Dokl Akad Nauk* **174,** 1202-1204.

Vogels, G. D. & Van der Drift, C. (1976). Degradation of purines and pyrimidines by microorganisms. *Bacteriol Rev* **40,** 403-468.

Wang, G. P., Lundegaard, C., Jensen, K. F. & Grubmeyer, C. (1999). Kinetic mechanism of OMP synthase: a slow physical step following group transfer limits catalytic rate. *Biochemistry* **38,** 275-83

White, O., Eisen, J. A., Heidelberg, J. F., Hickey, E. K., Peterson, J. D., Dodson, R. J., Haft, D. H., Gwinn, M. L., Nelson, W. C., Richardson, D. L., Moffat, K. S., Qin, H., Jiang, L., Pamphile, W., Crosby, M., Shen, M., Vamathevan, J. J., Lam, P., McDonald, L., Utterback, T., Zalewski, C., Makarova, K. S., Aravind, L., Daly, M. J., Minton, K. W., Fleischmann, R.D., Ketchum, K. A., Nelson, K.E., Salzberg, S., Smith, H. O., Venter, J.C., Fraser, C. M. (1999). Genome sequence of the radioresistant bacterium *Deinococcus radiodurans* R1. *Science* **286**, 1571-1577.

Wild, J. R., Foltermann, K. F. & O'Donovan, G. A. (1980). Regulatory divergence of aspartate transcarbamoylases within the *Enterobacteriaceae*. *Arch Biochem Biophys* **201**, 506-517.

Wolff, J. A., MacGregor, C. H., Eisenberg, R. C. & Phibbs, Jr., P. V. (1991). Isolation and characterization of catabolite repression control mutants of Pseudomonas aeruginosa PAO. *J Bacteriol* **173,** 4700-4706.

Yamamoto, S., Kasai, H., Arnold, D. L., Jackson, R. W., Vivian, A. & Harayama, S. (2000). Phylogeny of the genus *Pseudomonas*: Intrageneric structure reconstructed from the nucleotide sequences of *gyrB* and *ropD* genes. *Microbiology* **146,** 2385-2394.

Yan, Y. & Demerec, M. (1965). Genetic analysis of pyrimidine mutants of *Salmonella typhimurium*. *Genetics* **52**, 643-651.

Yarchuk, O., Jacques, N., Guillerez, J. & Dreyfus, M. (1992). Interdependence of translation, transcription and mRNA degradation in the *lacZ* gene. *J Mol Biol* **226,** 581-596.

Yates, R. A. & Pardee, A. B. (1956a). Pyrimidine biosynthesis in *Escherichia coli*. *J Biol Chem* **221**, 743-756.

Yates, R. A. & Pardee, A. B. (1956b). Control of pyrimidine biosynthesis in *Escherichia coli* by feedback mechanism. *J Biol Chem* **221**, 757-770.

Yates, R. A. & Pardee, A. B. (1957). Control by uracil of formation of enzymes required for orotate synthesis. *J Biol Chem* **227**, 677-692.

Yurgel, **S.**, **Mortimer**, **M**. **W.**, **Rogers**, **K**. **N**. & **Kahn**, **M**. **L. (2000).** New substrates for the dicarboxylate transport system of *Sinorhizobium meliloti*. *J Bacteriol* **182,** 4216-21.

Zubay, G. (1973). *In vitro* synthesis of proteins in microbial systems. *Ann Rev Genet* **7**, 267.